REPORT DOCUMENTATION PAGE

AFRL-SR-AR-TR-04-

0079

the ng ntly

1. REPORT DATE (DD-MM-YYYY) 11-01-2004	2. REPORT TYPE Final	3. DATES COVERED (From - To) 25-07-2003 to 31-12-2003

4. TITLE AND SUBTITLE The 8th Int'l Meeting on Hole Burning, Single Molecules, and Related Spectroscopies: Science and Applications	5a. CONTRACT NUMBER
	5b. GRANT NUMBER F49620-03-1-0417
	5c. PROGRAM ELEMENT NUMBER
6. AUTHOR(S) Wm. Randall Babbitt	5d. PROJECT NUMBER
	5e. TASK NUMBER
	5f. WORK UNIT NUMBER

7. PERFORMING ORGANIZATION NAME(S) AND ADDRESS(ES) The Spectrum Lab and Physics Department Montana State University PO Box 173840 Bozeman, MT 59717-3740	8. PERFORMING ORGANIZATION REPORT NUMBER SL-WRB-0401

9. SPONSORING / MONITORING AGENCY NAME(S) AND ADDRESS(ES)
Air Force Office of   Research
4015 Wilson Blvd Room 713
Arlington, VA 22203-1954
        Program Manager: Gernot Pomrenke
        Grant Officer: Donna L. Moran
	10. SPONSOR/MONITOR'S ACRONYM(S)

	11. SPONSOR/MONITOR'S REPORT NUMBER(S)

12. DISTRIBUTION / AVAILABILITY STATEMENT Approved for public release; distribution unlimited Distribution Statement A:

20040213 115

14. ABSTRACT
    The 8th International Meeting on Hole Burning, Single Molecule, and Related Spectroscopies: Science and Applications (HBSM 2003) was held in Bozeman, Montana on July 26 to 31, 2003. The Co-Chairs were Wm. Randall Babbitt, Aleksander Rebane, and Rufus L. Cone of the Montana State University Physics Department and Randy W. Equall of Scientific Materials Corporation. Meetings have been held since 1987 to disseminate the latest developments in fundamental science and applications of site-selective spectroscopies, spectral hole burning and single molecule spectroscopy, photon echoes, and related topics. The 2003 topics included: Hole-burning materials and mechanisms, Photon echoes and coherent transients, Photophysics and photochemistry, Single molecule detection and spectroscopy, Laser frequency stabilization to SHB references, Optical storage and signal processing, Dephasing and spectral diffusion, Time and space domain holography, Biological systems, Nanosystems and nano-optics, Multi-photon and nonlinear effects, and Novel microscopies.
    The 99 scientists that attended the meeting came from 12 countries around the world. The conference program had 55 talks and 56 posters. Tours of research laboratories at MSU and Scientific Materials were part of the program. The Journal of Luminescence HBSM 2003 Proceedings to be published in 2004 contains 46 papers based on the presentations made at the meeting.

15. SUBJECT TERMS
Optical Coherent Transients, Spatial-Spectral Holography, Single Molecules, Photon Echoes, Spectral Hole Burning, Nanocrystals Spectroscopy, wideband signal processing, Inhomogeneously broadened materials

16. SECURITY CLASSIFICATION OF:			17. LIMITATION OF ABSTRACT	18. NUMBER OF PAGES	19a. NAME OF RESPONSIBLE PERSON Wm. Randall Babbitt
a. REPORT UNCLASSIFIED	b. ABSTRACT UNCLASSIFIED	c. THIS PAGE UNCLASSIFIED	UL	11	19b. TELEPHONE NUMBER (406) 994-6156

Standard Form 298 (Rev. 8-98)
Prescribed by ANSI Std. Z39.18

8th International Meeting on Hole Burning, Single Molecule, and Related Spectroscopies: Science and Applications

"HBSM 2003"

Bozeman, Montana USA
July 27 to 31, 2003

The HBSM Conference is held regularly to disseminate the latest developments in high-resolution optical spectroscopy of solids: spectral hole burning, single molecule spectroscopy, photon echoes and related topics.

The main conference themes include:
- Hole-burning materials and mechanisms
- Photon echoes and coherent transients
- Photophysics and photochemistry
- Single molecule detection and spectroscopy
- Novel microscopies
- Optical storage and signal processing
- Dephasing and spectral diffusion
- Time and space domain holography
- Biological systems
- Nanosystems and nano-optics
- Multi-photon and nonlinear effects

The purpose of this international meeting is to draw together participants from all over the world to discuss the latest developments in the fundamental science and applications of site-selective spectroscopies, spectral hole burning and single molecule spectroscopy. Since the first meeting in Estonia (1987), the meeting has been held in California, Switzerland, Japan, Minnesota, France and Taiwan.

The 8th meeting is being held in Bozeman, Montana, USA, in the Rocky Mountains. The program consists of invited and contributed talks and poster sessions. Posters will be displayed continuously during the meeting. Tours to Montana State University research laboratories and to Scientific Materials are part of the program.

Bozeman has a strong optics industry and is a resort travel destination. Bozeman is a portal for travel to Yellowstone Park, Big Sky, and Western Montana.

The conference proceedings will be published as full-length reviewed papers in a special issue of Journal of Luminescence. The planned publication date is May 2004.

Conference Co-Chairs

Wm. Randall Babbitt (Montana State University, Bozeman, Montana)
Rufus Cone (Montana State University, Bozeman, Montana)
Randy Equall (Scientific Materials Corporation, Bozeman, Montana)
Aleksander Rebane (Montana State University, Bozeman, Montana)

International Advisory and Program Committee

Thomas Basché (Universitaet Mainz, Mainz, Germany)
Ta-Chau Chang, (Academia Sinica, Taiwan, ROC)
Rufus Cone (Montana State University, Bozeman, Montana)
Alan Craig (Montana State University, Bozeman, Montana)
Josef Friedrich (Munich Technical University, Munich, Germany)
Kazuyuki Horie (Tokyo Univ. of Agriculture and Tech., Tokyo, Japan)
Jaak Kikas (University of Tartu, Tartu, Estonia)
Jean-Louis Le Gouët (CNRS-Laboratoire Aime Cotton, Orsay, France)
H. Peter Lu (Pacific Northwest National Lab., Richland, Washington)
W. E. Moerner (Stanford University, Stanford, California)
Norio Murase (National Institute of AIST, Osaka, Japan)
Michel Orrit (Universiteit Leiden, Leiden, Netherlands)
Gernot S. Pomrenke(Air Force Office of Sci. Res., Arlington, Virginia)
Seishiro Saikan (Tohoku University, Tohoku, Japan)
Matthew Sellars (Australian National University, Canberra, Australia)
Robert Silbey (Massachusetts Inst. of Tech, Cambridge, Massachusetts)
James Skinner (Univ. of Wisconsin, Madison, Wisconsin)
Gerald Small (Univ. of Iowa, Ames, Iowa)
Toshiro Tani (Tokyo Univ. of Agriculture and Technology, Tokyo, Japan)
Hans-Peter Trommsdorff (Université Joseph-Fourier, Grenoble, France)
Silvia Völker (Leiden University, Leiden, The Netherlands)
Kelvin Wagner (University of Colorado, Boulder, Colorado)

Local Organizing Committee

Alan Craig (Montana State University, Bozeman, Montana)
Ralph Hutcheson (Scientific Materials Corporation, Bozeman, Montana)
Yongchen Sun (Montana State University, Bozeman, Montana)
Robert Vrooman (Montana State University, Bozeman, Montana)

Saturday	Sunday	Monday	Tuesday	Wednesday	Thursday
	Breakfast 8:00 - 9:00	Breakfast 8:00 - 9:00	Breakfast 6:00 - 7:00	Breakfast 8:30 - 9:30	Breakfast 8:00 - 9:00
	Opening Remarks & Single Molecules I 9:00 - 10:30	Quantum Computing 9:00 - 10:30		Photophysics & Photochemistry 9:30 - 11:00	Rare Earth Systems 9:00 - 11:00
	Break 10:30 - 11:00	Break 10:30 - 11:00		Poster Session A 11:00 - 13:00	Break 11:00 - 11:30
	Nanosystems 11:00 - 12:30	Applications II 11:00 - 12:40	Excursion Yellowstone National Park 7:00 - 18:00		Novel Microscopies 11:30 - 12:30
	Lunch 12:30 - 13:30	Lunch 12:40 - 13:40		Lunch 13:00 - 14:00	Lunch 12:30 - 13:30
	Applications I 13:30 - 14:50	Single Molecules II 13:40 - 15:00		Lab Tours 14:00 - 17:00	Organic Systems 13:30 - 14:30
	Break 14:50 - 15:20	Break 15:00 - 15:30			Break 14:30 - 15:00
	Coherent Transients 15:20 - 17:00	Dephasing & Spectral Diffusion 15:30 - 17:50		Break 17:00 - 18:00	Dephasing, Diffusion, and Dynamics 15:00 - 17:00
Welcoming Reception 18:00 - 22:00	Dinner 18:00 - 19:00	Dinner 18:00 - 19:00	Conference Banquet Chico Hot Springs 18:00 - 21:00	Dinner 18:00 - 19:00	Dinner 18:00 - 19:00
	Biological Systems 19:00 - 20:20			Poster Session B 19:00 - 21:00	

Arrival (Tuesday)

HBSM2003 Program Schedule
GranTree Hotel, Bozeman, Montana

Saturday, July 26

Welcoming Reception in Foyer	18:00 - 20:00

Sunday, July 27

Breakfast served in Atrium	8:00 - 9:00
Opening Remarks	9:00 - 9:15

Single Molecules I   Chair: Taras Plakhotnik   page

W.E. Moerner	Single Molecules as Local Nanoscopic Probes	9:15 - 10:00	1
H. Peter Lu	Single-Molecule Spectroscopy at Nanoscale Interfaces	10:00 - 10:30	2
	Break /Refreshments served in Foyer	10:30 - 11:00	

Nanosystems   Chair: Fredy Meixner

Vladimir Shalaev	Plasmonic Nanoantennas for Guiding Light and Sensing Molecules	11:00 - 11:30	3
Frank Cichos	Non-Stationary Blinking of Individual Silicon Nanocrystals	11:30 - 11:50	4
Jörg Woehl	Local and Remote Addressing of Single Nano-Objects	11:50 - 12:10	5
Norio Murase	Single-Particle Spectroscopy of Doped Nanocrystals	12:10 - 12:30	6
	Break /Lunch served in Atrium	12:30 - 13:30	

Applications I   Chair: Mike Jefferson

Kelvin Wagner	Spatial-Spectral Holography for RF Antenna Array Multi-Beam Imaging	13:30 - 14:00	7
Kristian Merkel	Multi-Gigahertz Radar Range Processing of Baseband and IF Modulated Signals in Tm:YAG	14:00 - 14:20	8
Jean-Louis Le Gouët	Wide-Band, Flexible, Radio Frequency Spectrum Analyzer	14:20 - 14:50	9
	Break /Refreshments served in Foyer	14:50 - 15:20	

Coherent Transients   Chair: Kris Merkel

Vincent Lavielle	Efficient Engraving of Dispersive Filters for Time-to-Frequency Fourier Transform	15:20 - 15:40	10
Todd Harris	Chirped Inversion of Inhomogeneously Broadened Optically-Dense $Eu^{3+}:Y_2SiO_5$	15:40 - 16:00	11
Stefan Kröll	Photon Echoes from Accumulated Single Photon Excitations	16:00 - 16:20	12
Mingzhen Tian	Geometric Phase in Two-Level Atomic Systems	16:20 - 16:40	13
Yongchen Sun	Spectral Diffusion in Erbium-Doped Transient Spectral Hole Burning Materials	16:40 - 17:00	14
	Break /Dinner served in Atrium 18:00-19:00		

Biological Systems   Chair: Ta-Chau Chang

Silvia Volker	Optical High-Resolution Spectroscopy of Biological Systems: Some Examples of What Can Be Learnt	19:00 - 19:30	15
Ryszard Jankowiak	Spectral Holeburning Studies of the Isolated Reaction Center of Photosystem II of Green Plants.	19:30 - 19:50	16
Josef Friedrich	Hole Burning Spectroscopy of Biomolecules in External Fields	19:50 - 20:20	17

HBSM2003 Program Schedule
GranTree Hotel, Bozeman, Montana

Monday, July 28

	Breakfast served in Atrium	8:00 - 9:00	

Quantum Computing — Chair: Krishna Rupavatharam — page

Matthew Sellars	Rare Earth Quantum Computing	9:00 - 9:30	18
Lars Rippe	Preparing Rare-Earth-Ion-Doped Crystals for Quantum Gate Operations	9:30 - 10:00	19
Marlan Scully	Using Quantum Coherence to Detect Anthrax	10:00 - 10:30	20
	Break /Refreshments served in Foyer	10:30 - 11:00	

Applications II — Chair: Geoffrey Burr

Karl Rebane	Purely Electronic Zero-Phonon Line as the Cornerstone of Spectral Hole Burning and Single Impurity Molecule Spectroscopy: Prospects and Bottlenecks for Applications	11:00 - 11:20	21
Randy Babbitt	Power Budget Analysis of Image-Plane Storage in Spectral Hole Burning Materials	11:20 - 11:40	22
Zameer Hasan	Atomic Tailoring of Rare Earth Transitions in Wide Band Gap Semiconductors for Ultra-Dense Spectral Storage	11:40 - 12:00	23
Zeb Barber	Optical Coherent Transient High Bandwidth Arbitrary Waveform Generation and Pulse Shaping	12:00 - 12:20	24
Friso Schlottau	Demonstration of a Continuous Scanner and Time-Integrating Correlator using Spatial-Spectral Holography	12:20 - 12:40	25
	Break /Lunch served in Atrium	12:40 - 13:40	

Single Molecules II — Chair: W. E Moerner

Erwin Thiel	Surface and Resonance Enhanced Microraman Spectra: From Single Molecule to Excited States	13:40 - 14:10	26
Eli Barkai	From Sub-Poissonian Photon Statistics in Two-Level Molecules to Levy Photon Statistics in Blinking Quantum Dots.	14:10 - 14:40	27
Chris Hollars	Non-Classical Light Emission from Single Conjugated Polymers	14:40 - 15:00	28
	Break /Refreshments served in Foyer	15:00 - 15:30	

Dephasing and Spectral Diffusion Chair: Richard Meltzer

Michel Orrit	In Memory of Roman I. Personov	15:30 - 15:40	
Michael Fayer	Ultrafast Infrared Vibrational Echo Correlation Spectroscopy: Hydrogen Bond Dynamics in Water and Methanol	15:40 - 16:10	29
Seishiro Saikan	Correlated Fields Hole Burning Spectroscopy in Tm^{3+}:YAG	16:10 - 16:30	30
Roger Macfarlane	Optical Dephasing by Disorder Modes in Yttrium Orthosilcate (YSO) Doped with Eu^{3+}	16:30 - 16:50	31
Geoffrey Burr	Numerical Modeling of Excitation-Induced Dephasing	16:50 - 17:10	32
Taras Plakhotnik	Line "Narrowing" in Strong Optical Fields	17:10 - 17:30	33
Andrei Naumov	Single-Molecule Spectra and Low-Temperature Dynamics of Amorphous Solids: Standard and Non-Standard Temporal Behaviour	17:30 - 17:50	34

Dinner served in Atrium 18:00-19:00

HBSM2003 Program Schedule
GranTree Hotel, Bozeman, Montana

Tuesday, July 29

Breakfast served in Atrium	6:00 - 7:00

Yellowstone Tour and Banquet

Tour busses depart from GranTree Hotel	7:00
Arrive at Chico Hot Springs	18:00
Cash Bar	18:00 - 18:30
Conference Banquet: Western BBQ	18:30 - 21:00
Return to GranTree	22:00

Wednesday, July 30

Breakfast served in Atrium	8:30 - 9:30

Photophysics and Photochemistry Chair: Josef Friedrich

			page
Michel Orrit	Charge Transfer as a Source of Blinking in Single Molecules and Nanocrystals	9:30 - 10:00	35
Sybrand Bonsma	Light-Induced Conformational Changes in Red Fluorescent Protein	10:00 - 10:20	36
Mariusz Bednarz	Theoretical Study of Fluorescence Kinetics, Stokes Shift and Intra-Band Relaxation of Frenkel Excitons in J-Aggregates at Low Temperatures	10:20 - 10:40	37
Ta-Chau Chang	Satellite Hole Investigation of Hole Filling Induced by Fluorescence Energy Transfer	10:40 - 11:00	38

Poster Session A

Odd numbered posters presented in Hyalite Room	11:00 - 13:00
Break/Lunch served in Atrium	13:00 - 14:00

Labs Tours

Busses to MSU campus	14:00 - 17:00
Break/Dinner served in Atrium 18:00-19:00	17:00 - 19:00

Poster Session B

Even numbered posters presented in Hyalite Room	19:00 - 21:00

HBSM2003 Program Schedule
GranTree Hotel, Bozeman, Montana

Thursday, July 31

	Breakfast served in Atrium	8:00 - 9:00	

Rare Earth Systems   **Chair: Yongchen Sun**   *page*

			page
Richard Meltzer	Photon Echo Studies of $LaF_3:Pr^{3+}$ Nanocrystals in Glass	9:00 - 9:30	39
Laurent Bigot	Transient and Permanent Spectral Hole Burning in Erbium-Doped Glasses	9:30 - 10:00	40
Vladimir Hizhnyakov	Phase Relaxation in the Vicinity of the Dynamic Instability: Anomalous Temperature Dependence of Zero-Phonon Lines	10:00 - 10:20	41
Charles Thiel	Locating the Electronic States of Rare-Earth Ions Relative to Host Band States for the Development of Photon-Gated Hole Burning Materials	10:20 - 10:40	42
G. Mackay Salley	Enhanced Mo^{3+} and Re^{4+} Near-IR-to-Visible Upconversion	10:40 - 11:00	43
	Break /Refreshments served in Foyer	11:00 - 11:30	

Novel Microscopies   **Chair: Jorg Woehl**

M. Andreas Lieb	A Parabolic Mirror Objective with High Numerical Aperture for Imaging and Spectroscopy at the Nanometer Scale	11:30 - 11:50	44
Recep Avci	Antibody-Antigen Interactions and Atomic Force Microscopy: Another Approach to Single Molecule Detection	11:50 - 12:10	45
Volkmar Dierolf	Microscopy Studies of Lithium Niobate Waveguide Devices Using Spatially Dependent Fluorescence Line Narrowing	12:10 - 12:30	46
	Break/Lunch served in Atrium	12:30 - 13:30	

Organic Systems   **Chair: Silvia Volker**

Jean-Pierre Galaup	Naphthalocyanine Based Time Reversal Mirror at 800 nm	13:30 - 13:50	47
Mikhail Drobizhev	Electron-Phonon Coupling in Selectively-Excited Two-Photon Transition: Role of Molecular Symmetry	13:50 - 14:10	48
Kazuyuki Horie	PHB Study on Nanoscopic Aggregation in Random-Copolymer Bulk Films of Methyl Methacrylate with Butyl and Benzyl Methacrylates	14:10 - 14:30	49
	Break /Refreshments served in Foyer	14:30 - 15:00	

Dephasing, Diffusion, and Dynamics   **Chair: Lothar Kador**

Yuri Vainer	Parameter Distributions of Single-Molecule Spectra and Low-Temperature Dynamics of Disordered Solids	15:00 - 15:20	50
Toshiro Tani	Microscopic Exciton Properties of Fibril-Shaped Molecular J-Aggregates Prepared in Ultra-Thin Polymer Films	15:20 - 15:40	51
Claudine Crepin	Vibrational Dynamics of H(D)Cl in Cryogenic Matrices: from van der Waals Interaction to Weak Hydrogen Bond	15:40 - 16:00	52
Jaak Kikas	Site-Selection Spectroscopy of Low-Temperature Incommensurate Phases	16:00 - 16:20	53
Eric Chronister	Impulsive Stimulated Scattering on Metal and Semiconductor Interfaces Under High Pressure	16:20 - 16:40	54
	Closing Remarks	16:40 - 17:00	

Dinner served in Atrium 18:00-19:00

HBSM2003 Poster Program

GranTree Hotel, Bozeman, Montana

All posters will be on display throughout the conference

	Posters	Session	page
Dehong Hu	Single-Molecule Nanosecond Anisotropy Dynamics of Tethered Protein Motions	A	55
Josef Friedrich	UV-Hole Burning of Proteins via Photobleaching of Intrinsic Aminoacids	B	56
Valter Zazubovich	Correlation Between Energy Disorder and Excitonic Couplings in the LH-2 Complex from Rhodopseudomonas Acidophila. (A High Pressure Spectral Hole Burning Study.)	A	57
Peter Geissinger	A Quantum-Mechanical Model for Determination of Internal Electric Fields at Protein Active Sites from the Stark Effect on Persistent Spectral Holes	B	58
M. Andreas Lieb	Rotational Diffusion of the Transmembrane Anion Exchange Protein AE1 at the Single Molecule Level	A	59
Jan Hala	Hole Burning Study of Cyanobacterial Photosystem II Complexes Containing Small Putative Chlorophyll-Binding Proteins	B	60
Flurin Könz	Optical Dephasing in Light-Harvesting Complexes of Purple Bacteria	A	61
Pat Callis	Quantitative Predictions of Fluorescence Quantum Yields for Tryptophan in Proteins	B	62
Jean-Pierre Lemaistre	Intraband Relaxation of Frenkel Excitons in Molecular Aggregates of Low Dimensionality	A	63
Joanne Harrison	Optically Induced Spin Polarisation of the Nitrogen-Vacancy Centre in Diamond	B	64
B. R. Reddy	Persistent Spectral Hole Burning Studies in Lithium Fluoride Color Centers	A	65
B. R. Reddy	Optical Hole Burning in Europium Doped Borate Glasses	B	66
Tonu Reinot	A New Way to Model Spectral Hole Burning	A	67
Hiromasa Hanzawa	Hole Burning of Inorganic-Organic Hybrid Materials Prepared by Sol-Gel Method	B	68
Jaak Kikas	Hole Burning And Single-Molecule Spectroscopy Of Terrylene In Incommensurate Biphenyl	A	69
Koji Fujita	Room-Temperature Persistent Spectral Hole Burning of Eu_{3+} in Alkali Borate Glasses	B	70
Norio Murase	Function of Eu Ions and Defect Centers in Photochemical Hole-Burning in Glasses	A	71
Jaak Kikas	Persistent Spectral Hole Burning in Mn-Doped Al_2O_3 ceramics	B	72
Anshel Gorokhovsky	Diamond With Impurity Ions As A Hole Burning Material	A	73
Aras Konjhodzic	Holeburning In Rare Earth Doped Nanoparticles of MgS and CaS	B	74
Imbi Tehver	A Possibility of Separating the Inhomogeneous Broadening via Coherent Raman Spectra	A	75
Judith Grimm	Near-Infrared to Visible Upconversion Studies in Tm^{2+} Doped Halide Crystals	B	76

SUMMARIES

Single Molecules as Local Nanoscopic Probes

W. E. Moerner and Kallie Willets

Department of Chemistry, Stanford University

Optical spectroscopy of single molecules in condensed phases provides a tool to sense local nanoenvironments that complements and extends conventional bulk ensemble-averaged measurements. Since typical single-molecule fluorophores are on the order of a few nm in size, detecting the state of the single molecule allows exploration of several features of the local interaction of the molecule with its immediate neighbors in the material or biomolecule. Molecular state variables that sense aspects of the local environment range from signal strength, orientation, and lifetime, to the emission spectrum of the molecule and the degree of energy transfer with neighboring molecules. For example, the time-dependent fluctuations in the orientation of a single kinesin motor as a function of nucleotide state were detected by single-molecule polarization microscopy. Recently, some groups have begun to explore the behavior of individual fluorescent molecules in the challenging environment of living cells. By extrinsic labeling of an antigenic peptide, we have completed a detailed study of the diffusion of single copies of major histocompatibility complexes of type II (MHCII) in the membranes of CHO cells. The results from this study bear on fundamental properties of the cell membrane, in particular on the presence of significant confinement restricting the motion of the MHCII transmembrane proteins and the role of cholesterol.

In recent work, we have discovered a new class of fluorophores that can be imaged at the single-molecule level at room temperature (Figure 1) and offer additional beneficial properties such as a significant ground state dipole moment, moderate hyperpolarizability, and sensitivity to local rigidity. These molecules contain an amine donor and a dicyanodihydrofuran (DCDHF) acceptor linked by a conjugated unit (benzene, thiophene, alkene, styrene, etc.). These molecules were originally designed to deliver both high polarizability anisotropy and dipole moment as nonlinear optical chromophores for photorefractive applications. Surprisingly, we have found that these molecules are also well-suited for single-molecule fluorescence applications in polymers and other reasonably rigid environments.
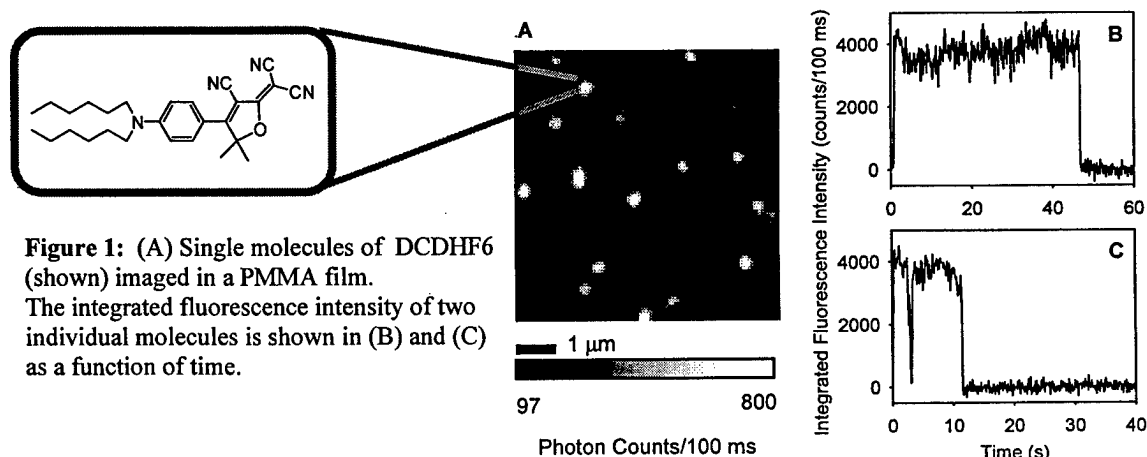

Figure 1: (A) Single molecules of DCDHF6 (shown) imaged in a PMMA film.
The integrated fluorescence intensity of two individual molecules is shown in (B) and (C) as a function of time.

1

Single-Molecule Spectroscopy at Nanoscale Interfaces

H. Peter Lu

Pacific Northwest National Laboratory, Fundamental Science Division, P.O.Box 999, Richland, WA 99352, USA

Surface Enhanced Raman Scattering (SERS) fluctuation observed at confined "hot spots" at nanometer scale has been studied using combined AFM-enhanced multi-channel Raman microscopy, theoretical modeling, and computational simulation.[1-3] We report our laser intensity dependent studies of the nano-SERS fluctuation to demonstrate and characterize that the photoinduced and spontaneous nature of the nano-SERS fluctuation. The origin of the nano-SERS fluctuation has been attributed to the fluctuation of the interaction of the molecules with the local electromagnetic field that depends on the substrate nano-metallic structures.[1,3] We have applied a frequency-domain three-dimensional finite element method to solve Maxwell's equations of electric field enhancement distributions encountered in atomic force microscopy (AFM) tip-enhanced surface-enhanced Raman spectroscopy (SERS) experiments (AFM-SERS).[2] We simulated the near- field enhancement in the vicinity of an AFM tip in close proximity to silver spherical nanoparticles under a laser illumination. Our results suggest new approaches for using AFM-SERS tip-enhanced near-field technique to image samples on surfaces. Single-molecular spectroscopy studies of electron-hole recombination dynamics at the dye-sensitized TiO_2 semiconductor interface have begin to shed light on the molecular-level understanding of the inhomogeneous interfacial electron transfer dynamics at this system.[4] E-mail: peter.lu@pnl.gov

Reference:
1. Yung Doug Suh, Gregory K. Schenter, Leyun Zhu, and H. Peter Lu, "Probing Nano-Surface Enhanced Raman Scattering Fluctuation Dynamics using Correlated AFM and Confocal Ultramicroscopy," *Ultramicroscopy*, in press.
2. Miodrag Micic, Nicholas Klymyshyn, Yung Doug Suh, H. Peter Lu, "Finite Element Method Simulation of the Field Distribution for AFM Tip-Enhanced Surface Enhanced Raman Scanning Microscopy," *J. Phys. Chem. B*, **2003**, *107*, 1574-1584..
3. Leyun Zhu, Gregory K. Schenter, Miodrag Micic, Yung Doug Suh, Nicholas Klymyshyn, H. Peter Lu, "Nano-Surface Enhanced Raman Scattering Fluctuation Dynamics," *Proceedings of SPIE*, in press.
4. Miodrag Micic, Dehong Hu, H. Peter Lu, "Single-Pair Electron-Cation Recombination Dynamics at a Dye-Sensitized Semiconductor Nanoparticle Interface," Submitted.

Plasmonic Nanoantennas
for Guiding Light and Sensing Molecules

Vladimir M. Shalaev

School of Electrical and Computer Engineering, Purdue University, West Lafayette, IN 47907, email shalev@purdue.edu

We study optical properties of metal nanocomposites and specially engineered metal nanostructures where impingent electromagnetic wave effectively couples to surface plasmon modes. Such coupling leads to extremely high local fields if the incident radiation resonantly excites the plasmon modes. Thus, metal nanostructured materials open new avenues for manipulating light and sensing molecules [1-5]. Engineered plasmonic structures can act as "smart" optical nano-antennas focusing light on nanometer scale areas, with high spatial and spectral control of the energy concentration. In this presentation, the optical properties of plasmonic nanomaterials and their novel applications in nano-photonics and spectroscopy will be discussed. I'll outline new phenomena in plasmonic nanomaterials, such as negative refraction [2,3,5], enhanced optical transmittance [1,4,5], plasmonic nano-lithography, disorder-induced localization of plasmons [1], and surface-enhanced nonlinear optical phenomena [1]. Plasmonic nanomaterials open up the feasibility to detect molecules with unsurpassed sensitivity and develop photonic nano-circuits allowing the control of photons in a similar manner as electrons are manipulated and controlled in conventional electronic circuits.

REFERENCES:

1. Vladimir M. Shalaev, *Nonlinear Optics of Random Media: Fractal Composites and Metal-Dielectric Films* (Springer, Berlin Heidelberg 2000); A. K. Sarychev and V. M. Shalaev, Physics Reports **335**, 275-371 (2000)
2. J.B. Pendry, Phys. Rev. Lett. **85**, 3966 (2000)
3. D.R. Smith, et al., Phys. Rev. Lett. **84**, 4184 (2000); R. A. Shelby and D. R. Smith, Science **292**, 77 (2001).
4. H.J. Lezec, et al., Science **297**, 820 (2002); T. Thio, et al., Nanotechnology **13**, 492 (2002)
5. V. A. Podolskiy, A. K. Sarychev, V. M. Shalaev, J. of Nonlinear Opt. Physics & Materials, V. 11, 65 (2002); K. Seal, et al., Phys. Rev. B **67**, 035318 (2003).

Non-stationary Blinking of Individual Silicon Nanocrystals

Frank Cichos, Jörg Martin and Christian von Borczyskowski
Institute of Physics 122501, Chemnitz University of Technology
09107 Chemnitz, GERMANY
Phone: +49/(0)371 531 3066
Fax: +49/(0)371 531 3060
email: cichos@physik.tu-chemnitz.de

Silicon nanocrystals are of potential interest not only for opto-electronics but also for astrophysics. It is supposed that silicon nanocrystals are responsible for the so called extended red emission (ERE) – a broad emission feature of interstellar matter in the wavelength region of 600 nm to 900 nm. As support for this argumentation a detailed knowledge of the photophysical/photochemical processes (i.e. the emission quantum yield, surface chemistry) in silicon nanocrystals is needed. Although a large number of studies on silicon nanocrystal ensembles exists, no uniform picture on these processes is available.

We present results of room temperature confocal microscopy studies on individual silicon nanocrystals produced from porous silicon. The particles show narrow emission spectra (150 meV) between 500 nm and 650 nm and the typical blinking as observed for other semiconductor nanocrystals. During the course of our longest observations (20 min), all studied particles show no bleaching event. The probability density to find certain *on* and *off* time durations obeys the commonly observed power law ($p(t_{on/off}) \propto t_{on/off}^{-\alpha}$), however, the exponent α of the *on* time duration statistics is found to be larger than 2. This is observed for the statistics of many nanocrystals as well as for individual nanocrystals and implies a finite mean *on* time $<t_{on}>$ and thus a different physical process behind the blinking as compared to other semiconductor nanocrystals. The *off* time statistics on the other hand shows an exponent between 1.1 and 1.4 which is close to the values found i.e. for CdSe.

Besides this, the duration of *on* and *off* times is non-stationary on the timescale of our observation. This is observable in the histograms of *on* and *off* times as a function of the observation time as well as in the persistence probability that *off-on/on-off* switches occur. At the beginning of the recorded time traces longer *on* times and shorter *off* times are observed. With increasing observation time (timescale of several ten seconds) the *on* times decrease by a factor of three while the *off* times increase. This time dependence is responsible for an apparent bleaching of nanocrystal ensembles which we observe and which is found to be reversible.

Local and remote optical addressing of single nano-objects

Mickaël Brun, Aurélien Drezet, Serge Huant,
Jean-François Motte, and Jörg C. Woehl*

Laboratoire de Spectrométrie Physique
Université Joseph Fourier Grenoble et CNRS
BP 87, 38402 Saint Martin d'Hères cedex, France

* Phone +33 4 76 51 48 20, Fax +33 4 76 63 54 95, email jorg.woehl@ujf-grenoble.fr

Aperture-type near-field scanning optical microscopy (NSOM) is the tool of choice for confining light to subwavelength dimensions in order to address single nano-objects (like single molecules, quantum dots, nanocrystals, or nanospheres). The usual procedure is to position the optical probe, a tapered and metal-coated optical fiber with an aperture at the tip apex, over the object under study, to excite it optically, and to construct, point by point, the corresponding emission image. While this **local addressing** is usually employed in order to learn about the object's intrinsic properties, we will show that it can, inversely, be used to image the optical properties of the probe itself. For this purpose, we use single, fluorescent nanospheres as scalar detectors in order to map the electric field intensity transmitted by an optical tip. Paradoxically, the recorded fluorescence images show two intensity lobes if the sphere diameter is smaller that the aperture diameter (see Fig.) which is expected only in the case of vector detectors like single molecules [1]. The widely used Bethe-Bouwkamp model [2] fails to explain these results even qualitatively. We therefore present a simple but realistic, analytical model for the electric field created by light emitted by a NSOM tip that is not only in qualitative but also quantitative agreement with the experimental data. This analysis leads to a better understanding of the physics of the optical tip with important implications for the local, optical addressing of single nano-objects.
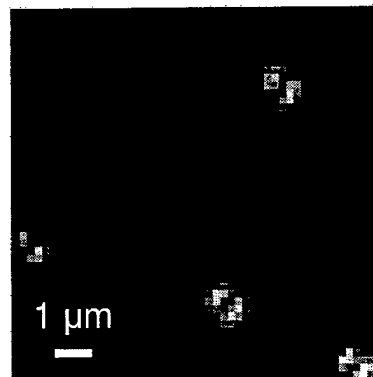
But NSOM also offers an interesting way to **remotely address** single objects by making use of one of the most fundamental properties of electromagnetic radiation: its polarization. In our method, an optically active medium is covered with a thin but opaque metallic film presenting sub-wavelength holes. The method, easily applicable to other systems, will be demonstrated for the remote addressing of single quantum dots at low temperature. When the optical tip is positioned some distance away from a sub-wavelength hole, surface plasmons in the metal coating are generated [3] and, by turning the polarization plane of the excitation light, can be selectively directed towards a chosen hole. Subsequent scattering at the hole boundaries allows to recover the original excitation energy in the form of light [4] and to stimulate emission from the underlying quantum dots. In contrast to other methods, our approach does not rely on external waveguide structures, and most experimental parameters (hole diameter, geometry, polarization) are continuously tunable over a wide range of values. Therefore, we expect the proposed method to become a valuable tool for future optical and optoelectronic applications.

[1] E. Betzig, R. J. Chichester, *Science* **262**, 1422 (1993)
[2] H. A. Bethe, *Phys. Rev.* **66**, 163 (1944); C. J. Bouwkamp, *Philips Res. Rep.* **5**, 321 (1950)
[3] B. Hecht, H. Bielefeldt, L. Novotny, Y. Inouye, D. W. Pohl, *Phys. Rev. Lett.* **77**, 1889 (1996)
[4] C. Sönnichsen, A.C. Duch, G. Steininger, M. Koch, G. von Plessen, J. Feldmann, *Appl. Phys. Lett.* **76**, 140 (2000)

Single-particle spectroscopy of doped nanocrystals

Norio Murase
Photonics Research Institute, National Institute of Advanced Industrial Science & Technology (AIST),
Ikeda-City, Osaka 563-8577, Japan, Tel. +81-72-751-8483, Fax. +81-72-751-9637
•E-mail: n-murase@aist.go.jp

Single-particle spectroscopy of Te-doped CdSe nanocrystals (ca. 6 nm in diameter, passivated by ZnS, dopant ratios of Te relative to Se upon synthesis were 2.0 and 3.5%) has been performed at room temperature. The results were compared with those of undoped one prepared by a same method. There was no difference in emission widths of individual particles of doped and undoped samples, in spite of the wider ensemble bands of the doped emissions. Some of the individual emissions from doped ones show irreversible blue shift by successive measurements significantly larger than those of the undoped ones. This means every particle emits from only one energy site during emission. However, the emission from a dopant changes its energy position easily due to instability of the dopant upon excitation. To the best of the knowledge of the author, this is the first report on a single particle spectroscopy of a dopant in nanocrystals.

Spatial-Spectral Holography for RF Antenna Array Multi-Beam Imaging

K. Wagner and F. Schlottau
Univ. Colorado, Boulder, CO 80309 USA
kelvin@colorado.edu

Jaap Bregman
ASTRON 7900 AA Dwingeloo NL
bregman@astron.nl

Jean-Louis Le Gouët
Aimé Cotton 91405 Orsay FR
jean-louis.legouet@lac.u-psud.fr

Abstract: The optically-modulated signals from a fiber-remoted, coherently-fed, randomly-spaced, RF array antenna can be cohered with a photorefractive crystal and processed to form squint-free broad-band RF images using a Fourier-plane spatial-spectral hologram to accumulate the RF scene, and a frequency-scanned, synchronously-magnified, holographic-readout system to produce the squint-free output image and spectrally analyze every source in the field of view simultaneously.

RF imaging and spectral analysis of far-field sources illuminating a large, broadband, sparse antenna array is an exceedingly computationally demanding task required for applications in radio-astronomy, SETI, or surveillance receivers.[1] These large antenna arrays provide dramatically increased sensitivity by coherently combining the RF signals from individual array elements to point high gain, narrow angular resolution beams, but require true-time-delay beam steering, or alternatively spectrally-selective processing to compensate for the aperture scaling and resulting beam-steering with frequency (squint). This RF array imaging task requires a cross-correlation between every antenna signal with every other signal to produce a frequency dependent complex coefficient of the scene component in $(\vec{k}_T, \omega)$-space determined by the frequency and element separations. Spatial Fourier transformation of the samples in $(\vec{k}_T, \omega)$-space at each frequency forms a monochromatic RF image which can be detected, while different frequency-component images must be scaled proportional to their RF frequency. The squint-free array imaging and spectral-analysis of thousands of multi-GHz bandwidth RF signals from an irregularly-spaced antenna array is a demanding task beyond the capabilities of electronic signal processing for which we propose a novel spatial-spectral holography solution.

Our solution to this demanding application uses a fiber-fed, coherently-modulated array, phase cohered with a photorefractive crystal.[2] The cohered output is spatially Fourier transformed onto a thin cryogenically-cooled spatial-spectral holographic (SSH) crystal, in which each pair of antennas interferes and accumulates a spatial-spectral grating at each resolvable frequency bin of 1MHz (corresponding to a coherence time $T_2 = 1\mu s$) with a $\vec{K}_g$-vector proportional to the antenna element separation. After accumulating for about $T_1 = 10$ms (the lifetime), a frequency-scanned, plane-wave laser diffracts off these gratings, and is imaged onto a 2-D CCD detector array. As the frequency of the laser is scanned, the system magnification is synchronously varied over a range corresponding to the bandwidth ratio of the maximum to minimum RF frequencies, producing a high resolution spectra for each RF source as a function of time.

This new SSH based array imager overcomes the key limitations of previous Fourier optical approaches by harnessing the frequency domain parallelism inherent to SSH materials, and reading out each frequency band sequentially as the zoom lens is scanned. This processor solves the previously intractable problem of squint-free, broadband, randomly-spaced, large antenna-array RF imaging and source spectral analysis in a simple system with huge processing gain.
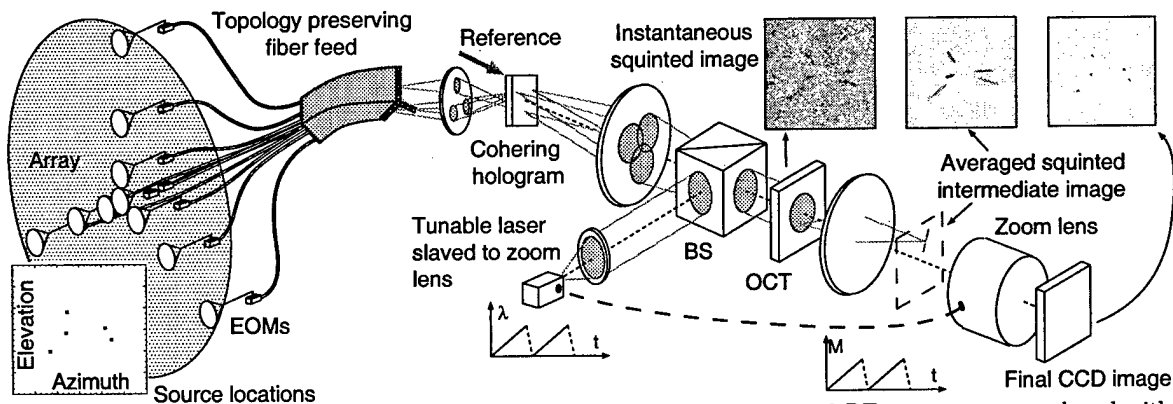
Figure 1: Sparse-array correlation imager using a coherently-modulated, fiber-remoted RF antenna array cohered with a photorefractive hologram and then spatially Fourier transformed with a lens onto a spatial-spectral holographic (SSH) medium. The time-integrated, spectrally-selective hologram is read out with a scanned, tunable laser using a variable magnification zoom lens whose magnification is proportional to the laser frequency offset. The inset simulated images are for an array with 360 randomly positioned antenna elements, 1km diameter, and 1-10GHz bandwidth, as required for the Allen radio-telescope.

1. A. R. Thompson, J. M. Moran, et al, *Interferometry and synthesis in radio astronomy.* Wiley, 1986.
2. K. H. Wagner, F. Schlottau, and J. Bregman, "Array imaging using SSH," in *Optics in Computing*, SPIE, 2002.

Multi-Gigahertz Radar Range Processing of Baseband and IF Modulated Signals in Tm:YAG

K. D. Merkel, R. Krishna Mohan, Z. Cole, A. Olson, and W. R. Babbitt
Spectrum Lab, Montana State University, Bozeman, Montana 59717
Phone (406) 994-7241, Fax (406) 994-7676, Email: merkel@spectrum.montana.edu

The Spectral-Spatial Coherent Holographic Integrating Processor (S^2-CHIP) performs coherent signal processing operations on high bandwidth analog optical signals with large time bandwidth products. The device integrates the results of multiple acquisitions and resolves time delays up to microseconds with high precision and large dynamic range. High-resolution Doppler processing is also achievable. Experimental results will be presented on time delay (range) resolution, integration of spectral correlations, and effects of dynamic coding as applied to a radar range processor. Processing of both baseband and intermediate frequency (IF) modulated signals is demonstrated. The baseband demonstrations used a code length of 2048 chips clocked at 2.5 Gcps (Giga-chips per second), which were binary phase shift keying (BPSK) modulated onto the optical carrier. The IF demonstrations used code lengths up to 500 chips at 1.0 Gcps that were BPSK modulated on a 1.75 GHz RF carrier and then modulated onto the optical carrier.

In a radar range processor, an optimally encoded RF waveform is transmitted and an antenna receives a signal that is delayed, attenuated and buried in a noisy background after being reflected back by a target. A single analog correlation of the received and reference signals yields the round-trip delay and thus the target's range. Integration of multiple coherent returns increases signal strength and can allow for target velocity determination. In the S^2-CHIP design, two coded RF signals are modulated on a stable optical carrier and correlative processing occurs between the signals in a spectral-spatial holographic (SSH) material. This correlation yields the delay, τ, as a periodic spectral grating with primary period $1/\tau$. The persistence of the SSH material allows for integration of multiple correlative results. For J coherent correlations, the grating strength increases by a factor of J, while incoherent noise grows as $\sqrt{J}$.

The S^2-CHIP device consists of a frequency stabilized diode lasers, broadband electro-optic modulators and optical amplifiers, a spectral-spatial holographic material in a cryocooler, frequency-swept laser pulses, and low bandwidth photoreceivers and A-to-D converters. Since the high bandwidth processing occurs in the SSH material, the conventional high bandwidth optical-to-electronic bottleneck is eliminated. The practicality of the device stems from the use of a swept frequency readout of the broadband grating that creates a low bandwidth optical output signal that is detected, digitized and post processed, all at low bandwidths. In order to ensure sufficient spectral resolution in readout, the frequency chirp rate should be less than $(1/\tau_m)^2$, where τ_m is the maximum delay of interest.. For τ_m = 1 μs, the chirp rate should be 1.0 MHz / μs and the required detection bandwidth is 1 MHz. A 10 GHz bandwidth grating can be read out in less than 10 msec, the persistence time of Tm:YAG.

In our experiments, a frequency stabilized Ti:Sapphire laser was resonant with the 793 nm transition of a Tm:YAG crystal (0.1 at. %) held at 5K. The laser beam was split into processing and readout beams. Each programming shot consisted of a N-chip BPSK waveform (i.e. radar reference signal) and a single time delayed replica (i.e. radar return signal), where a unique BPSK pulse pair was introduced at the pulse repetition frequency of 100 kHz. The BPSK codes were created by a pulse pattern generator and modulated onto the processing beam by an electro-optic phase modulator. The readout bandwidth was limited to 40 MHz by the acousto-optic modulator currently used to create the chirped (~1 MHz/μs) readout pulse. Broadband readout techniques are being developed. The processing (0.3 to 2.5 mW) and readout (100 μW) beams were combined and focused to a ~50 μm F spot in the crystal. Figure 1 shows the signal to noise enhancement achieved by integration of multiple coherent radar returns. The calculated peak strength of the rms power spectrum of the readout signal is plotted versus the number of programming shots (log-log scale) with a fixed 1 μs delay, for baseband coding and for four different processing beam powers. As expected, the processed signal strength initially grows as the square of the number of shots in each data set and the strength grows as the square of the programming power. The grating exhibits shot and power dependent material saturation. Studies of range resolution, dynamic coding, and integration dynamics will be presented.
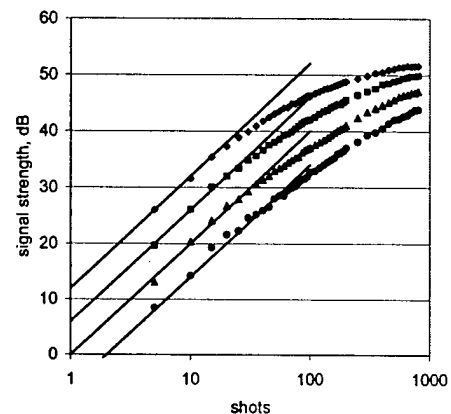

Figure 1 Integration dynamics plotted as rms peak strength of the power spectral density of the grating readout signal versus number of shots, J, for programming powers of 2.5 mW (top curve) and powers decreased by factors of 2 from 2.5 mW (lower curves), along with curves for ideal integration, J^2 (solid lines).

8

WideBand, Flexible, Radio Frequency Spectrum Analyzer

I. Lorgeré, V. Lavielle, F. De Seze, J.-L. Le Gouët
Laboratoire Aimé Cotton, CNRS, Bâtiment 505, 91405 Orsay, France
Tel 33 1 69 35 20 00, Fax 33 1 69 35 21 00, ivan.lorgere@lac.u-psud.fr

**Sylvie Tonda, Daniel Dolfi and Jean-Pierre Huignard**
Thales TRT-France, Domaine de Corbeville, 91404 Orsay, France

Abstract: Recent results demonstrating broadband, versatile operation of a Radio Frequency spectrum analyzer based on spectral hole burning are reported. The device aims at becoming the next generation spectrum analyzer for broadband radar and astronomical applications.

Astronomers are expecting valuable information from the sub millimeter window where numerous important molecular and atomic species uniquely express through their spectral lines. In heterodyne receivers, mixing with a THz range local oscillator shifts the astronomical signal frequency to the 1-10 GHz range. In this frequency range amplifiers and high resolution spectrometers are available. Cryogenic conditions are necessary, both for the high frequency mixers and the low noise amplifiers.

Also, one need broad band spectrometers at the back end. Available spectrometers do not answer the bandwidth demand. The forthcoming HERSCHEL space observatory will use four acousto-optical spectrometer (AOS) to cover an instantaneous bandwidth of 4GHz with a resolution of 1MHz. Since the AOS have fixed resolution and bandwidth, an autocorrelation spectrometer (ACS) will also be used, with a maximum resolution of 100kHz. Flexible, the ACS still suffers from limited bandwidth, below 500MHz, and high power consumption. If such combinations of spectrometers can handle a 4GHz bandwidth, they cannot cope with increasing bandwidth demand. Alternative technology with great potential is required for future space laboratories.

Fig. 1. Counter propagating box geometry for independent access to engraving (#1,#2), reading (#3) and diffracted beams. The insert shows the architecture of the analyzer. A Mach-Zehnder modulator MZM transfers the RF signal S(t) on the optical carrier from laser L. The crystal C diffracts the RF signal frequency components in different directions.
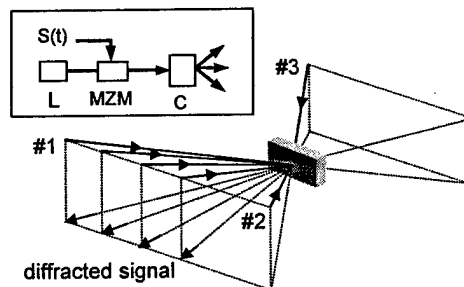
The Spectral Hole Burning (SHB) technology has this potential. Specifically, the inhomogeneously broadened absorption bands of rare-earth doped crystals have bandwidths exceeding 10 GHz, together with spectral resolution below 100 kHz at low temperature. With the advent of broadband integrated electro-optic modulators, these materials are particularly suited to processing broadband RF signals with impressive time-bandwidth product. We recently proposed and demonstrated the principle of a spectral analyzer for broadband RF signals based on SHB [1]. The principle is the following (see Figure 1). One first engraves an holographic filter in the absorption band of the crystal. The two engraving beams, labeled #1 and #2, issue from the same laser. During the engraving stage the frequency of the laser is linearly swept over a frequency interval Δv while the angle between the two beams is simultaneously scanned over the angular range $\Delta \theta$ by acousto optic deflectors. Thanks to the intrinsic frequency selectivity of the SHB process in the crystal, this assigns a specific diffraction direction to each frequency component. The beam #3, modulated by the RF signal, is directed to the engraved holographic filter that achieves the instantaneous angular separation of the optically carried RF spectral components. The dispersion law is given by the coefficient $\Delta \theta / \Delta v$ and is inherently flexible since the angular and spectral ranges are independent parameters at engraving. The spectral resolution is ultimately limited by the homogeneous linewidth of the ion transition and the bandwidth by the inhomogeneous width.

We shall present recent results including attractive features such as multiscale spectral analysis and optical carrier suppression.

[1] L. Ménager, I. Lorgeré, J.-L. Le Gouët, D. Dolfi, J.-P. Huignard, Opt. Lett., **26**, 1245, (2001) ; V. Lavielle, I. Lorgeré, J.-L. Le Gouët, S. Tonda, D. Dolfi, Opt. Lett., **28** (2003) *in press*.

Efficient engraving of dispersive filters for time-to-frequency Fourier transform

V. Lavielle, J.-L. Le Gouët, I. Lorgeré

Laboratoire Aimé Cotton, CNRS, Bâtiment 505, 91405 Orsay, France
Tel 33 1 69 35 20 00, Fax 33 1 69 35 21 00, ivan.lorgere@lac.u-psud.fr

F. Schlottau, K. Wagner

Optoelectronic Computijng Systems Center, University of Colorado, CO 80309-0525, Boulder

Abstract: An new method is presented for engraving a dispersive filter in a rare-earth doped crystals. Experimental results are presented and discussed in the perspective of broadband operation.

Optical processing of radio frequency signals is a growing field. One of the attractive feature of this approach is the wide instantaneous bandwidth offered by optical processing. Nonetheless spectral resolution is also required. Optical processing using optical coherent transients in rare earth doped crystals is particularly attractive because it offers both wide bandwidth and high spectral resolution. A number of RF processing applications have been pursued during the last years. The longest studied ones approach today the benchmarks required to reach the development stage [1,2]. Optical coherent transients have recently demonstrated their ability to perform time-to-frequency Fourier transform of RF signals [3]. The operation relies on the so-called chirp transform algorithm. The RF signal modulates an optical chirp (chirp rate r). This modulated chirp is then filtered through a group-delay dispersing line (dispersion rate 1/r) engraved in the crystal's absorption band. The filtered output is an optical chirp (rate r) modulated by the Fourier transform of the RF signal.
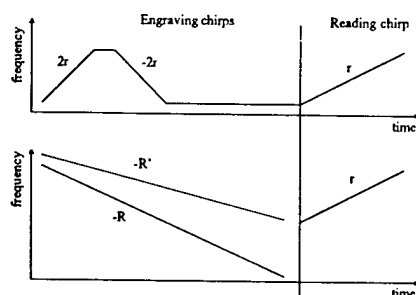

Figure 1: The successive chirp (a) and the co-temporal chirp (b) approaches for engraving. In (a) two successive chirps of rate 2r and (-2r) respectively, engrave a dispersive filter with dispersion rate (1/r). In (b) two co-temporal chirps of rate (-R) and (-R') respectively, engrave the dispersive filter with dispersion rate 1/R'-1/R=1/r. In both cases (a) and (b) the reading optical chirp rate is r.
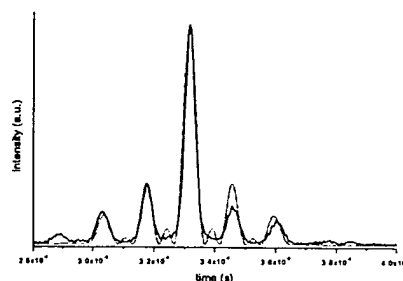

Figure 2: Experimental (solid line) Fourier transform of a two-frequency RF signal obtained with the co-temporal approach. The dotted line is the simulation.

In order to get an efficient process, one must efficiently engrave the dispersive filter in the crystal. This implies two optical chirps. In the first demonstration [3] the two engraving chirps were two successive chirps (see Figure 1a). With this approach, the total duration of the engraving stage is limited to the coherence time of the optical transition. Hence little energy can be deposited at each frequency. We propose here another approach to engrave the dispersive filter. Now the two engraving chirps are co-temporal chirps (see Figure 1b). Therefore the duration of the engraving stage is no longer limited to the coherence time of the transition, yielding higher engraving efficiency. This approach has been experimented in a low bandwidth experiment in a Tm^{3+}:YAG crystal. Experimental results (Figure 2) demonstrate its validity. This new scheme will be presented and discussed.

[1]   V. Lavielle, I. Lorgeré, J.-L. Le Gouët, S. Tonda, D. Dolfi, Opt. Lett., **28** (*in press*)(2003).
[2]   Z. Cole, T. Böttger, R.K. Mohan, R. Reibel, W.R. Babbitt, R.L.Cone, K.D.Merkel, App. Phys. Lett., **81**, 3525 (2002)
[3]   L. Ménager, J.-L. Le Gouët, I. Lorgeré, Opt. Lett., **26**, 1397 (2001).

Chirped inversion of inhomogeneously broadened optically-dense Eu^{3+}:Y_2SiO_5

T. L. Harris[2], G. W. Burr[1], J. A. Hoffnagle[1], M. Tian[2], W. R. Babbitt[2], and C. M. Jefferson[1]

[1]IBM Almaden Research Center, 650 Harry Road, San Jose, California 95120-6099
[2]The Spectrum Lab, Montana State University, PO Box 173510, Bozeman, Montana 59717-3510
harris@spectrum.montana.edu; tel:406-994-7881; fax: 406-994-6767

Abstract: Novel pump-probe experiments provide practical, sensitive diagnostics of average population inversion created by linear frequency chirped optical pulses. Maxwell-Bloch simulations and Landau-Zener calculations support the experiments and provide a general prescription for inversion by chirps.

Optical coherent transients, used extensively for nonlinear optical spectroscopy, have been proposed and demonstrated as the basis of storage and processing of classical and quantum information. For these applications, it is often desirable to uniformly excite a superposition state comprised of an equal mixture of ground and excited states over a wide frequency interval within the inhomogeneously broadened absorption of a medium. In practice, a transform-limited $\pi/2$-pulse can only induce such a half-inversion over a narrow bandwidth. Linear frequency-chirped optical pulses (chirps) have been used[1] to circumvent this problem. Many storage and processing demonstrations have been conducted using chirps, but there is no consensus regarding the choice of the parameters of the chirp in order to achieve precisely the desired inversion, especially for optically-dense media.

We have developed a pump-probe technique that sensitively identifies a half-inversion, where "inversion" here is defined as the population inversion averaged over all atoms in the beam path and probe-pulse bandwidth. A dye laser, stabilized in both frequency (<1kHz) and amplitude (<1 % rms), excited the Eu^{3+}:Y_2SiO_5 Site 1 transition at 579.879 nm with optical density $\alpha L = 1.2$.[2] An acousto-optic modulator produced both the chirps and square-envelope π-pulses used to pump and subsequently probe the inversion in the media (Figure 1). The figure inset highlights how the shape of the transmitted probe pulse is modified by the media and can be used as a sensitive, experimentally accessible diagnostic of the degree of inversion. The desired half-inversion (averaged in space and frequency) was achieved by systematically varying the chirp power and was indicated when a linear fit to the transmitted probe pulse had zero slope.
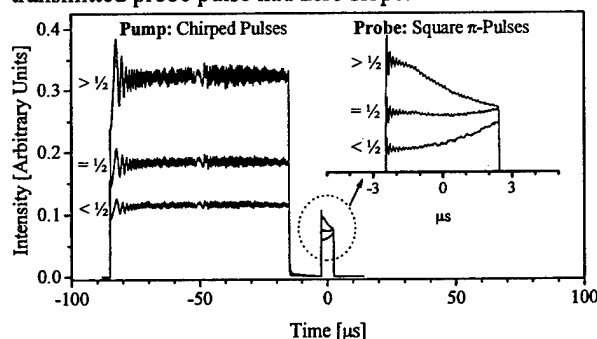

Fig.1. Examples of pump-probe experiments. The chirp that drives a half- inversion, and the subsequent probe pulse indicating that condition, are labeled "= ½". Chirps that create <½ and >½ inversions are labeled accordingly; the corresponding probe pulses show evidence of absorption and stimulated emission.
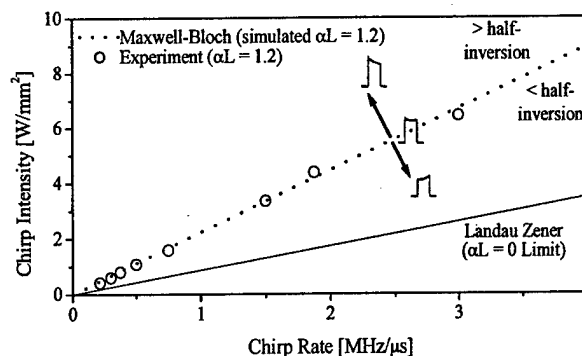

Fig.2. Circles indicate combinations of chirp intensity and chirp rate that created a half-inversion experimentally. The slope of the dotted line was computed from the Maxwell-Bloch simulation results. The solid line is the low optical-density limit predicted by Landau-Zener.

The relationship between the chirp power and the chirp rate needed for such a half-inversion was found to be linear (Figure 2) and the slope of that line was found to depend upon optical density. Both Landau-Zener theory[3] and extensive Maxwell-Bloch numerical simulation[4] confirmed the linear relationship between optical power and chirp rate for constant inversion. Landau-Zener sets a low optical density bound on the slope of that linear relationship and extends it to arbitrary inversion. Maxwell-Bloch simulations support the association of the transmitted probe pulse shape with medium inversion and extend the linear power-chirp rate relationship to high optical density.

References

1. Y. S. Bai, W. R. Babbitt, and T. W. Mossberg, *Opt. Lett.* **11**, 724-6 (1986).
2. R. W. Equall, Y. Sun, R. L. Cone, and R. M. Macfarlane, *Phys. Rev. Lett.* **72**(14) 2179-2181 (1994).
3. N. V. Vitanov and B. M. Garraway, *Phys. Rev. A.* **53**, 4288- 4304 (1996).
4. C. Sjaarda Cornish, W. R. Babbitt, and L. Tsang, *Opt. Lett.* **25**, 1276-8 (2000).

Photon echoes from accumulated single photon excitations

Nicklas Ohlsson, Mattias Nilsson and Stefan Kröll
Dept. of Physics, Lund Institute of Technology (LTH), Box 118, S-221 00 Lund, Sweden
phone: +46 (0)46 2229626, fax: +46 (0)46 2224250, e-mail: Stefan.Kroll@fysik.lth.se

If a single photon is split into two wave-packets using a beam splitter, and the two possible photon paths are made to overlap, an interference pattern due to interference between the two wave-packets can arise. If a classical detector, e.g. a photographic plate, is used for detecting the interference, the interference pattern will only be visible if the difference in optical path length between the two possible photon paths is less than the length of the photon wave-packet, i.e. the two wave-packets must overlap in both space and time. If however, instead of the normal detector, a material that can record and remember the phase of the electro-magnetic field is placed in the region where the overlap takes place, it has been proposed that interference can take place even if the path difference is much larger than the length of the photon wave-packet [1]. In this case, only the phase memory time of the material will limit the path difference still allowing interference to take place. As generally is the case in a photon echo experiments the interference of the photon wave-packets will be manifested as a frequency dependent modulation of the population of absorbing atoms within an inhomogeneously broadened optical transition in the material. Here the periodicity of this modulation is related to the time differences between the two possible photon paths. The frequency dependent modulation of the population is the time domain analogue of a spatial two-slit interference pattern. The detection of the interference is done using a photon echo process, where a strong light pulse interacting with the frequency dependent modulation of the population will give rise to the emission of a coherent light pulse after a time exactly matching the difference in arrival time between the two possible paths for the single photon wave-packet.

We have experimentally investigated a modified version of the delayed single-photon self-interference experiment described above using a sample of $Pr:Y_2SiO_5$ for detecting the interference pattern [2]. Instead of using a beam splitter and two spatially separated paths for the light to travel towards the material, we used acousto-optic modulators to create two light pulses and let the pulses travel along the same path towards the material. We used attenuated laser pulses, with energies down to less than 0.6 photons per pulse pair, and accumulated $7*10^9$ such pulse pairs before reading out the resulting frequency dependent modulation of the population in the material. We have also compared the signals for different average photon numbers in the pulse pairs to conclude that our observed signal is due to the pulse pairs containing a total of only one photon.

Our experiment is a three-pulse stimulated photon echo experiment, but with one photon divided into two of the pulses. In a photon echo process the interaction between the first two pulses and the material is normally considered to be a nonlinear multiphoton process, but in this experiment it is performed using only one photon. This addresses questions about the connections between quantum and nonlinear optics. How do we for instance interpret the phase matching and energy conservation diagrams when one photon is shared between two of the fields?

In the delayed single-photon self-interference experiment, the absorption of a single photon is divided into two events separated in time. The time separation between the two interactions is recreated at the read-out. The absorption of the single photon is also spread out over a large number of atoms in a material of macroscopic size, but without the normal loss of coherence. We therefore believe that the single-photon self-interference experiment is a new and exciting tool for studying microscopic and macroscopic quantum states.

[1]   A.R. Kessel and S.A. Moiseev, *JETP Lett.*, **58**, 80 (1993)
[2]   N. Ohlsson, M. Nilsson and S. Kröll, "Experimental investigation of delayed self-interference for single photons", Submitted to Phys. Rev. A (also at http://xxx.lanl.gov/abs/quant-ph/0301157).

Geometric Phase in Two-level Atomic Systems

Mingzhen Tian, Zeb W. Barber, Joe A. Fischer, Hongyan Li, and Wm. Randall Babbitt
(The Department of Physics, Montana State University, Bozeman, MT 59717, USA
phone: (406)994-6286, Fax: (406)994-4452, email: tian@physics.montana.edu)

A geometric phase is an intrinsic property associated with the evolution path of a quantum-mechanical system.[1] After a cyclic evolution the system's wave function acquires an extra phase factor other than the Hamiltonian dependent dynamic phase. This extra phase is a geometric property because it depends solely on the amount of the solid angle enclosed by the system's evolution path in the projected wave function vector space. It does not depend on the driving Hamiltonian, the initial and the final states, the time spent, nor even the specific path. For a two-level quantum system, such as a spin-half or an atomic system, the geometric phase is equal to the half of the solid angle enclosed by the movement of the Bloch vector on the Bloch sphere. Study of the geometric phase of two-level system is of interest to understanding of quantum theory and performing fault tolerant operations and logic gates for quantum computing. Often a geometric phase change causes only a global phase factor of a two-level system wave function, in this case this phase can only be observed through the coupling of the two level system to a third reference level.[2,3] However, a geometric phase can also introduced a phase change within the wave function as a relative phase between the components of a superposition state. Unlike the global phase, this phase change results can be observed in a closed two-level system.

In this paper, we report the observation of the optical control of the geometric phase in a closed two level atomic system. The two levels studied are the two electronic energy levels ($^3H_4$ and $^3H_6$) of Tm^{3+} doped in YAG crystal. The geometric phase change of the atomic wave function was induced and controlled by two laser pulses resonant to the $^3H_6$-$^3H_4$ transition and observed using photon echoes on the same trabsition. According to Bloch's theory and the property of the geometric phase, when an atom is excited successively by two pulses, both with pulse areas of π with a relative phase shift ϕ on the second pulse, the ground and the excited state components of the atomic wave function gain a relative phase of 2ϕ. In an inhomogeneously broadened atomic system, such as Tm^{3+}:YAG, photon echo can be generated by two coherent pulses. The first creates the coherence by exciting the atoms. After the atoms have dephased for a specified time (delay) a second pulse rephrases the coherence generating a macroscopic electric field (the echo pulse) at the same delay after the second pulse. The echo field carries the information about the atomic state composition. A phase shift is introduced to the wave function by a pair of phase-control pulses (two π pulses with relative phase of ϕ) between the two echo-generating pulses, the echo will carry an extra phase of 2ϕ, which can be measured by heterodyne detection. In our experiment, we observed the phase shift introduced by the phase-control pulses and tested the relation between the phase shifts between the two control pulses (ϕ) and the echo field (2ϕ) by varying ϕ from 0 to π in increments of 0.05π. The experimental results confirmed the theoretical prediction with a standard deviation of $0.03\ \pi$, which is mostly attributed to the resolution of the phase measurement limited by the frequency jitter of the laser source. The related dynamic phase and the effects of control pulse areas were also studied.

References:
[1]. "Geometric phase in Physics" ed. A. Shapere, and F. Wilczek, (World Sicientific, Singapore, 1989).
[2]. D. Suter, K. T. Mueller, and A. Pine, Phys. Rev. Lett. **60**, 1218 (1988).
[3]. M. Tian, R. R. Reibel, Z. W. Barber, J. A. Fischer, and Wm. R. Babbitt, Phys. Rev. A **67**, 011403(R) (2003).

Spectral Diffusion in Erbium-Doped Transient Spectral Hole Burning Materials

C. W. Thiel, T. Böttger, Y. Sun[*], and R. L. Cone

Physics Department, EPS 264, Montana State University, Bozeman, MT 59717

The general subject of spectral diffusion in rare earth doped materials is important from the perspective of basic science and practical device applications. We report detailed modeling of our extensive data on spectral diffusion in Er^{3+}:Y_2SiO_5 and related Er^{3+} oxide materials. Such modeling has been a valuable tool for assessing the capabilities of these materials, understanding the role of important variables, and demonstrating how material properties may be optimized for technological applications.

It is well known that spatial-spectral-holography can perform real-time, wide-bandwidth information storage and signal processing. Both for devices operating directly in the communication bands and for the realization of other devices exploiting communications component infrastructure, the $^4I_{15/2} \rightarrow {}^4I_{13/2}$ transition of Er^{3+} is the only known solution. Er^{3+} materials have been used successfully in our laboratory for both laser frequency stabilization[1] and high bandwidth optical correlators.[2]

Spectral diffusion has been measured using stimulated photon echo spectroscopy on Er^{3+}:Y_2SiO_5 and modeled as a function of magnetic field magnitude and direction, crystal temperature, and Er^{3+} dopant concentration. From Fig. 1, spectral diffusion is evident at low magnetic fields as a significant broadening of the effective linewidth as the waiting time between the second and third pulses in the echo sequence is increased. With the measurements and extensive modeling, spectral diffusion can be successfully controlled in devices by choosing appropriate operating conditions.

To describe the observed stimulated echo decays, the spectral diffusion model incorporates Er^{3+} spin flips into a generalized echo decay function that enables us to extract the time evolution of the effective linewidth and to significantly extend our previous data analysis.[3] In addition to describing the observed echo decays, the model gives insight into the microscopic dynamics of these materials through

Figure 1: Evolution of the effective linewidth in 0.02 at. % Er^{3+}:Y_2SiO_5 at 1.6 K as the waiting time T_W is varied in a stimulated photon echo experiment. The magnetic field varies from B = 0.8 T to B = 3 T. Solid lines are least-squares fits using the model.

model parameters describing the saturated effective linewidth for long waiting times and the rate of perturbations causing the spectral diffusion. These parameters were modeled as a function of magnetic field by considering the magnitude of the dipole-dipole interactions between Er^{3+} ions and the one-phonon (direct) absorption and emission process as the physical mechanism driving the spin flips. Excellent agreement with the experimental data was obtained. The model describes spectral diffusion over a wide range of operating conditions including higher temperature, allows broad predictions, leads to material optimization for applications, and improves fundamental understanding of Er^{3+} materials as well as the Nd^{3+} and Yb^{3+} materials that we have studied more recently.
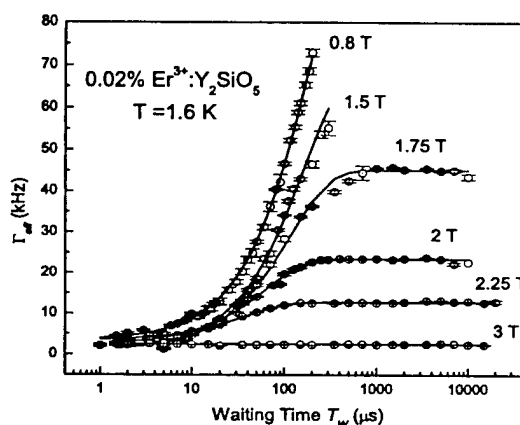
1. T. Böttger, G. J. Pryde, N. M. Strickland, P. B. Sellin, and R. L. Cone, Optics in 2001, Optics & Photonics News 12, no.12, 23 (2001).
2. Z. Cole, T. Böttger, R. Krishna Mohan, R. Reibel, W. R. Babbitt, R. L. Cone, and K. D. Merkel, Applied Physics Letters 81, 3525 (2002).
3. T. Böttger, Y. Sun, G. J. Pryde, G. Reinemer, and R. L. Cone, J. Lumin. 94-95, 565 (2001).

[*]Corresponding Author. Tel.: +1-406-994-6163; fax: +1-406-994-4452.
E-mail address: sun@physics.montana.edu (Y. Sun)

OPTICAL HIGH-RESOLUTION SPECTROSCOPY OF BIOLOGICAL SYSTEM: SOME EXAMPLES OF WHAT CAN BE LEARNT

Silvia Völker

Huygens and Gorlaeus Laboratories, University of Leiden,Leiden, The Netherlands

At ambient temperature, optical spectra of chromophore-protein complexes are rather featureless because of inhomogeneous broadening and thermal fluctuations. At low temperature, hole-burning, single-molecule detection and fluorescence line-narrowing allow an increase of spectral resolution by a factor of 10^4-10^6 compared to that at ambient temperature. These techniques, thereby, enable us to retrieve two types of information that normally remain hidden underneath the broad absorption bands:

a) *A fingerprint of the species* provided by the origin of the spectrum (0-0 transition) and its vibronic structure. An example is provided by the mysteries that surrounded the photochemistry of green fluorescence protein (GFP) and several of its mutants. We have proven that each of the proteins can exist in at least three conformations which are associated with the protonation state of the chromophore and established the photochemical pathways of their interconversions [1]. Our results disprove the idea that some of the GFP mutants might be "one colour emitters" [2]. Based on our energy-level diagrams, we also proposed an explanation for the 'on-off' and 'blinking' behaviour [3] reported in the literature for single GFP-molecules at room temperature. In addition to reversible optical switching observed in GFP, red fluorescent protein (DsRed) [4] shows intra-molecular energy transfer [5] that originates from its tetrameric structure [6].

b) *Quantitative determination of the rates of dynamic processes.* The homogeneous linewidth determined from the width of narrow holes reflects the dephasing of the electronic transition and from this one obtains information on dynamic processes such as the thermal fluctuations of the chromophore in interaction with its surrounding protein and the transfer and trapping of the excitation energy within a system. In DsRed, for instance, we have found narrow (MHz-resolution) holes and determined, for the first time in an autofluorescent protein, the homogeneous linewidth and its temperature dependence [7]. Moreover, rates of energy transfer and their spectral distributions have been obtained from hole widths and hole depths for light-harvesting complexes of photosynthetic purple bacteria and the photosystem II reaction center of green plants. Owing to the frequency-selective nature of hole-burning, questions can be answered that can not be solved by ultrafast (fs or ps) techniques like pump-probe or photon-echoes, because of the inherently large optical bandwidth of short laser pulses. With time-resolved hole-burning, furthermore, we can probe structural changes occurring within a time-span from 10^{-6} to 10^5 seconds.

[1] T.M.H. Creemers et al., *Nature Structural Biology* 6 (1999) 557-560.
[2] T.M.H. Creemers et al., *Proc.Natl.Acad.Sci.USA* 97 (2000) 2974-2978.
[3] T.M.H. Creemers et al., Chemical Physics 275 (2002) 109-121.
[4] M.V. Matz et al., *Nature Biotechnology* 17 (1999) 969-973.
[5] S. Bonsma et al., to be published.
[6] L.A. Gross et al., *PNAS* 97 (2000)11990-11995; M.A. Wall et al., Nat.Struct.Biol. 7 (2000) 1133-1138.
[7] F. Könz et al., to be published.

Spectral Holeburning Studies of the Isolated Reaction Center of Photosystem II of Green Plants.

R. Jankowiak, V. Zazubovich, K. Riley, M. Rätsep[+] and G. J. Small
Ames Laboratory, USDOE and Department of Chemistry, Iowa State University, Ames, Iowa, 50011;
[+] Institute of Physics, University of Tartu, 142 Riia str. 51014 Tartu, Estonia.
Phone: (515)-294-43-94; Fax: (515)-294-16-99; E-mail: jankowiak@ameslab.gov

Summary:

Reaction centers of Photosystem II containing 5 Chl a per 2 Pheo a (PS II RC5) were investigated by means of hole burning spectroscopy, combined with electric field and high hydrostatic pressure. Even though PS II RC is a fairly simple system, analysis of its Q_y absorption spectrum is complicated due to the overlap of several bands. Thus, several important issues remain unsettled. One example is the rate of the primary charge separation. Another is the nature of the so-called trap states at ~684 nm, first observed in [1,2].

Due to comparable electrostatic couplings between core cofactors, the RC core should be treated as a multimer. Calculations show that the lowest exciton state of that multimer is localized primarily on P_1 and P_2 (analog of the special pair of the bacterial reaction center), but has significant contributions from other core pigments. Simulations of triplet-bottleneck hole spectra and results of photon echo experiments [3] indicate that the triplet associated with the recombination of charge-separated state is localized on Chl_1.
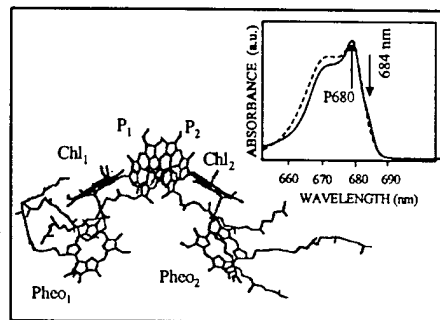
Concerning the trap states, we argue that they are not due to monomeric chlorophyll. We also argue that the absorption maximum near 680 nm is not a vibronic replica of the 684 nm shoulder. The properties of the 680 and 684 nm bands are quite similar. Consequently, the RC samples most likely contain two different subpopulations, the P680-type (dominant) and the P684-type, with their lowest exciton bands peaked near 680 and 684 nm, respectively. The P684-type RCs exhibit somewhat stronger P_1–P_2 coupling and smaller degree of disorder. We interpret the trap states as the lowest states of a fraction of P680- and P684-type RCs whose charge separation is inhibited.

We also demonstrate that a large amount of spectral hole burning data on PS II RC obtained so far can be reinterpreted with the same model used to explain the results of photon echo experiments [3]. According to that model, comparable couplings between pigments in RC core and (diagonal) energy disorder result in large variations of primary charge separation rates from RC to RC. These variations are manifested in hole-burning as variations in homogeneous line widths and hole burning efficiency. Results of simulations of persistent and triplet-bottleneck holes are presented. An important consequence of invoking the distribution of charge separation rates is that electron-phonon coupling for P680 (and P684) is smaller than it was previously believed.

References:
1: Groot, et al, *J. Phys. Chem.* **1996**, 100, 11488
2: den Hartog, et al. *J. Phys. Chem. B* **1998**, 102, 9174.
3: Prokhorenko and Holzwarth, *J. Phys. Chem.* B **2000**, 104, 11563.

HOLE BURNING SPECTROSCOPY OF BIOMOLECULES IN EXTERNAL FIELDS

Josef Friedrich
Physik-Department E14 und Lehrstuhl für Physik Weihenstephan, TU-München,
Freising, Germany

The high sensitivity of spectral holes to weak external perturbations, such as electric fields or pressure, makes them attractive sensors for probing chromophore-solvent interactions. This is especially interesting for biological molecules because they are characterized by a rich scenario of interactions which can easily be modified by changing, for instance, the pH or by inducing photochemical changes in the chromophore.

We have been using Stark-spectroscopy as well as pressure tuning hole burning spectroscopy to shed light on the chromophore-solvent interactions in a series of well characterized dye-labeled DNA-strands, in chromoproteins and aromatic amino acids. With Stark-spectroscopy internal protein fields, charge redistribution processes (e.g. as a function of pH) as well as molecular symmetries can be probed. An attractive feature of high resolution frequency selective techniques is the possibility to tune the chromophore-solvent interaction and to investigate so-called color effects in the inhomogeneous spectra. Some of these aspects are also accessible to computer modeling. With pressure tuning spectroscopy it seems possible to probe effective interaction volumes and to measure the compressibility of globular proteins. The compressibility of proteins is a very interesting quantitiy: It determines the volume fluctuation, hence, is a measure of the flexibility of the protein molecule which is important for functioning. It may strongly depend on small structural changes. Also the compressibility is accessible to computer modeling.

Most hole burning experiments on proteins are confined to chromoproteins. Recently we succeded to use aromatic amino acids to probe the protein *bovine pancreatic trypsin inhibitor* with Stark-and pressure tuning spectroscopy. This could open a much wider class of proteins to hole burning spectroscopy.

I will present results on heme proteins, on dye-labeled DNA-strands as well as on UV-hole burning with aromatic amino acids as probes.

Rare Earth Quantum Computing

M. Sellars, J.J. Longdell, E.L. Fraval and N.B. Manson
Laser Physics Center, Research School of Physical Science and Engineering
Australian National University, Canberra, ACT, 0200, Australia.

Rare-earth ions doped into inorganic crystals are promising candidates for demonstrating quantum computing operations [1,2,3]. The properties that make rare-earth ion doped crystals amenable for quantum computing demonstrations include:

- Optical transitions with long coherence times, up to 2.6 ms, have been observed [4].

- Long coherence times in their ground state nuclear spin transitions, up to 82 ms, have been observed.

- Strong coupling between the electronic states and nuclear spin states enables the optical manipulation and readout of the spin states [5,7]

- Large inhomogeneous broadening in the optical transitions. This is typically GHz and enables many homogeneous broadened ensembles or even single ions to be addressed individually [4]

- Strong electric dipole-dipole interactions (as large as GHz) enabling coupling between the ions [7].

In the quantum computing scheme being developed at the Australian National University each qubit is a packet of ions chosen from the inhomogeneous line based on their optical frequency, all ions that are not part of this packet but have similar resonant frequencies are optically pumped to an auxiliary hyperfine level. Ensembles of this type were first realized and their usefulness to quantum computing recognised in 2000 by Pryde et. al [1]. A clear demonstration that such systems perform well as qubits is given in [8]

I will report on recent advances made at the ANU. Highlights of this work include, full quantum state tomography of single qubit operations, development of a method to extend the hyperfine coherence time by two orders of magnitude and significant advances in the demonstration of two qubit operations.

[1] G.J. Pryde, M. J.Sellars and N.B. Manson, Phys. Rev. Lett. 84, 1152 (2000).

[2] K. Ichimura, Optics Comm. 196, 119 (2001).

[3] N. Ohlsson, R.K. Mohan and S Kroll, Optics Comm. 201, 71 (2002).

[4] R.W. Equall, Y. Sun, R.L. Cone and R.M. Macfarlane, Phys. Rev. Lett. 72, 2179 (1997).

[5] J. Mlynek, N.C. Wong, R.G. DeVoe, E.S. Kintzer and R.G. Brewer, Phys. Rev. Lett. 50, 993 (1983).

[6] L.E. Erickson, Opt. Comm. 21, 147 (1977).

[7] J.J. Longdell, and M.J. Sellars, (2002), quant-ph/0208182.

Correspondence:
Email: Matthew.Sellars@anu.edu.au
Ph: 61 2 61254571
Fax: 61 2 61250029

Preparing rare-earth-ion-doped crystals for quantum gate operations

Mattias Nilsson, Nicklas Ohlsson, Lars Rippe, Ingela Roos and Stefan Kröll
Dept. of Physics, Lund Institute of Technology (LTH), Box 118, S-221 00 Lund, Sweden
Klaus Mølmer
QUANTOP, Danish Research Foundation Center for Quantum Optics,
Department of Physics and Astronomy, University of Aarhus, DK-8000 Århus C, Denmark

A scheme for extracting quantum computer hardware from randomly located ions doped into a solid-state material has been presented [1]. In this scheme ensembles of rare-earth ions (e.g. Er^{3+}, Eu^{3+} or Tm^{3+}) in inorganic crystals (e.g. YAG, Y_2SiO_5 or $YAlO_3$) are used as qubits. Interaction between qubits is accomplished using the change in permanent dipole moment that is induced at the optical excitation of the ions. Initial experiments have demonstrated the two most important aspects of the scheme: The isolation of a single qubit in a pure state and the ion-ion interaction that will be used to entangle qubits [2].

When cooled to liquid helium temperatures, a rare-earth ion in an inorganic crystal can have a very narrow homogeneous absorption line (<1 kHz), corresponding to a long dephasing time, while the absorption frequencies of different ions can differ by many GHz, due to slightly different surroundings in the host. The inhomogeneously broadened optical transitions of the ions are utilised for creating qubits, consisting of sub-sets of ions, which are addressable because of their different absorption frequencies. Two of the long-lived hyperfine levels of the ion ground state are used as qubit states and optical pumping can be used for moving ions between these levels in the qubit preparation stage. Resonant Raman transitions via the excited state can be used to perform qubit operations. We have shown experimentally that it is possible to isolate ions in a selected frequency channel and (almost) all ions residing at a specific frequency have been pumped into one of the hyperfine levels and thereby one qubit has been prepared in a (nearly) pure state.

Quantum computing requires controlled interactions between different qubits. In the present scheme, this interaction is mediated by the change in permanent dipole moment experienced by the rare-earth ions when they are optically excited from the ground state to an excited state. The change in dipole moment changes the electric field experienced by ions situated close to the excited ion, thus their absorption frequencies are changed. The important aspect, in order to use this frequency shift for controlled logic, is that the shift is sufficiently large that ions, originally resonant with a certain laser frequency, are shifted out of resonance with this laser field. Excitation induced frequency shifts have been experimentally observed and compared with the theoretical calculations indicating that a sufficiently large fraction of ions indeed do experience the shift required. This opens the way for the realisation of the first quantum gate in this type of solid state materials.

In this scheme each qubit consists of an ensemble of rare-earth-ions which ideally should respond identically to the laser pulses for the gate operations. In practice the ions have slightly different transition frequencies and they may have different transition oscillator strengths for a given light polarisation due to their orientation in the crystal and their Rabi frequencies may be different due to intensity variations across the laser beam profile. To carry out reliable quantum gate operations it is necessary to compensate for the fact that the ions not are identical. It is theoretically shown that by appropriately tailoring excitation pulses and excitation pulse sequences excellent quantum gate fidelities can be obtained also when the ions have slightly different properties [3]. The quantum computing scheme and the experimental and theoretical results will be discussed in this contribution.

[1] N. Ohlsson, R. Krishna Mohan and S. Kröll, "*Quantum computer hardware based on rare-earth-ion-doped inorganic crystals*", Opt. Commun. **201**, 71-77 (2002)

[2] M. Nilsson, L. Rippe, N. Ohlsson, T. Christiansson and S. Kröll, "*Initial experiments concerning quantum information processing in rare-earth-ion doped crystals*", Physica Scripta **T102**, 178-185 (2002)

[3] "*Theoretical investigation of the quantum gate fidelity in the rare-earth-ion quantum computing scheme*", I. Roos, Diploma paper, Lund Reports on Atomic Physics, **LRAP-298**, LTH, Lund (2003).

Using Quantum Coherence to Detect Anthrax

Marlan Scully

Texas A&M University

No Abstract Available

PURELY ELECTRONIC ZERO-PHONON LINE
AS THE CORNERSTONE OF SPECTRAL HOLE BURNING (PSHB) AND
SINGLE IMPURITY MOLECULE SPECTROSCOPY (SMS).
PROSPECTS AND BOTTLENECKS FOR APPLICATIONS

Jaak Kikas[1,2] and Karl K. Rebane[1*]

[1] Institute of Physics, University of Tartu, Riia 142, Tartu 51014, Estonia

[2] Department of Physics, University of Tartu, Tähe 4, Tartu 51010, Estonia

Purely electronic zero phonon line (ZPL) is a remarkable and useful feature in low-temperature spectra of quite a broad glass of impurity-doped solids (crystals, glasses, complex biological and other systems). Based on ZPLs methods of high- and ultra-high spectroscopy of solids have essentially contributed to our understanding of structure and microdynamics in solids of different degree of disorder. They still seem to keep a good potential to provide fine novel utilization in physics,chemistry,biology,engineering.

Historically a number of applications based on ZPLs have been born in science and brought to practical proposals of their technological design (see [1] and references therein). The most instructive educationally and spectacular on their own have been space-and-time-domain holography (STDH, see [2] and references therein) and space-and-frequency-domain holography (see [3] and references therein) realized for optical data storage and parallel ulrofast processing. An exceptional and remarkable feature of these and other applications of ZPL is that practically everything proposed theoretically has been realized experimentally *in laboratory environment* , the main condition being liquid He temperatures. Would there be found systems exhibiting good ZPLs at room temperatures, a great field of commercial applications would be opened. Several other fields for which the properties of ZPL form a crucial bottleneck are considered and the possibilities to overcome the respective limitations are discussed, e.g., prospects to increase the oscillatory strength of strongly forbidden transitions in rare-earth ions. Quantum computing (QC) - a "hot" area of research and development – may be a particular field, which essentially gains from the concept of ZPL. A recent proposal to increase the number of qubits available for processing by a factor of up to 1000 utilizing the frequency dimension through PSHB is discussed (4). Some promises of QC have been, in fact, already realized in STDH – we draw this comparison further and point to some of its new aspects [5].

* Phone: +372 7428159, fax: +372 7383033, e-mail: rebanek@fi.tartu.ee

[1] K. K. Rebane, J. Lumin. **100** (2002) 219.

[2] K.K. Rebane, A. Rebane, in: G. Mahler, V. May, M. Schreiber (Eds.), Molecular Electronics, Properties, Dynamics and Applications, Marcel Dekker, New York, 1996, p. 257 (Chapter 13).

[3] C. De Caro, S. Bernet, A. Renn, U.P. Wild, *ibid*, p. 303 (Chapter 14).

[4] M.S.Shahriah,P.M.Hemmer,S.Lloyd,P.S.Bhatia,and A.E.Craig,Phys.Rev.A,66,(2002) 032301

[5] K. K. Rebane, Opt. Spectrosc. (St. Petersburg) **91** (2001) 472.

Power Budget Analysis of Image-Plane Storage in Spectral Hole-Burning Materials

M. A. Neifeld[1], W. R. Babbitt[2], R. Krishna Mohan[2], and A. E. Craig[3]
[1]Dept. of Elect. and Comp. Eng., Optical Sciences Center, Univ. of Arizona, Tucson, AZ 85821
[2]Spectrum Lab and [3]Physics Department, Montana State University, Bozeman, MT 59717
Phone: 520-621-6102, Fax: 520-621-8076, Email: mark@ece.arizona.edu

High performance parallel computing architectures place extreme demands on the storage sub-systems near the bottom of the memory hierarchy. These demands include ultra-high capacity (petabytes and higher), low-to-moderate latency (microseconds), and high data rates (tens of gigabytes per second). The Digital Photonics Group at Montana State University has been leading an effort to utilize spectral holeburning (SHB) optical memory to meet the storage demands of next generation supercomputers. Unlike photorefractive materials in which multiplexed pages share atoms, each data page in a frequency-multiplexed SHB memory utilizes a distinct set of atoms. The SHB system therefore offers readout efficiency/fidelity that is nearly independent of the number of stored pages. In this paper, we perform a power budget analysis of page-oriented SHB memory.

We consider a page-oriented memory in which a two-dimensional (2D) spatial light modulator (SLM) is imaged into the SHB storage material. The wavelength of the illumination is used to define the memory address. The recording process results in a spatially varying material absorption that mimics the data pattern on the SLM and the readout process uses uniform illumination to detect this absorption signal as a spatially varying transmittance function. A 2D detector array is used to sense the retrieved the data. The material thickness is restricted to be less than the depth of focus of the imaging optics so that spatial cross-talk can be ignored. The collinear architecture examined here eliminates the need for holographic stability and/or complex angled-beam geometries.

The supercomputer's random access memory is assumed to comprise 100,000 modules, each with a capacity of 10 GBytes, a latency of 10 μsec, and a burst data rate of 10 GBytes/sec (80 Gbps). This data rate can be met with pages consisting of 1000 x 1000 pixels and read out with the required 10 μsec latency. An 80 Gbit module requires 80,000 such spectrally addressed pages and thus a SHB material with 80,000 distinct spectral channels. The width of the spectral channels must be at least 100 KHz for 10 μsec read out. This requires homogeneous linewidth slightly less than 100 kHz and inhomogeneous linewidth greater than 8 GHz. These constraints are both easily achieved using inorganic crystals doped with ions such as Eu or Pr (if hyperfine interactions are ignored). Our analysis assumes that the holes are coherently written and read out with a narrow band (<100 KHz) laser. The ratio of the read to write power (γ), is fixed and sets a limit on the number of readouts (roughly $1/\gamma$). The readout is assumed to be shot-noise-limited and we seek to minimize the required writing power. Our optimization proceeds by fixing the SLM pixel size and finding both the crystal length and the hole depth that minimizes the required writing laser power to achieve a readout signal-to-noise-ratio (SNR) of 10. The analysis includes the non-linearities associated with coherent writing, hole saturation, and optically thick media.

The figure shows the required write power to achieve SNR=10 as a function of pixel radius for several values of γ in 1% Eu:YSO. Also plotted is the maximum laser power, defined as the power to achieve a 50% hole depth. The assumed materials parameters are an absorption coefficient of 400/m, a Rabi frequency of 1,350 (rad/sec) per $(W/m^2)^{1/2}$, a quantum yield of 25% (estimates range from 6% to 66%), an index of 1.8, and a wavelength of 580 nm. One significant finding is that a range of viable operating points exists with pixel radii below 10 μm (a roughly 2 cm x 2 cm page). For γ=1 (read once memory), the minimum required write power occurs at a radius of 3 μm and requires a write power of 200 nW (only 200 mW per page) and a material thickness of 180 μm (αL=0.07), well within practical limits. Note that minimum power occurs at maximum storage density for this system. Other materials systems were analyzed including organic systems, as well as the effects of incoherent writing and incoherent erasure and these will be presented.
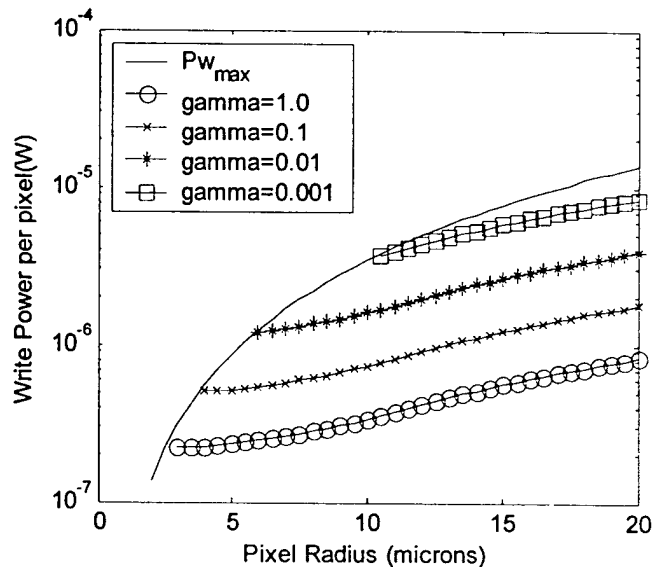
Atomic Tailoring of Rare Earth Transitions in Wideband Gap Semiconductors for Ultra-Dense Spectral Storage*

Zameer Hasan[#]

Physics Department, Temple University, Philadelphia. PA 19122.

Summary

Rare Earth doped Wide Bandgap Semiconductors are uniquely suited for some fascinating photonics applications especially where two visible or IR photons are involved. Here we present a detailed study of such a case.

Spectral storage provides ultra-high density memories approaching several terabits per square inch. The information is stored in the absorption spectrum of an optical center in a solid, for example, a rare earth impurity in a wide bandgap semiconductor. The realization of such high-density atomic scale storage is a very challenging task. The optical transition of the rare earth impurity, where the memory is stored, should meet strict requirements to facilitate efficient storage and read-out. Also, depending on the method of storage, the energy levels of the rare earth impurity should be aptly tailored with respect to the electronic bands of the host.

A detailed study of the rare earth 4f-5d transitions in wide bandgap sulfides has been performed. By appropriate tailoring of rare earth impurity and host energy levels, a new and unique process of storage was demonstrated, the Power-Gated Spectral Hole-Burning (PGSHB). PGSHB results from a resonant two-photon ionization of rare earth impurities. The requirement of two-photon-ionization restricts the band gap of the host to 3-5 eV, therefore making the wide bandgap II-VI sulfides the perfect host.

We have demonstrated that 4f-5d transitions of rare earths are ideally suited for hole-burning based storage. These transitions are strongly electric dipole allowed as opposed to f-f (rare earths) or d-d (transition metal) transitions that are extremely weakly allowed in solids. The fact that d-electrons are more susceptible to the host crystal field has been used to tune the 4f-5d transition energies in the red region of the spectrum, which is conveniently accessible by using the tunable dye lasers. Further tailoring of 4f-5d transitions down to 1.5 micron, the communication wavelength, is under serious investigation.

By atomic scale manipulation of rare earths and some other impurities in the host such as oxygen halogens and alkali metals, a variety of optical centers have been created in sulfides. Site symmetry of these centers has been tailored to enhance the radiative transition probabilities (for high photo-luminescence efficiencies) and to reduce the electron-phonon coupling in order to minimize the loss of optical energy to the phonon bath. The best demonstration of ultra-dense spectral storage was possible in multi-layer thin film structures of sulfides. In these structures each layer consisted of a unique rare earth associated center and the information was stored in spectrum of these centers.

This talk will review atomic tailoring of rare earth and rare earth-other impurity associated centers in alkaline earth sulfides. It will describe the ways to manipulate their energy levels and transition strengths. It will focus on new techniques developed by us for fabricating these materials in the form of multi-layer thin films and nano-structures. A detailed account of applications such as ultra-dense optical storage, memories for scalable quantum computers, and potential materials for optical manipulation of nuclear states will be presented.

Optical Coherent Transient High Bandwidth Arbitrary Waveform Generation and Pulse Shaping

Zeb W. Barber, Jesse Law, Mingzhen Tian, and W.R. Babbitt

Montana State University-Physics Dept. Rm. 264 EPS Bldg. Bozeman, MT 59717

Ph: (406) 994-7988 Fax: (406) 994-4452 Email: zwb@montana.edu

Applications for optical pulse shaping and arbitrary waveform generation (AWG) range from coherent chemistry to optical time-domain multiplexing and radar processing applications. Previous methods in the pico to femtosecond regime have utilized gratings and spatial light modulators to filter the Fourier spectrum of the pulse.[1] These methods have spectral resolutions of > 10 GHz limiting their coherence time and usefulness in the MHz to multi-gigahertz regime. In this presentation, we discuss a new method for performing pulse shaping and AWG that utilizes spectral holeburning materials. Utilizing fast broadband chirps from specialized chirp lasers and low bandwidth frequency shifting acousto-optic modulators, we can program complex spectral gratings to shape the echo output of a high bandwidth probe pulse. The programming method shown below [2] schematically extends the temporally overlapped frequency offset chirped (TOLFC) programming method by using multiple programming chirps and or different chirp rates. Using different chirp rates determined by $\frac{1}{\alpha_3} = \frac{1}{\alpha_1} - \frac{1}{\alpha_2}$ where 1,2,3 are the reference, control, and probe chirps respectively, the probe chirp can be compressed to a brief pulse with a specific delay given by the start frequency offset between the programming chirps. By controlling the amplitude and phase of the corresponding frequency offset chirps the echo output can be used to synthesize complex waveforms. Low bandwidth proof-of-concept and some high bandwidth demonstration results in Tm^{3+}:YAG are presented.
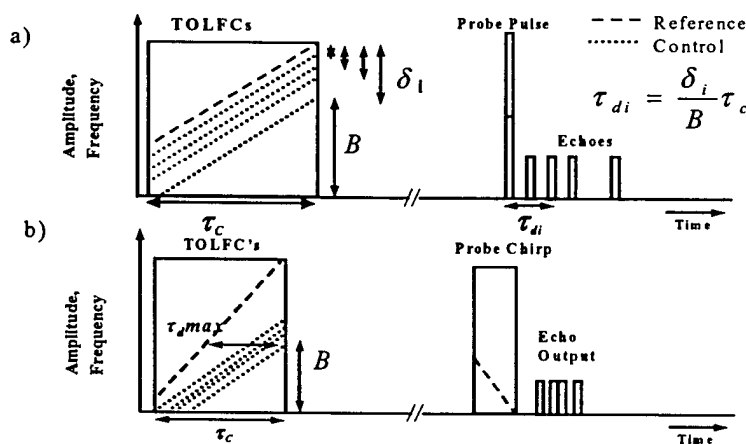

Fig. Schematic of a) pulse shaping and b) AWG utilizing chirps. In both cases each control chirp corresponds to a certain echo with delay determined by the frequency offset with respect to the reference chirp. In case a) the echoes are delayed copies of the probe. In case b) the larger chirp rate of the reference compared to the control chirps causes a chirped time delay grating allowing a properly chosen chirped probe pulse to be compressed.

References:
1. A.M. Weiner, Prog. Quant. Electr. **19**, 161 (1995).
2. Z.W. Barber, R. Reibel, M. Tian, W.R. Babbitt. "Optical Pulse Shaping Using Optical Coherent Transients." Optics Express. Vol. **10** No. 20

Demonstration of a Continuous Scanner and Time-Integrating Correlator using Spatial-Spectral Holography

Friso Schlottau and Kelvin H. Wagner

Optoelectronic Computing Systems Center
Dept. of Electrical and Computer Engineering, Campus Box 425
University of Colorado, Boulder, CO 80309-0425, friso.schlottau@colorado.edu

Spatial-spectral holography (SSH) has the potential for massive signal processing capabilities due to the high spatial and spectral resolutions that these materials offer at cryogenic temperatures. Some of the systems which are designed to take advantage of this processing capability include three dimensional space-time correlators[1] and broadband array imagers.[2] As a stepping stone towards implementing high bandwidth, optically coherent processors - such as ambiguity function generators - we present here the first experimental results of a Tm:YAG based, SSH time-integrating correlator (TIC).

The initial experiments were based on a modified version of an acousto-optic heterodyne TIC. The scrolling time-delay functionality of a Bragg cell is recorded into the SSH by injecting the same 50 μS chirp spanning 30MHz of bandwidth into an acousto optic modulator (AOM) and a slow-shear wave acousto optic deflector (AOD), and imaging both into the SSH (see Fig. 1). During this programming phase, the chopper (located after the cryo) is closed, preventing light from the AOD from reaching the 1-D CCD. When the chopper opens, the waveform $s(t)$ that is to be correlated (generated by the programming AOM) illuminates the SSH, resulting in a spatio-temporally scanned diffraction $s(t - \frac{x}{v})$ in the same direction and with the same velocity, v, as the acoustic wave in the AOD had at the time of programming. Around the time of the diffraction, the correlation reference signal $r(t)$ is generated in a second (TIC reference) AOM, and is interfered with the echoed, scanned output and accumulated on the 1-D CCD, yielding an intensity distribution $I(x) = \int_0^T r^*(t)s(t - \frac{x}{v})dt + c.c. + bias$. A correlation peak is thus generated on the CCD, where it can be integrated for a time, T, up to the lifetime of the SSH. Therein lies the key difference to previous spectrally-integrating SSH correlators that produce time-domain outputs,[3] because the correlation length in this experiment is not limited by the coherence time of the material, but rather only by the lifetime of the grating (see Fig. 2), which can even be extended further through continuous refreshing of the spatio-temporal scanner SSH. By using a wideband chirped laser and a synchronized Doppler matched scanner[4] the BW of this TIC could approach 20 GHz. Reading out the resulting SSH grating in multiple, Bragg-degenerate planes, one could envision a multichannel time-integrating correlator with a bandwidth spanning tens of GHz.
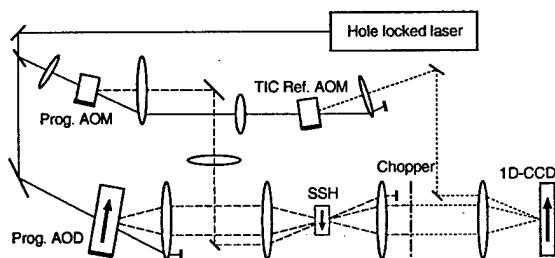

Figure 1: Setup for SSH-TIC: Programming AOM and AOD record Bragg cell function into SSH (chopper closed), which is then read out with Prog. AOM while chopper is open. The diffracted echo then interferes with signal from TIC ref. AOM and gives correlation peak on 1D-CCD.
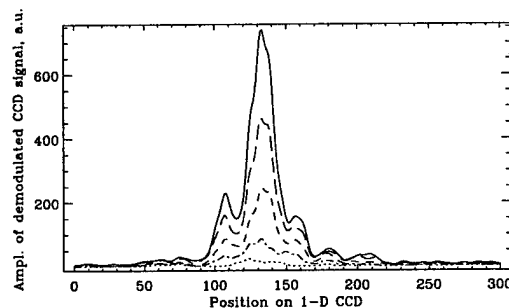

Figure 2: Correlation peaks for different length correlation waveforms, ranging from 50 to 250 μS in 50 μS intervals, showing correlation times greater than T_2.

References

[1] W. R. Babbitt, "Multidimensional signal processing with spatio-spectral holography," *SPIE*, vol. 3802, pp. 164–172, 1999.

[2] K. H. Wagner, F. Schlottau, and J. Bregman, "Array imaging using spatial-spectral holography," in *IOG*, (Mannheim), 2002.

[3] Y. S. Bai, W. R. Babbitt, N. W. Carlson, and T. W. Mossberg, "Real-time optical waveform convolver cross correlator," *Applied Physics Letters*, vol. 45, pp. 714–716, 1984.

[4] I. Lorgere, L. Menager, V. Lavielle, J. L. Legouet, D. Dolfi, S. Tonda, and J. P. Huignard, "Demonstration of a radio-frequency spectrum analyzer based on spectral hole burning," *Journal of Modern Optics*, vol. 49, pp. 2459–2475, 2002.

Surface and Resonance Enhanced Microraman Spectra:
From Single Molecule to Excited States

E. Thiel, T. Vosgroene, H. Kneppe, I. Gregor, R. Brnemann and A. J. Meixner
University of Siegen, Physical and Theoretical Chemistry Laboratory, Adolf-Reichweinstr, 57068 Siegen,
Germany, Phone +0175 74 55 129, Fax +49(0)271 740 2883, e.thiel@zess.uni-siegen.de

As known for decades Raman scattering is a very useful indicator for analysing the chemical structure of substances. The distribution of Raman lines can also be used in order to get information about the condition of certain chemical bounds. Moreover the interaction between molecules and its environment influences the Raman scattering of the molecule. Thus Raman spectra can even be used to investigate intermolecular interaction. However the cross section of Raman scattering is very low. Therefore the measurement of Raman spectra is difficult especially when the probes emit also fluorescence light. The cross section of Raman scattering can be increased by orders of magnitudes by using resonance or surface enhancement. By using this effects until today many research groups could show that it is possible to measure Raman spectra even of single fluorescing molecules.

By using of a confocal microscope with a feedback controlled scanning stage followed by a cooled CCD-spectrograph[1] we have recorded spatially resolved emission of isolated adsorbed rhodamine 6G molecules. As shown in the figure the dye molecules are clearly located. However from this result it can not be distinguished between fluorescence and Raman light. The ability of our CCD-spectrograph was high enough to register high resolution emission spectra of individual dye molecules. A typical spectrum is also shown in the figure. From the narrow spectral distribution of the detected lines one can conclude the origin of the emission is Raman scattering. The individual character of the adsorbed dye molecule can also be investigated by the inspection of the measured space resolved spectra. The individuality is revealed by a wavelength, intensity and background variation. Nevertheless the most Raman bands has been allocated clearly.
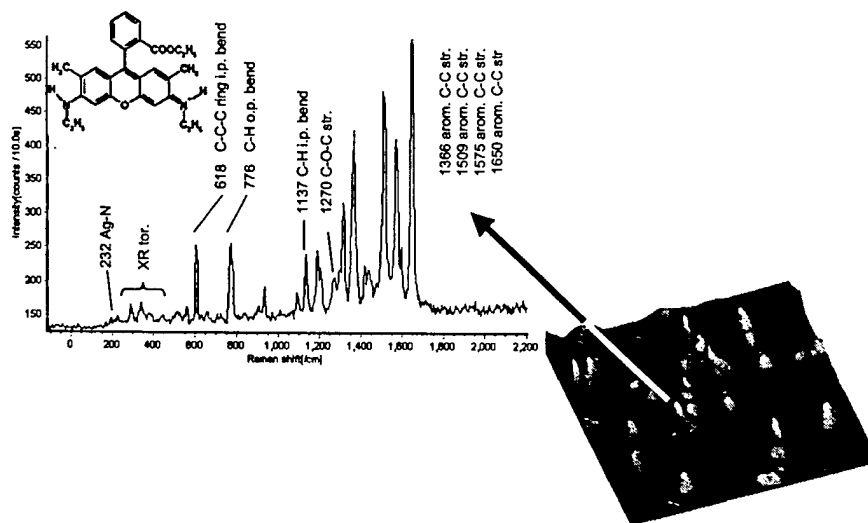
From this experiment we are able to observe the condition of the chemical bounds of each molecule in its electronically ground state. By using of a time resolved confocal microscope we are also able to detect Raman spectra of electronically excited dye molecules[2]. It is clearly shown that lines which are caused by scattering on chemical groups close to the chromophor are shifted to lower energies. This is explained by the expected loosening of the chemical bound in excited state. In contrast the frequency of scattering on peripheral groups is not influenced by the electronically state.

1. A. J. Meixner, T. Vosgröne, M. Sackrow, „Nanoscale surface-enhanced Raman scattering spectroscopy of single molecules on isolated silver clusters" J. Lumin. in press.
2. Ingo Gregor, "Resonanz-Ramanspektren transienter Molekülzustände stark fluoreszierender Farbstoffe", Ph. D. Thesis, 2003, University of Siegen

From Sub-Poissonian photon statistics in two level molecules, to Lévy photon statistics in Blinking quantum dots.

Eli Barkai[a], YounJoon Jung[b], and Bob Silbey[c]

[a] Dept. of Chemistry, Notre Dame University, Notre Dame, IN 46556.
E-mail: jbarkai@nd.edu, Fax: (574) 631-6652, Phone: (574) 631-5235
[b] Dept. of Chemistry, University of California, Berkley, CA 94720-1460
[c] Dept. of Chemistry, MIT, 77 Mass. Ave., Cambridge, MA 02139

The current of photons emitted from a single molecule is used in many laboratories to investigate molecular processes, light matter interaction, and dynamical processes in the molecule's environment. The mathematical characterization of the photon counts is through the second order correlation function $g^{(2)}(t)$ or the related Mandel's Q parameter. The latter is a measure of deviations from Poissonian statistics. We review and analyze four typical behaviors of Q[1].

(i) Using the quantum jump approach, for a simple two level molecule, we (briefly) re-derive Mandel's well known result $Q < 0$ exhibiting *sub–Poissonian statistics*.

(ii) Using a simple rate equation approach, we discuss Q for a three level system, describing for example triplet blinking.

(iii) For the case where the molecule performs fast or slow spectral diffusion processes[2,3], and when the laser field is weak, we find rich physical behaviors for $Q > 0$ indicating *super Poissonian statistics*. Classification of Q in different regimes of spectral jumps magnitude, life time of the excited state, and jump rate is made.

(iv) We then discuss blinking quantum dots[4], where the photon counting statistics is non–ergodic, non–stationary, the mean on and off time diverge. We show that Q exhibits a new type of behavior, it increases with measurement time, even in the long time limit. In this case photon counts are described using *Lévy statistics*.

---

[1] E. Barkai, Y. Jung and R. Silbey *Theory of Single Molecule Spectroscopy: Beyond the (ensemble) Average* **Annual Review of Physical Chemistry** invited review and http://www.nd.edu/jbarkai/

[2] E. Barkai, Y. Jung, and R. Silbey *Time-Dependent Fluctuations in Single Molecule Spectroscopy: A Generalized Wiener–Khintchine Approach* **Phys. Rev. Lett.** *87*, 207403 (2001).

[3] Y. Jung, E. Barkai and R. Silbey *A Stochastic Theory of Single Molecule Spectroscopy* **Adv. in Chem. Phys** *123* 199 (2002).

[4] Y. Jung, E. Barkai, and R. Silbey, *Lineshape Theory and Photon Counting Statistics for Blinking Quantum Dots: a Lévy Walk Process* **Chemical Physics** *284* 181 (2002).

NON-CLASSICAL LIGHT EMISSION FROM SINGLE CONJUGATED POLYMERS

T. Huser[†], C.W. Hollars[†], S.M. Lane[¶]

[†]Department of Chemistry and Materials Science,
[¶]Department of Physics and Advanced Technology,
Lawrence Livermore National Laboratory, Livermore, CA 94551, U.S.A.

We have studied the fundamental photophysics of conjugated polymer conformational changes at the single molecule level. This effort to helps elucidate complex process dependant photophysical behavior and its impact on optoelectronic device performance. Single polymer molecules of MEH-PPV (poly[2-methoxy,5-(2'-ethyl-hexyloxy)-p-phenylene-vinylene) spun from polar and non-polar solvents adopt very different conformational states. This solvent-dependence of the chain conformation is carried forward into films and affects the photophysical properties of polymer molecules prepared on solid supports. Spectroscopic evidence from single polymer molecules indicates that only a few centers, i.e. those with the lowest transition energy, dominate the photoluminescence of the entire chain in samples prepared from non-polar solvents such as toluene. This result is in contrast to very different spectroscopic behavior for chloroform-spun samples, where the majority of the single polymer chains behave as a large ensemble of luminescent centers. This solvent dependent behavior is observed for the analysis of samples prepared from different solvent polarities using the quantum optical effect of photon antibunching. This effect manifests itself as a dip at short time intervals in the second-order intensity correlation function of the photon emission.

We have observed photon-antibunching from single, isolated molecules of collapsed-chain MEH-PPV by a Hanbury-Brown and Twiss photon correlation experiment, where the photon flux is divided equally between two single-photon-counting avalanche photodiodes. We have observed emission from an average of only 2-3 active sites on a folded polymer chain that is composed of hundreds of quasi-chromophores. These results indicate that MEH-PPV molecules exhibit considerable intrachain energy transfer. The controlled tuning of the number of active sites, if combined and addressed in an electroluminescent device, could find applications as a source for single or few photons in quantum cryptography, quantum computing, and data storage.

References:
Huser, T., Yan, M., and Rothberg, L.J., PNAS **97**, 11187-91(2000)
Huser, T., and Yan, M., J. Photochem. Photobiol. A **144**, 43-51(2001)
Hollars, C.H., Lane, S.M., and Huser, T., Chem. Phys. Lett. **370** (2003), 393-398 (2003)

Corresponding author information: Dr. Thomas Huser, ph.: (925) 423-6952, fax: (925) 423-0579, email: huser1@llnl.gov

Ultrafast Infrared Vibrational Echo Correlation Spectroscopy: Hydrogen Bond Dynamics in Water and Methanol

Michael D. Fayer*, John B. Asbury, Tobias Steinel, and C. Stromberg
Department of Chemistry, Stanford University, Stanford, CA 94305

Ultrafast (< 50 fs) infrared multidimensional stimulated vibrational echo correlation spectroscopy with full phase information is used to examine the dynamics of hydrogen bonds in water and methanol. By using pulses that are transform limited in the sample and by controlling path lengths with accuracy of a small fraction of a wavelength of light along with proper data analysis, correlation spectra are obtained with correct phase relationships across the entire very broad (~400 cm^{-1}) hydroxyl stretch spectrum in a manner that is similar to 2D NMR spectroscopy. Using a "dual scan" technique, the dispersive contribution to the correlation spectrum is eliminated and only the absorptive contribution remains, greatly narrowing the spectral features. The correlation spectra contain information that is not available from any other spectroscopic probes of vibrational relaxation and dynamics. The multidimensional stimulated vibrational echo correlation spectroscopy technique measures the vibrational dephasing and population dynamics in two frequency dimensions, ω_m and ω_τ.

The OD hydroxyl stretch of HOD in H_2O is probed. The time evolution of the vibrational echo correlation spectrum reflects the structural evolution of the hydrogen bond networks. The correlation spectra are found to evolve on multiple time scales. Molecular dynamics simulations/electronic structure calculations are used to obtain the time correlation functions (TCF) for two water models, TIP-4P and SPC/E. The TCFs are inputs to full time dependent diagrammatic perturbation theory calculations, which yield theoretical correlation spectra. Quantitative comparison with the data demonstrates the two water models somewhat over emphasize the fast fluctuations in water and do not contain a slow enough component to account for the slowest fluctuations. Fits to the data using a phenomenological tri-exponential TCF yield a slowest component of 2 ps, while TIP-4P and SPC/E have slowest components of < 1 ps.

In methanol hydrogen bond dynamics represent a photochemical system in which vibrational excitation of the hydroxyl stretch results in hydrogen bond breaking. Therefore, the ω_m axis provides information on the identity of the species that result from hydrogen bond breaking like a pump-probe experiment. The $\omega_\tau$nsion of information that is contained only in the correlation spectrum. The positions and signs of peaks in the correlation spectra contain the history of the various species involved in the hydrogen bonding dynamics. Separation of the peaks in the 2D correlation spectrum is equivalent to separation of quantum pathways even though the pathways result in optical emission at the same frequency. The experiments provide detailed information on hydrogen bond breaking and the production of photoproducts. Vibrational echo correlation spectra are obtained on time scales long compared to the vibrational lifetime (~500 fs) because of hydrogen bond breaking. The breaking of hydrogen bonds following the second pulse of the 3 pulse echo sequence leaves a ground state frequency grating (one of the rephasing Feynman diagrams) that produces a vibrational echo following the third pulse. The nature of hydrogen bond breaking dynamics is elucidated from the time evolution of the correlation spectra.

*email: fayer@stanford.edu; phone: 650 723-4446; Fax: 650 723-4817

Correlated Fields Hole-Burning Spectroscopy in Tm^{3+} : YAG

S. Saikan, T. Ishii, S. Ohno, T. Sonehara, and A. Koreeda

Department of Physics, Graduate School of Science, Tohoku University, Sendai 980-8578, Japan

The correlated fields spectroscopy, which was developed first by Steel and coworkers, yields the spectral resolution less than kHz even if large frequency jitter is present in the laser sources. We have recently improved this jitter-free technique in order to extend the available offset frequency range up to }40 MHz by compensating the frequency dependent Bragg diffraction of acousto-optic frequency shifter. As an example, figure 1 is the observed spectrum in Nd:glass, which indicates the present spectral resolution of 8 kHz. This signal arises from the nonlinear optical effect called as two-beam coupling. By using this technique, we have successfully measured the temperature dependence of orientation relaxation time of liquid crystal around the nematic-isotropic phase transition. This technique was found to work quite well for the non-resonant light scattering experiment. However, it is not clear whether this technique is also applicable to the hole-burning experiment, because the frequency jitter during the life times of the excited or bottleneck states might smear out the sharp hole spectrum. In this paper, we present the results on the hole burning experiment in Tm^{3+} : YAG and point out that the spectral resolution can be improved significantly by means of the correlated fields spectroscopy. Figure 2 is the observed hole-burning spectrum at 2K. The spectrum consists of two components, that is, the spike due to the population modulation effect (T$_1$ spike) and hole burning spectrum. The half width of the two components is, respectively, 19 kHz and 136 kHz, which is significantly narrower than the frequency jitter of the external cavity diode laser. The non-Lorentzian line shape of the hole spectrum might be ascribable to the effect of spectral diffusion. In fact, it has been observed that the hole-burning spectrum broadens as the modulation frequency for the lock-in detection is decreased. The temperature- and modulation frequency- dependence of the homogeneous line width in Tm^{3+} : YAG will be discussed taking account of the spectral diffusion.
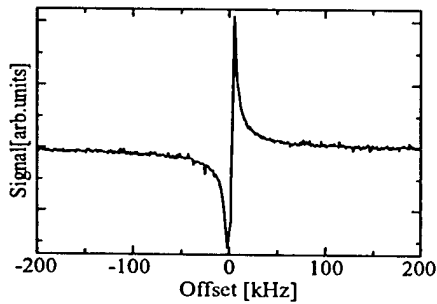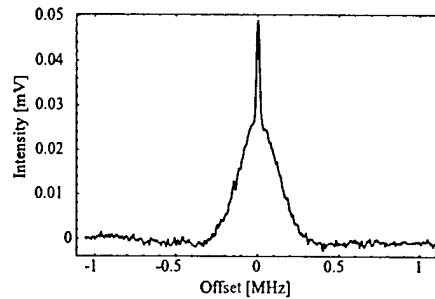

Fig.1:Two beam coupling in Nd:glass

Fig.2:Hole burning spectrum in Tm^{3+} : YAG

Optical Dephasing by Disorder Modes in Yttrium Orthosilicate (YSO) Doped with Eu^{3+}

R. M. Macfarlane,[a, b] Y. Sun,[a] R. L. Cone,[a] C. W. Thiel,[a] and R. W. Equall,[c]

[a]Physics Department, Montana State University, Bozeman, MT USA, [b]IBM Almaden Research Center, San Jose, CA USA, [c]Scientific Materials Corporation, Bozeman, MT USA

Yttrium orthosilicate (Y_2SiO_5 or YSO) doped with Eu^{3+} shows one of the narrowest homogeneous linewidths (Γ_h) observed in solid state systems with a width 100-200Hz for the $^5D_0 - {}^7F_0$ transition at 1.5 K^1. This width is the value obtained by extrapolation to zero excitation density in a 2-pulse photon echo experiment and has contributions from the population decay time and fluctuating local fields due to the Y nuclear spins. Such narrow lines can be very sensitive probes of static and dynamic environments in solids. We found in one lightly doped (0.02% Eu^{3+}) sample of YSO, that the inhomogeneous linewidth Γ_{inh} of 23 GHz is approximately 30x broader than in normal crystals, and that Γ_h is also significantly larger i.e. 600Hz at 1.5 K. The homogeneous linewidth is independent of concentration up to doping levels of at least 1%. An 'anomalous' 1% sample showed a linear dependence of Γ_h on temperature between 1.5 K and 4.5 K (Fig. 1); it is expected that the linewidth of that crystal would reach the same value as in 'normal' crystals at T~0.5 K. This behavior, i.e. the combination of broader inhomogeneous lines, excess dephasing at 1.5 K, and a linear temperature dependence, has been seen in other crystalline materials doped with Eu^{3+} (Ref. 2) or Pr^{3+} (Ref. 3) and is strong evidence for dephasing produced by disorder modes of the kind found in glassy systems and commonly designated as 'two-level systems' or TLS. The anomalous dephasing suggests that certain crystals of YSO exhibit microscopic disorder with a small density of TLS modes. It is postulated that optical coherence, measured by Γ_h, can be an extremely sensitive probe of the presence of *dynamic* disorder modes in crystalline systems. In contrast, the inhomogeneous linewidth Γ_{inh} is a measure of the *static* component of the disorder. Since rare-earth doped YSO is a material suitable for applications to storage and signal processing using spectral-spatial holography, it is desirable to be able to increase the bandwidth by increasing the inhomogeneous linewidth without significantly increasing the homogeneous linewidth, i.e. without decreasing the optical coherence time. Thus, one can optimize the overall capacity of a system with the upper limit set by the ratio Γ_{inh}/Γ_h. Further characterization of the anomalous crystals is under way with the goal of determining the nature of the disorder that has led to the excess dephasing.
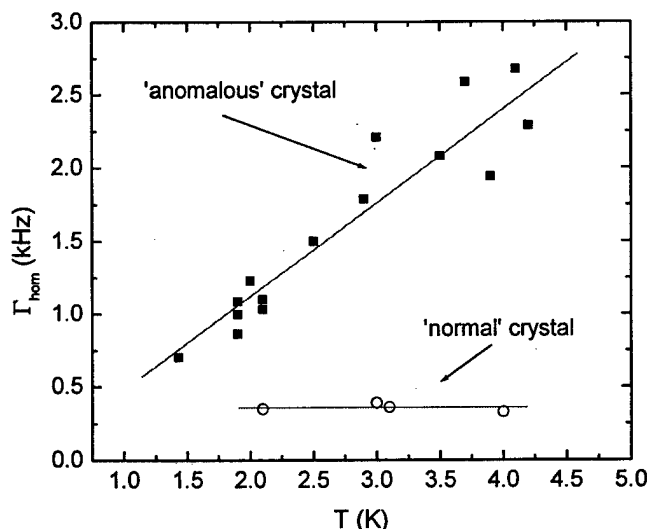

Fig. 1 Temperature dependence of the homogeneous linewidth in anomalous and normal crystals of Eu^{3+}:YSO

1. R. W. Equall, Y. Sun, R. L. Cone and R. M. Macfarlane, Phys. Rev Lett. 72, 2179 (1994).
2. G. P. Flinn, K. W. Jang, J. Ganem, M. L. Jones, R. S. Meltzer and R. M. Macfarlane, J. Lumin. 58, 374 (1994);
3. K. Tanaka,T. Okuno, Y. Yugami, M. Ishigami and T. Suemoto, Opt. Comm. 86, 45 (1991); R. S. Borisov ,B. V. Grinev, Y. V. Malyukin, B. I. Minkov, N. V. Znamenskii, E. A. Manykin, D. V. Marchenko, E. A. Petrenko, JETP 88, 385 (1999); R. M. Macfarlane, F. Könz, Y. Sun and R. L. Cone, J. Lumin. 86, 311 (2000).

Corresponding Author: R. M. Macfarlane, Phone 408 927 2428, FAX 408 927 2100, macfarla@almaden.ibm.com

Numerical modeling of excitation–induced dephasing

Geoffrey W. Burr[1], Todd L. Harris[2], Wm. Randall Babbitt[2], and C. Michael Jefferson[1]

[1] *IBM Almaden Research Center, 650 Harry Road, San Jose, California 95120*
Tel: (408) 927–1512, Fax: (408) 927–2100, E-mail: burr@almaden.ibm.com

[2] *The Spectrum Lab, Montana State University, PO Box 173510, Bozeman, Montana 59717*

An improved understanding of excitation–induced dephasing (EID) [1, 2], also known as instantaneous spectral diffusion, would not only facilitate engineering tradeoff analysis and optimization when EID limits system performance (such as in coherent transient storage and signal processing applications), but also enable novel functionality where EID might be used to advantage (solid–state quantum computation [3]).

Previous attempts at modifying the Bloch equations to model EID have addressed only the simple case of few-pulse echoes at low optical density [6,7]. Here we describe the incorporation of excitation–induced dephasing directly into the numerical integration of the Maxwell–Bloch equations. This allows modeling of arbitrary pulse inputs (including chirps) in media that can be also optically thick, as well as quantitative evaluation of tradeoffs between time, bandwidth, and signal strength.

To phenomenologically incorporate EID into the conventional Maxwell–Bloch equations [4,5], we stochastically impose random frequency jumps on each homogeneous ensemble of ions based on the overall excitation. After the usual evolution of the Bloch vector at each time–step of the numerical simulation, all three components of the Bloch vector for each detuning are scrambled with the Bloch vectors of neighboring detunings by convolution with a Lorentzian kernel of variable width.

In essence, the instantaneous change in any ion's resonance frequency depends on the degree to which its local environment has changed, as quantified by the overall change in population. If not much excitation is occurring, then few ions are changing state and the scrambler function is narrow and has little impact. If some part of the simulated bandwidth is being strongly excited, the resonance frequencies of all ions are more likely to undergo a significant random perturbation. These ions then dephase from how they would have evolved at their original resonance frequency, leading to weaker photon echoes.

Figure 1 shows preliminary results of simulated photon–echo decay with and without the excitation–induced dephasing feature enabled. For simplicity, results are shown for an optically–thin media with three different pulse sequences of identical pulse areas, but with different intensity in the second pulse. Without EID, all three decay curves are identical. With EID, however, the expected behavior [1,2] of faster decay rate with wider excitation bandwidth is observed.

In addition to describing the numerical implementation, we will try to connect these simulation results with experimental measurements of excitation–induced dephasing, both from the literature and from our own experiments. Conceivably, this modeling approach could be connected to microscopic modeling of the environment around an "average" ion, including the effects of doping density, dipole orientation, and Stark coefficient. We will also discuss the possibility of designing experiments that could independently determine the parameters used in the EID modeling (the choice of scrambler function and its width scaling with total change in r_3).
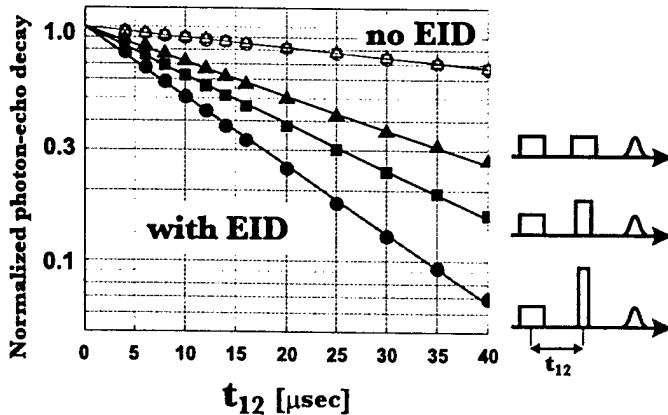
References

[1] G. K. Liu, M. F. Joubert, R. L. Cone, and B. Jacquier. *Journal of Luminescence*, 38(1-6):34–36, 1987.

[2] J. Huang, J. M. Zhang, A. Lezama, and T. W. Mossberg. *Physics Review Letters*, 63(1):78–81, 1989.

[3] N. Ohlsson, R. K. Mohan, and S. Kroll. *Optics Communication*, 201(1-3):71–77, 2002.

[4] T. L. Harris, C. M. Jefferson, G. W. Burr, J. A. Hoffnagle, M. Tian, and W. R. Babbitt. Chirped excitation of optically-dense inhomogeneously broadened media using Eu^{3+}:Y_2SiO_5. manuscript submitted to JOSA-B.

[5] M. Azadeh, C. S. Cornish, W. R. Babbitt, and L. Tsang. *Physical Review A*, 57(6):4662–4668, 1998.

[6] P. R. Berman. *Journal of the Optical Society of America B*, 3(4):564–571, 1986.

[7] N. Y. Asadullina, T. Y. Asadullin, and Y. Y. Asadullin. *Journal of Physics: Condensed Matter*, 13(22):5231–5240, 2001.

Fig. 1 Simulated photon–echo decay with and without the excitation–induced decay feature turned on (Lorentzian of width $\sigma_0 = 10^{-3}$). Pulse areas are kept constant while the duration of the second pulse is decreased, increasing excitation bandwidth and thus the effects of EID. Lines show exponential fits.

Line "narrowing" in strong optical fields

Taras Plakhotnik

Physical Chemistry Laboratory, ETH-Zürich, CH-8093, Switzerland.
Fax: +41 1 632 1021, E-mail: taras@phys.chem.ethz.ch

Linewidths of impurity centers in solids are broaden due to dephasing. One part of this dephasing is related to the decay of the excited electronic states. The decay rate equals $1/T_1$ and determines the lifetime-limited linewidth. A second contribution to the dephasing is related to fluctuations in the surrounding matrix. Frequently this contribution can be well approximated by a T_2^* time. The total dephasing rate $1/T_2$ is than $1/(2T_1) + 1/T_2^*$.
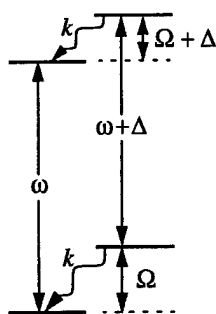
Fig. 1. A four-level energy scheme is a standard model for an impurity center in solids at low temperatures. Matrix related dephasing is caused by coupling between electronic states and a local vibration. Due to the coupling, the transition frequency fluctuates when the molecule jumps from the pure electronic state to the vibronic state. Dephasing depends also on k, the relaxation rate of the local vibration.

Usually a single degree of freedom, a so-called local vibration contributes to the matrix related dephasing at low temperatures. The corresponding level diagram is shown in Fig.1 and is explained in the figure caption. When the molecule interacts with a laser field, a new parameter that is a Rabi frequency Ω_R appears in the problem. At low laser powers the interaction is just a small perturbation which does not change the characteristics of the four-level system shown in Fig.1. Figure 2 demonstrates what happens when the Rabi frequency becomes larger than Δ and k. The matrix related dephasing disappears. This effect is connected (but not in a straightforward manner) to decrease of the decay rate of the Rabi oscillations, which are the oscillations with frequency Ω_R of the reduced density matrix elements describing the molecule. The measurements shown in Fig. 2 were done using *single molecule spectroscopy*. It is essential for interpretation, that contributions to the signal from molecules which have different transition frequencies do not cover the effect.

Fig. 2. The linewidth (FWHM), whose experimental values were measured at 2.1 K and are given by circles, always increases in strong optical fields due to saturation. The inset shows that this increase can be described by a simple function represented by the solid line $\Gamma = 1/(\pi T_2)\sqrt{1 + I/I_{sat}}$, where I is the laser intensity and I_{sat} is the dependent on T_2 saturation intensity. Because even at cryogenic temperatures $T_2 < 2T_1$, the linewidth is broader than a lifetime limited value which is achieved only when $T_2 = 2T_1$. The doted curve is the curve calculated assuming that $T_2 = 2T_1$. However, at high laser powers the experimental points deviate from the T_2-approximation and approach the dotted curve. In other words, at very high laser powers dephasing and broadening caused by the interaction between the molecule and the local vibration disappears.
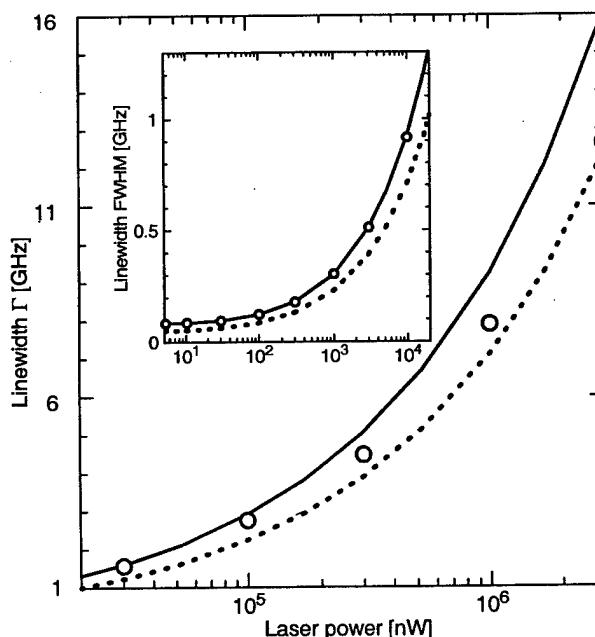
SINGLE-MOLECULE SPECTRA AND LOW-TEMPERATURE DYNAMICS OF AMORPHOUS SOLIDS: STANDARD AND NON-STANDARD TEMPORAL BEHAVIOUR

A.V. Naumov[1*], Yu.G. Vainer[1], M. Bauer[2], L. Kador[2]

(1) Institute of Spectroscopy, Russian Academy of Sciences, Troitsk, Moscow reg, 142190 Russia
(2) Institute of Physics and BIMF, University of Bayreuth, Bayreuth, D-95440 Germany

The observation of the temporal evolution of single molecule (SM) spectra in a disordered solid matrix is a powerful way for obtaining information about the dynamics of such a matrix and the validity of the two-level system (TLS) model on microscopic level.

We studied the temporal behavior of SM spectral trails detected on the purely amorphous polymer - *polyisobutylene* doped with *tetra-tert-butylterrylene* chromophore molecules. The experiments were performed at different low temperatures (2-15 K), the total observation time of each SM spectrum was in the range of 30-120 min. For each SM we recorded a number of fast (about 5-10s) repeated fluorescence excitation spectra. The evolution of the spectra was analyzed in 2D-plots, where the horizontal axis corresponds to the number of scan, the vertical axis to the laser frequency, and the grey scale of each data point is proportional to the fluorescence intensity (see Fig. 1 a,b).
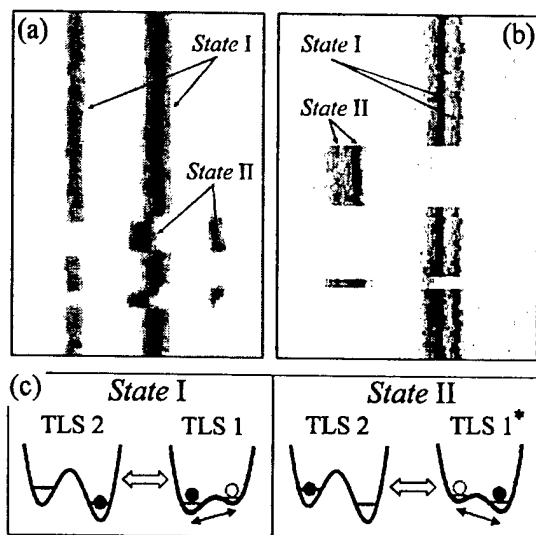

Figure 1. Examples of "nonstandard" spectral trails (a,b) and possible explanation of their temporal behavior as an interaction of the chromophore with two "strong" TLSs interacting with each other (c,d).
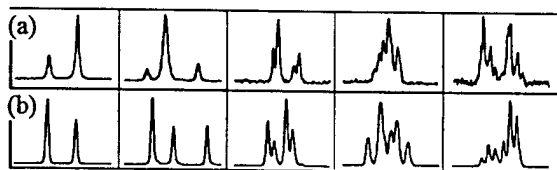

Figure 2. Examples of measured (a) and simulated (b) SM spectra of different multiplet orders.

Main results: ❶ The temporal evolution (number of spectral positions, ratio of peak intensities etc.) of most spectra was found to be consistent with the TLS model. ❷ Interactions of the chromophores with different types of TLSs ("strong", "weak", "fast fluctuating", "slow fluctuating", "non-fluctuating" TLSs) and with the quasi-localized low-frequency modes have been observed and analyzed. ❸ Spectral trails inconsistent with the TLS model and their temperature behavior were detected and analyzed: (a) Trails which have some "holes" during short time intervals (from milliseconds up to seconds); (b) Several trails which can be explained as an interaction of the chromophore with a "three-level" system; (c) Trails with slow spectral drifts of their components; (d) Trails with intensity redistribution of their spectral components during spectral jumps (see examples in Fig. 1 a,b). ❹ A few spectral trails, which can be interpreted as a direct experimental proof (visualization) of an interaction between TLSs were detected (see Fig. 1).

A statistical analysis of the multiplet structure of SM spectra at different temperatures was performed. For this purpose the relative number of multiplets of different orders (see examples in Fig. 2) was calculated for SM spectra which were measured and simulated on the base of a stochastic SMS theory [E. Geva, J.L. Skinner, *J. Phys. Chem.* B **101**, 8920 (1997)]. It allowed us to obtain new information about the dynamics of the chromophore environment.

CHARGE TRANSFER AS A SOURCE OF BLINKING IN SINGLE MOLECULES AND NANOCRYSTALS

Rob Zondervan, Rogier Verberk, Florian Kulzer, and Michel Orrit*

Molecular Nano-Optics and Spins (MoNOS, LION)

Huygens Laboratory, Universiteit Leiden, P.O. Box 9504, 2300 RA Leiden

The sudden brightness variations of single fluorescent objects, known as blinking, may have various origins. Photo-induced transfer of a charge to a trap in the environment leaves a charged, usually dark object, until the trapped charge tunnels back. This blinking mechanism seems common to various kinds of nano-objects, including semiconductor nanocrystals and organic dyes.

Blinking semiconductor nanocrystals present long off-times, which we attribute to transfer of an electron to traps in the neighborhood. A uniform spatial distribution of traps leads to power-law statistics of the off-times, with exponent between 1 and 2. This simple model explains most of the current observations of nanocrystal blinking, including power-law dependence of the correlation function over 6 decades of time [1]. For capped nano-crystals, the on-times are also distributed according to a power-law, with a nearly flat correlation function. A slight modification of our model accounts for this difference.

We measured the bulk fluorescence kinetics of Rhodamine 6G in polyvinylalcohol. We find a long-lived dark state, with a widely distributed lifetime, which is confirmed by the slow blinking of single molecules. The lifetime of the dark state is independent of temperature, which hints at electron tunneling. ESR experiments under illumination show an intense peak at g=2, which we think is the radical-anion created by electron transfer from donor sites in polyvinylalcohol [2]. We also studied photo-bleaching at various temperatures, in air and nitrogen, and find strongly dispersive kinetics. In that case, however, the temperature dependence is strong, pointing to photo-chemical reactions.

1. R. Verberk, A. van Oijen, M. Orrit, Phys. Rev. B 66 (2002) 233202.
2. R. Zondervan, F. Kulzer, S. Orlinsky, M. Orrit, submitted (2003)

*tel. 31 71527 1720, fax 31 71527 5819, e-mail orrit@molphys.leidenuniv.nl

LIGHT-INDUCED CONFORMATIONAL CHANGES IN
RED FLUORESCENT PROTEIN

S. Bonsma[1], F. Könz[1], J. Gallus[1], V. Subramaniam[2], T.M. Jovin[2] and S. Völker[1]

[1] Huygens and Gorlaeus Laboratories, University of Leiden, The Netherlands.
[2] Max-Planck-Institute for Biophysical Chemistry, Göttingen, Germany.

Green fluorescent protein (GFP) and its mutants have become highly popular in the life sciences as strong luminescent markers for visualization of dynamic events in living cells [1]. Through the discovery of a red fluorescent protein (DsRed), emitting at wavelengths well separated from those of GFPs, the possibilities of multicolor labeling have greatly expanded [2, 3]. The red-shift in DsRed as compared to GFP (see figure) originates from the structure of the chromophore [4, 5], which in DsRed has a more extended conjugated π-electron system (see the extra C=N bond in the figure, upper right). However, the mechanism leading to the red (and green) fluorescence is still poorly understood.
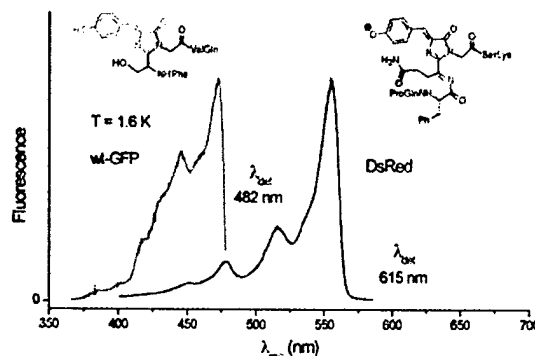
Here we will present results on the photophysics of DsRed, which we studied by time-dependent fluorescence line-narrowing and spectral hole-burning at temperatures between 1.2 and 300 K. By selective wavelength excitation, using three lasers simultaneously, we have found a number of conformations which can be switched back and forth by light. In addition to identifying their 0-0 transitions and vibrational frequencies, we have also observed energy transfer processes between these forms. From the temperature-dependence of the spectra, we could not only separate photo-induced from thermally-induced conformational changes, but also determine quantitatively the barrier heights for thermal interconversions and the energy-level differences in the ground states of the various forms. The energy-level scheme and the pathways for the photo-reactions will be discussed and compared to those of GFP and its mutants [6].

[1] R.Y. Tsien, *Annu. Rev. Biochem.* **67** (1998) 509-544.
[2] M.V. Matz et al., *Nature Biotechnology* **17** (1999) 969-973.
[3] R.E. Campbell et al, *Proc.Natl.Acad.Sci.USA* **99** (2002) 7877-7882.
[4] L.A. Gross et al., *Proc.Natl.Acad.Sci.USA* **97** (2000)11990-11995.
[5] M.A. Wall et al., *Nature Struct. Biol.* **7** (2000) 1133-1138.
[6] T.M.H. Creemers, A.J. Lock. V. Subramaniam, T.M. Jovin and S. Völker, *Nature Structural Biology* **6** (1999) 557-560; T.M.H. Creemers, A.J. Lock, V. Subramaniam, T.M. Jovin and S. Völker, *Proc.Natl.Acad.Sci.USA* **97** (2000) 2974-2978.

Theoretical study of fluorescence kinetics, Stokes shift, and intra-band relaxation of Frenkel excitons in J-aggregates at low temperatures

M.Bednarz[1,*], V.A. Malyshev[2], J. Knoester[1]

[1]*Theoretical Physics and Material Science Center, University of Groningen, Nijenborgh 4, 9747 AG Groningen, The Netherlands*
[2]*All-Russian Research Center "Vavilov State Optical Institute" Birzhevaya Linia 12, Saint Petersburg 199034, Russia*

The optical properties of linear molecular aggregates exhibit unusual temperature dependence, mainly originating from the fact that the optically active states in these species are Frenkel excitons. In particular, the fluorescence decay time in J-aggregates grows with increasing temperature [1], reflecting the superradiant nature of exciton states coupled to the light. Despite the fact that this observation is qualitatively understood, the quantitative description, taking into account the experimental conditions, is still lacking. Furthermore, for some aggregates, the Stokes shift of fluorescence spectra with respect to absorption spectra shows surprising non-monotonic temperature dependence [2].

In the present contribution, we propose a microscopic approach, based on the Pauli master equation, which is able to describe in a quantitative manner both peculiarities outlined above. We take into account the factors that are most relevant to experiments done in this field: i) - *localization* of the exciton states, ii) - coupling of localized excitons to the *host vibrations* (not only to the vibrations of the aggregate itself), iii) - a possible *non-equilibrium* of the subsystem of Frenkel excitons on the time scale of the emission process, and iv) - *excitation conditions* (blue-tail or resonant).

We demonstrate also that the local energy structure, which has been proved to exist at the tail of the density of state [3], can be measured by means of fluorescence line narrowing spectroscopy.

We discuss the relevance of our numerical results on the temperature dependence of the fluorescence decay time and Stokes shift to the existing experimental data of THIATS aggregate [2].

[1] S. de Boer and D. A. Wiersma, Chem. Phys. Lett. 165, 45 (1990).
[2] I. G. Scheblykin, O. Yu. Sliusarenko, L. S. Lepnev, A. G. Vitukhnovsky, and M. Van der Auweraer, J. Phys. Chem. B 105, 4636 (2001).
[3] A. V. Malyshev and V. A. Malyshev, Phys. Rev. B 63, 195111 (2001)

* Corresponding author: Mariusz Bednarz, e-mail: M.Bednarz@phys.rug.nl

Satellite hole investigation of hole filling induced by fluorescence energy transfer

Kai-Hsiang Huang, Jin-Yi Wu, Cheng-Chung Chang, Ta-Chau Chang

Institute of Atomic and Molecular Sciences, Academia Sinica
Taipei, Taiwan 106, Republic of China

We have demonstrated that the intermolecular energy transfer from 9-amino-6-chloro-2-methoxy-acridine (ACMA) to bodipy can trigger the filling of the primary holes of 4,4-difluoro-5-(2-thienyl)-4-bora-3a,4a-diaza-s-indacene-3-propionic acid (BP568).[1] Here we show the effect of energy transfer along the DNA in LIHF. Figure 1a and 1b show the ratios of hole-depths of the zero-phonon hole of BP568 and BP568-DNA as a function of filling time via the excitation of ACMA, respectively. The data were fitted to a bi-exponential decay of the form,

$$I(t) = \alpha_1 \exp(-t/\tau_1) + \alpha_2 \exp(-t/\tau_2),$$

where α_i are the amplitudes of the individual contributions and τ_i are the filling times. We used $\tau_1 = 5$ min and $\tau_2 = 125$ min for figure 3a, and $\tau_1 = 1$ min and $\tau_2 = 20$ min for figure 3b. It appears that the filling rate is much fast when the covalently linked BP568 to DNA interacts with ACMA. This is because ACMA can intercalate in the base pairs of DNA and hence to shorten the distance between the ACMA and BP568. In addition, the study of energy transfer from the excitation of donor to two different acceptors characterized by the filling of their distinct non-resonant holes will be discussed.
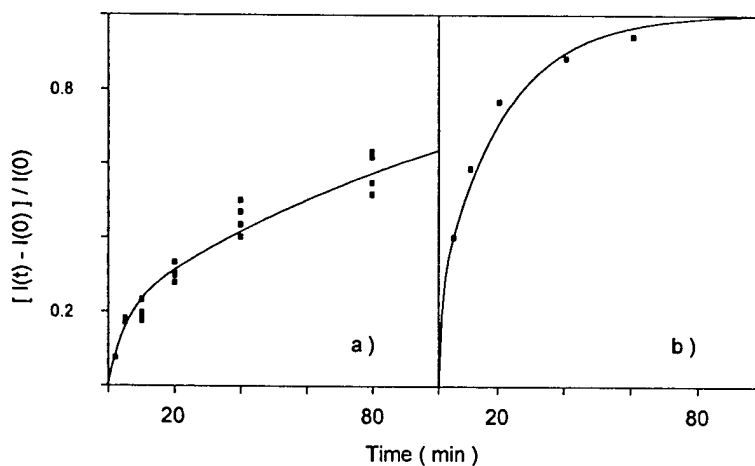
1. C. T. Kuo, T.-C. Chang, (1997) J. Chem. Phys. 106, 5947.

Photon Echo Studies of LaF$_3$:Pr^{3+} Nanocrystals in Glass

R.S. Meltzer and H. Zheng

Department of Physics and Astronomy
University of Georgia
Athens, GA 30602

Ph: (706) 542-5515   Fax: (706) 542-2492   Email: rmeltzer@hal.physast.uga.edu

The dynamics of rare earth ions in nanocrystals is quite different from their behavior in bulk crystals. For example, confinement of the phonon modes results in strongly-enhanced electron-phonon interactions.[1] Studies of spectral hole burning (SHB) of rare earth ions contained in LaF$_3$ nanocrystals embedded in oxyfluoride glass ceramics have shown that at low temperatures, an additional mechanism of optical dephasing dominates: i.e. interactions with the two-level systems (TLS) of the glass, even for nanoparticles whose diameters exceeds 20nm.[2] Since dephasing measurements obtained with SHB include the effects of spectral diffusion over the timescale (ms) necessary in these experiments, it is desirable to study the dynamics using photon echo measurements in order to obtain the "true" homogeneous linewidths. Here we report the results of two-pulse photon echo experiments on the ^{3}H$_4 \rightarrow$ ^{3}P$_0$ transition of Pr^{3+} in LaF$_3$ nanocrystals contained in these glass ceramics. Dephasing times for this transition fall between 30-50 ns at 1.3K. As was the case for SHB, the temperature dependence of the homogeneous linewidth is nearly linear, indicating the dominant role of interactions with the TLS in controlling dephasing. The corresponding homogeneous linewidths at 1.5K (7-10 MHz) are similar to those obtained from SHB measurements on the ^{3}H$_4 \rightarrow$ ^{1}D$_2$ transition. However, since it can be expected that the ^{3}H$_4 \rightarrow$ ^{3}P$_0$ transition will dephase more rapidly because of its larger transition dipole moment which will couple more strongly with the elastic dipoles of the TLS, the similar linewidths suggest the presence of spectral diffusion in the SHB results over the millisecond time scale of the SHB measurements.

[1] R.S. Meltzer and K.S. Hong, Phys. Rev. B**61**, 3396 (2000).
[2] R.S. Meltzer, W.M. Yen, H. Zheng, S.P. Feofilov, M.J. Dejneka, B.M. Tissue and H.B. Yuan, Phys. Rev. B **64**, 100201 (2001) and R.M. Macfarlane and M.J. Dejneka, Opt. Lett. **26**, 429 (2002).

TRANSIENT AND PERMANENT SPECTRAL HOLE-BURNING IN ERBIUM-DOPED GLASSES

L. BIGOT[*], S. CHOBLET, A-M. JURDYC, B. JACQUIER
Laboratoire de Physico-Chimie des Matériaux Luminescents
UMR-CNRS 5620, 10 rue André-Marie Ampère, Bâtiment A. Kastler
Campus de la Doua, 69622 Villeurbanne Cedex, France
T. BÖTTGER, Y. SUN, and R. L. CONE
Department of Physics, Montana State University
Bozeman, Montana 59717, USA

This paper reports the observation of transient Spectral Hole-Burning (SHB) in erbium-doped fluoride glass and of transient and permanent SHB in erbium-doped chalcogenide glass. The holes were burned around 1.53 µm in the $^4I_{15/2} \leftrightarrow {}^4I_{13/2}$ absorption band of Er^{3+}, using a pump/probe technique, between 1.5 and 15 K. In both glasses, hole width is around 100 MHz at 1.5 K. Burning efficiency can be as high as 15 % and saturation can be detected both in absorption and luminescence. Permanent holes are only observed for the chalcogenide composition, and they persist for a few minutes with the same width as the transient holes.
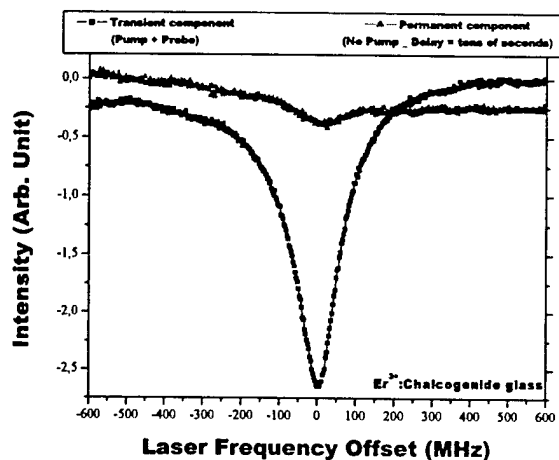
Figure 1: Example of transient and persistent holes burned at 3 K for the chalcogenide glass composition with a burning power of 177 µW @ 1538 nm.

Power dependence of the SHB has been investigated for the two glass compositions to characterize the roles of spectral diffusion effects and concentration for the fluoride glass. A nearly linear temperature dependence of the transient contribution is measured. Holes were detected up to more than 15 K. The measured linewidth at the highest temperature is in agreement with RFLN measurements already performed on the two glasses [1, 2]. Transient holes only have been recently observed in several oxide glass compositions [3]. Further dynamics of refilling holes on millisecond and longer time scales will be reported.

The origin of the saturation in the transient SHB (time ~ a few ms) is assumed to be related to the long lifetime of the $^4I_{13/2}$ level of Er^{3+} and to a coupling of Er^{3+} to Two-Level Systems (TLS) of the surrounding glassy matrix. In the permanent SHB observed for chalcogenide glass, the saturation is most likely associated with photo-induced modification of the glass.

References:

[1] L. Bigot, A-M. Jurdyc, B. Jacquier, L. Gasca and D. Bayart, Phys. Rev. B, **66** 214204 (2002)
[2] L. Bigot, A-M. Jurdyc, B. Jacquier and J-L. Adam, accepted in Opt. Mat.
[3] L. Bigot, S. Choblet, A-M. Jurdyc and B. Jacquier, DPC'03

[*]Corresponding author: *Laurent.Bigot@alcatel.fr*, Tel : (33).1.69.63.40.28, Fax : (33).1.69.63.44.30

Phase relaxation in the vicinity of the dynamic instability: anomalous temperature dependence of zero-phonon lines

V. Hizhnyakov, V. Boltrushko, H.Kaasik, and I.Sildos

Institute of Physics, University of Tartu, Riia 142, 51014 Tartu, Estonia;
E-Mail: hizh@fi.tartu.ee

We are studying the optical spectra of impurity centres in crystals in the case when in one or in both electronic states of the optical center, local elastic springs are strongly reduced, causing the appearance of a peseudolocal mode of a very low, or even of an imaginary frequency. In these cases, the optical transition takes place into the area of the flat minimum or the flat potential barrier in the configurational coordinate space, where the density of states of low-frequency phonons is strongly enhanced. One example of the systems of this type is the trigonal center with strong Jahn-Teller effect in the two-fold degenerate E-state, when the adiabatic surface has a shape of the so-called squeezed Mexican hat. In this case the adiabatic potential of the E-state has three shallow minima separated by three low barriers. There are also other examples of the centers with very weak local elastic springs. The goal of this communication is to investigate the temperature dependence of the width and the position of the zero-phonon line (ZPL) of the optical spectrum in the systems of this type. The peculiarity of the problem is that the change (weakening) of the elastic springs at the electronic transition in this case is so strong that the standard theory of the ZPL is not usable. To take this strong change into consideration, the mentioned strong change, a nonperturbative theory of the phase relaxation causing a temperature broadening and a shift of the ZPL is developed.

It has been found that, if the weakening of the elastic springs brings the system in the excited state close to the dynamic instability, then the usual T^7-dependence of the homogeneous width of the ZPL at $T \ll T_D$ is replaced by the T^3-dependence in a broad temperature interval (T_D is the Debye temperature). Besides, the usual T^4-dependent red shift of the line is replaced by the T^2-dependent shift. If the excited state is dynamically unstable then the homogeneous width of the ZPL gets a finite value already at T=0. In real systems the dynamic stability can be reduced or even disappear with respect to one or a few symmetrized displacements; other symmetrized displacements contribute to the ZPL characteristics in the usual way. Therefore, if one of the electronic states gets into the region of the dynamic instability, then one should expect the following temperature dependences of the width (γ) and the position (δ) of the ZPL:

$$\gamma = \gamma_0 + a\,T^3 + b\,T^7, \qquad \delta = \delta_0 + \mu T^2 - v T^4,$$

where a, b and v are positive parameters, while the parameter μ may be either positive or negative.

The proposed theory is applied to describe the homogeneous width and the temperature dependence of the zero-phonon line 637 nm of nitrogen-containing NV centers in good-quality diamond films ($T_D \approx 1900$ K). Here the excited state of the center belongs to E representation. We have carried through a detailed experimental investigation of the temperature dependence of this line in a broad temperature interval between 5 K and 300 K. We have found that in the temperature interval $50 < T < 200$ K both the width and the position of the ZPL were well described by the above-given expressions; thereby the main contribution to the width was given by the T^3 term.

Locating the electronic states of rare-earth ions relative to host band states for the development of photon-gated hole burning materials

C. W. Thiel[*], Y. Sun, and R. L. Cone

Department of Physics, Montana State University, Bozeman, Montana 59717, USA.

Rare-earth spectral hole burning materials are important for a wide range of applications including laser frequency stabilization, analog signal processing, and optical data storage. Many of these applications would benefit from an ability to probe the population distribution of the optical transition without perturbing the population through further hole burning. Photon-gated hole burning through two-step photoionization of the rare-earth ion provides a mechanism that enables this non-destructive readout. By employing a process that requires two photons of different frequencies, the hole burning is controlled by selective application of the second step "gating" photons, and little or no modification of the material occurs in the absence of the "gating" photons. This will enable, for example, secondary frequency standards based on rare-earth-doped materials and optical signal processors with pre-programmed patterns for searching and data routing.

We report several critical steps in developing practical photon-gated photoionization hole burning materials for device applications: (a) the determination of the energies of the excited $4f^{N-1}5d$ states relative to the host conduction band and (b) the energies of the $4f^N$ ground states relative to the host valence band. For the ionization hole burning process to produce stable, long-lived spectral holes, it is noted that the $4f^N$ ground state must have an energy higher than the valence band states of the host crystal. If there are occupied valence states at higher energy than the $4f^N$ ground state, an electron from the ligand ions, whose valence states primarily contribute to the valence band, can relax into the "hole" on the ionized rare earth, returning the rare earth to its original valence and filling the spectral hole. It is important to know the energy of the $4f^{N-1}5d$ states relative to the conduction band to determine which levels are degenerate with conduction band states and what corresponding gating wavelength is required to produce ionization by efficient transition pathways.

To better understand the relative energies of these states and provide practical information for optical material development, conventional and resonant electron photoemission was used to measure the relative energies of $4f^N$ and valence band states in a number of potential photon-gated hole burning materials, including YAG, $YAlO_3$, and $YLiF_4$. By combining these energies and ultraviolet spectroscopy, binding energies of $4f^{N-1}5d$ states relative to host bands were also determined. These results show that electron binding energies of the $4f^N$ states vary considerably between ions, while the $4f^{N-1}5d$ binding energies have similar values. In the oxides and fluoride materials, the trivalent ion ground state energies generally lie near or below the top of the host valence band and the lowest $4f^{N-1}5d$ states are typically within a few eV of the bottom of the conduction band. A simple empirical model accurately describes these observed electron binding energies for the lowest energy $4f^N$ and $4f^{N-1}5d$ states. The systematic changes in the relative energies for different states, different ions, and different host materials provide insight into photoionization, luminescence quenching, and ion valence stability. The results of that work indicate that by extending these methods to additional materials, potential photoionization hole burning materials may be identified and analyzed to determine their suitability.

[*]Corresponding Author. Tel.: +1-406-994-4363; fax: +1-406-994-4452.
E-mail address: thiel@physics.montana.edu (C. W. Thiel)

Enhanced Mo^{3+} and Re^{4+} Near-IR-to-Visible Upconversion Excitation Through Yb^{3+}-Host Sensitization

G. Mackay Salley[2*], Daniel R. Gamelin[1], and Hans U. Güdel[3]

[1]*Department of Physics, Wofford College, 429 N. Church St. Spatanburg, SC, 29303*

[2]*Department of Chemistry, University of Washington, Box 351700, Seattle, WA 98195*

[3]*Department of Chemistry and Biochemistry, University of Bern, Freiestrasse 3, CH-3000 Bern 9, Switzerland*

Abstract. Rare Earth (RE) sensitization of transition metal upconversion is demonstrated in the materials Mo^{3+}- and Re^{4+}-doped $Cs_2NaYbCl_6$. Absorption, emission, upconversion excitation, and time and power dependence spectroscopic methods have been used to determine the mechanistic roll of Yb^{3+} in these upconversion processes. In both materials, the Yb^{3+} host is found to serve as a photon antenna for the absorption and nonradiative transfer of excitation energy to the transition metal dopant ions. Essentially (~1000:1) every photon absorbed by Yb^{3+} leads to luminescence from the transition-metal "supertraps". Yb^{3+} sensitization transforms the relatively inefficient Mo^{3+}-doped chloro-elpasolite upconversion material into one with bright upconversion clearly visible by eye under ambient lighting conditions. Quantum yield measurements for 5% Mo^3:$Cs_2NaYbCl_6$ reveal that greater than 40% of all absorbed photons participate in upconversion under high power conditions. Yb^{3+} sensitized Re^{4+} upconversion is also extremely bright, with over 20% of all absorbed photons contributing to upconversion under high power conditions. The broad NIR absorption range, efficient sensitization, and efficient upconversion observed in Re^{4+}:$Cs_2NaYbCl_6$ at room temperature make this combination a promising new material for potential room-temperature NIR imaging and upconversion applications.

* Tel: (864)597-4610 Fax: (864)597-4629
  email: salleygm@wofford.edu

A parabolic mirror objective with high numerical aperture for imaging and spectroscopy at the nanometer scale

M. Andreas Lieb*, Andreas Drechsler, Christina Debus and Alfred J. Meixner

Physikalische Chemie, Universität Siegen, Adolf-Reichwein-Str. 2, 57068 Siegen, Germany
present address: The Institute of Optics, University of Rochester, Wilmot Building, Rochester, NY 14627

Phone: (585) 275 5104, Fax: (585) 244 4936, email: lieb@optics.rochester.edu

Parabolic mirrors with high numerical aperture (NA) have been used as efficient light collection devices in the early cryogenic single-molecule work [1], but for microscopy and imaging they have been avoided due to poor off-axis imaging properties. However, in a stage scanning confocal microscope one can ensure that the optical focus is always on the optical axis. It is possible to fabricate a concave parabolic mirror with an aperture close to one and hence it (1) can produce a tight diffraction limited spot, (2) can efficiently collect the radiation of a point light source in the focal spot, (3) has minimal chromatic aberrations since the rays are only deflected at one surface which is highly reflective over a large spectral range and (4) can be cooled down to cryogenic temperatures without loss of performance. Fig. 1 shows a confocal fluorescence image of a single terrylene molecule which demonstrates the good imaging properties with the confocal setup at 1.8 K [2].
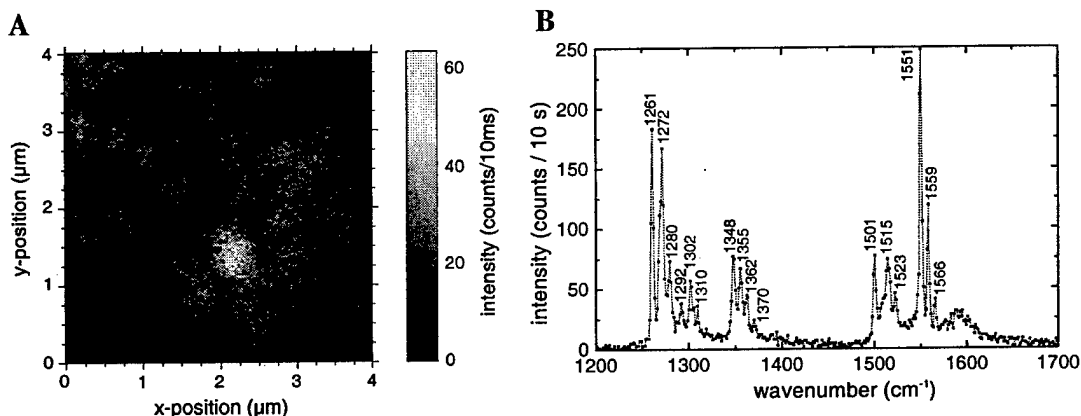
Fig. 1. A) Confocal fluorescence image of a single terrylene molecule, which is embedded in the Shpol'skii matrix octadecane. A two dimensional Gaussian fit leads to a FWHM of 0.46 µm, which corresponds to 0.8 λ for the excitation wavelength of λ = 571.6 nm. B) Fluorescence spectrum of a single terrylene molecule at 1.8 K, which has been excited in resonance at a wavelength of 572,2 nm. The values attributed to the peaks indicate the frequency shift compared to the excitation wavelength in wavenumbers.

Vector-field simulations have been performed for a parabolic mirror using linear as well as radially polarized light [3]. In a radially polarized beam the electric field vector is everywhere oriented in a radial direction from the optical axis. While linear polarized light yields the well known highly confined field component along the polarization direction in the focal plane of the mirror, radially polarized light leads to a strong, highly confined electrical field component along the optical axis which is about 15 times more intensive than the in-plane components, which are also present near the focus, for $NA \approx 1.0$. This makes it a well suited tool for local field-enhancement in near-field optics, or in conjunction with linear polarized light in two perpendicular directions it yields a platform for investigation of nanometer sized particles or single molecules with optical fields in the three spatial dimensions.

The numerical aperture of $NA \approx 1.0$ allows as well a very efficient collection of fluorescence light, especially from single molecules, which have their transition dipole moment oriented along the mirror axis. Overall, high resolution fluorescence spectroscopy of single molecules at low temperature can be performed with high signal-to-noise ratio, as shown in Fig. 1B.

References:
1. T. Basché, W. E. Moerner, M. Orrit, U. P. Wild (eds.) "Single-Molecule Optical Detection, Imaging and Spectroscopy," (VCH, Weinheim, 1997).
2. A. Drechsler, M. A. Lieb, C. Debus, A. J. Meixner, and G. Tarrach, "Confocal microscopy with a high numerical aperture parabolic mirror," Opt. Express 9, 637-644 (2001).
3. M. A. Lieb and A. J. Meixner, "A high numerical aperture parabolic mirror as imaging device for confocal microscopy," Opt. Express 8, 458-474 (2001).

Antibody-antigen interactions and atomic force microscopy: another approach to single molecule detection

Avci et al
MSU Physics, EPS 264, Bozeman, MT 59717

The ability to image antibody binding to specific antigenic sites holds great potential in biosciences, for example in the development of novel medical techniques, new biosensors and, of particular interest in our case, the detection of extinct and extant life in outer planets. Atomic force microscopy (AFM) offers a unique opportunity to localize antibody binding in real time and the ability to measure the strength of the antibody-antigen (ab-ag) binding at the single-molecular level. This is achieved by covalently tethering an appropriate antibody to one end of a *highly flexible* linker molecule while tying the other end covalently to a sharp tip located at the end of a soft cantilever of an AFM setup. The system is analogous to a micro fishing pole having a nano-hook to localize and measure individual ab-ag interactions in the natural environment of the biological systems. In this presentation we discuss the chemistry of AFM tip functionalization and give examples of its application for determining the strength of the ab-ag interactions on collagen fibers at the molecular level in terms of average pull-off forces and their distribution. The ab-ag interactions will be visualized by imaging gold nano-particles conjugated with secondary antibodies raised against the primary antibodies of the collagen fibers. Application of the technique is extended to the studies of ab-ag interactions on fossilized bacteria. These interactions are visualized by imaging gold nano-particles conjugated with secondary antibodies raised against the primary antibodies associated with the bio-molecules (such as hopanes) preserved within the fossilized bacteria. We will also discuss the difficulties as well as the advantages and disadvantages of this technique as compared with traditional immunological techniques and suggest ways to remedy the difficulties encountered in our approach.

MICROSCOPY STUDIES OF LITHIUM NIOBATE WAVEGUIDE DEVICES USING SPATIALLY DEPENDENT FLUORESCENCE LINE NARROWING

V. Dierolf and *Chr. Sandmann*

Lehigh University, Bethlehem, PA 18015 USA

Nonlinear light sources based on periodically poled $LiNbO_3$ have gained a great deal of attention due to low thresholds, ease of operation and wide tuning range. In particular, the integrated optical versions of them, achieve, due to the confinement of light over long interaction lengths, very high conversion efficiencies [1]. In order to optimize the latter, both the Ti-profile, which defines the waveguides, and the domain structure have to be engineered precisely and effects of interaction have to be under control. In order to achieve this goal we developed a novel characterization tool based on the luminescence of a well-characterized "designer defect" (e.g.: Er^{3+}) that we use as a local probe.

(1) Characterization of the Ti-profile within a waveguide. Under optical excitation with a *single* laser we found that the spectral width of the Er^{3+} transitions increase considerably in the presence of Ti^{4+} ions [2]. We were able to use this observation to image the diffusion profiles within waveguides. Furthermore, using a *two-photon* excitation scheme the luminescence lines narrow drastically and can be moved across the whole inhomogenously broadened line by varying the excitation laser wavelengths. Performing these measurements spatially selective using a confocal microscope reveals emission intensity distributions over a cross section of the Ti-diffused waveguide in $LiNbO_3$, which dependent on the choice of excitation wavelength (see Fig. 1). These observations make it apparent that the inhomogenous broadening, which is observed for a waveguide, is a result of convolution of Ti^{4+} concentration-dependent (and hence spatially dependent) spectral positions with the mode distribution of the guided wave.
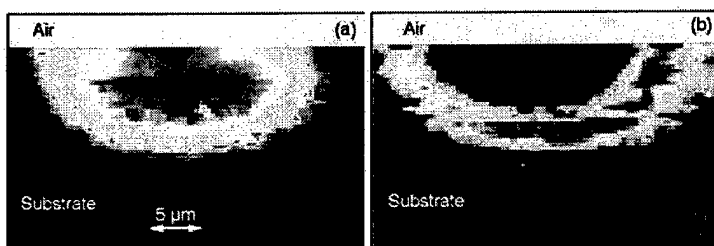

Fig. 1:
Er^{3+} intensity distribution over a cross section of a $Ti:LiNbO_3$ waveguide obtained under resonant two-photon excitation for two different combinations of excitation wavelengths
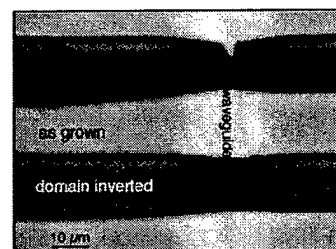
Fig. 2:
Periodically poled $LiNbO_3$ waveguide device imaged in a confocal luminescence microscope

(2) Characterization of domain structures. It has been shown that the domain inversion process, most notably the coercive field, is strongly influenced by the presence of defects [3]. We investigated this effect by addressing the reverse question: How does domain inversion influence intrinsic defects and dopants? Using again Er^{3+} as a probe ion we find drastic changes in the luminescence both in terms of spectral width and position. Based on a detailed analysis of these changes, using earlier studies of the defect systems [4], we conclude that a defect reconfiguration takes place during domain inversion. Obviously, some of the required charge compensators do not reposition themselves according to the reversed orientation of the spontaneous polarization vector at room temperature, while others do. Furthermore, we were able to detect a change in the intrinsic electric field experienced by the ion.

Combining (1) and (2) we investigated fine details of (periodically) poled $LiNbO_3$ waveguide devices. Measuring in a scanning confocal microscope the spatially dependent emission spectra and evaluating the moments of the spectra, enables us to image various aspects of the device, with high contrast and spatial resolution (<500nm). Different from other microscopic techniques, the waveguide, up and down domains, the domain wall region, and domain pattern imperfection become very apparent in our technique (see Fig. 2). This method is non-destructive, free of topographical artifacts, and can be employed in situ, allowing precise control of the domain structures.

[1] W. Sohler et al. Appl. Phys. B **73**, 501 (2001).
[2] V. Dierolf et al., Appl. Phys. B **73**, 443 (2001).
[3] V. Gopalan et al., Appl. Phys. Lett. **72**, 1981 (1998).
[4] V. Dierolf and M. Koerdt, Phys. Rev. B **61**, 8043 (2000).

* Corresponding author: e-mail: vod2@lehigh.edu; Phone: 610-758-3915

Naphthalocyanine based time reversal mirror at 800 nm.

J.-P. Galaup[a], S. Fraigne[a], J.-L. Le Gouët[a], J.-P. Likforman[b] and M. Joffre[b]

a-Laboratoire Aimé Cotton, CNRS, Bât 505, Université Paris-Sud, 91405 Orsay cedex, France
b- Laboratoire d'Optique et Biosciences, Ecole Polytechnique, 91128 Palaiseau cedex, France
E-mail : jean-pierre.galaup@lac.u-psud.fr, tel : (33) 1 69 35 20 59 ; fax : (33) 1 69 35 21 00

Broadband materials exhibiting persistent spectral hole burning (PSHB) in the near infra-red region, with photon-gating properties in particular, are of much interest for pulse spectral shaping as they can be used as frequency selective photographic plates for the recording of suitably programmed frequency-domain patterns. To our knowledge, few spectral holography experiments have been done in the frequency domain of Ti-Sa lasers and none demonstrated the control of the phase of femtosecond pulses shaped using spectral holography based on persistent spectral hole-burning.

In this work, we adapted spectral interferometry technique for measuring the amplitude and phase of photon echo signals produced by diffraction of fs pulses on a spectral hologram[1]. The technique was improved in terms of spectral resolution for measuring photon echoes delayed by a few tens of picoseconds. Our study was focused on the measurement of the coherence time of the sample using a photon echo experiment in the photochemically accumulated regime and on demonstrating the pulse-shaping and time-reversal potentialities of our photo-sensitive material.

Spectral holograms were formed through PSHB using a sequence of 2 pump pulses separated by a time delay, in a collinear geometry. Samples were free base naphthalocyanine or Si-naphthalocyanine doped polyvinylbutyral or silicate based xerogels. Absorption peaked at 783 nm and were 20 nm large (FWHM). Our laser source was a 15-fs, 100MHz, Ti:Sa oscillator. A chirp was introduced on one of the two pump pulses and the spectral interferences between chirped and unchirped pulses were engraved. By simply changing the time ordering between the two pulses, the sign of the spectral phase engraved in the sample can be changed. Then the chirped (unchirped) pulse can be recovered by diffraction on the spectral hologram of the unchirped (chirped) pulse. The amplitude and phase of the diffracted pulse are shown on the figure.
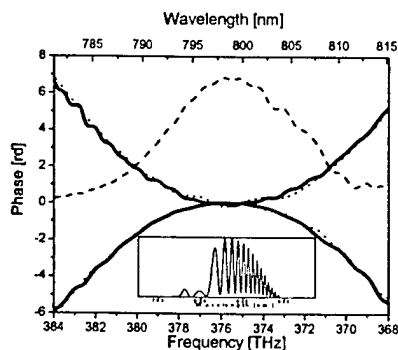
Demonstration of the phase control of femtosecond chirped pulses[2].

Solid lines: spectral phase of the diffracted pulse for two delays $+\tau$ and $-\tau$ between the writing pulses.
Thin dotted lines: spectral phase difference between the 2 writing pulses for the two cases $+\tau$ and $-\tau$.
We also show as a thin dashed line the diffracted pulse spectral amplitude.
Insert: spectral interference fringes between the unchirped and chirped writing pulses at time delay equal 0 at 800nm. The chirp is formed by propagation through a SF58 glass plate of thickness 1.7 cm.

[1] T. Chanelière, S. Fraigne, J.P. Galaup, M. Joffre, J.L. Le Gouët, J.P. Likforman and D. Ricard, "*Femtosecond pulse shaping based on spectral hole burning*", Eur. Phys. J. Appl. Phys. **20** (2002) 205.
[2] S. Fraigne, J.P. Galaup, J.L. Le Gouët, L. Canioni, B. Bousquet, M. Joffre and J.P. Likforman, "*Amplitude and phase measurements of femtosecond pulses shaped using spectral hole burning in free-base naphthalocyanine-doped films*", J. Opt. Soc. Am. B, *in press*, 2003.

Electron-Phonon Coupling in Selectively-Excited Two-Photon Transition: Role of Molecular Symmetry.

M. Drobizhev[1], A. Karotki, Yu. Dzenis, A. Rebane

Department of Physics, Montata State University, Bozeman MT 59717-3840.
Phone +1(406)-994-7826, FAX: +1(406)-994-4452, drobizhev@physics.montana.edu
[1]Permanent address: P.N. Lebedev Physics Institute, Leninsky pr, 53, 119991 Moscow, Russia.

We study spectral gratings in resonant one-photon fluorescence signal, obtained as a result of two-photon excitation of the lowest electronic Q(0-0) transition of tetrapyrrole molecules with a pair of phase-locked 100-femtosecond pulses.

These near-IR pulses (1200 – 1600 nm) were obtained from optical parametric amplifier (TOPAS, Quantronix), pumped with regenerative Ti-Sapphire amplifier (Clark MRX, CPA-1000). A pair of pulses with constant time delay (corresponding to spectral modulation period of 45 cm^{-1}) was delivered by Michelson interferometer and applied to a poly-(vinylbutyral) film, doped with tetrapyrrole dye and placed in a helium cryostat. Q(0-0) fluorescence spectrum was analyzed with a Jobin-Yvon TRIAX 550 spectrometer. In order to extract information on two-photon absorption (TPA) homogeneous spectrum, we have developed a mathematical model, which relates the excitation spectrum profile, TPA absorption, and one-photon fluorescence homogeneous spectral parameters to the observed temperature-dependent modulation contrast, $M(T)$ and phase shift of the spectral grating $\Delta\varphi(T)$. Fluorescence homogeneous spectrum was obtained in independent experiment and substituted in the simulations in form of accurate model function at each temperature. Model calculations show that the temperature-induced shift of the grating is determined by a decrease of Debye-Waller factors of both TPA (α_2) and one-photon homogeneous fluorescence (α_1) spectra, whereas the blurring of spectral modulation mainly results from the phonon sideband temperature broadening. The M value at lowest temperature (4K) is determined by both α_1 and α_2 values, as well as by phonon sideband widths.

We study a series of tetrapyrrole molecules, in which the inversion symmetry varies from almost perfect (Si-2,3- naphthalocyanine dioctyloxide, SiNc) through slightly perturbed (anthraceno-substituted phthalocyanine, AnPc) to completely broken (7,8-dihydroporphin, Chl). While we observe a continuous red shift of the grating with temperature in asymmetric Chl, there is no such shift in symmetric SiNc. Also, even though the α_1 value at 4K is larger for SiNc than for Chl (1.0 vs. 0.55), the contrast M is lower in the former case (0.30 vs. 0.32). These observations are consistent with $\alpha_1 \approx 1$ and $\alpha_2 \approx 0$ for SiNc molecule. This result is not surprising, because for centro-symmetrical molecules, selection rules for one- and two-photon zero-phonon absorption are alternative. On the other hand, the model gives comparable values of α_1 and α_2 for non-symmetrical Chl.

In conclusion, we present the parameters of TPA homogeneous spectrum (Stokes shift, phonon sideband width, Debye-Waller factors) for all the molecules studied and discuss the role of molecular symmetry and Herzberg-Teller effect in electron-phonon coupling.

PHB study on nanoscopic aggregation in random-copolymer bulk films of methyl methacrylate with butyl and benzyl methacrylates

Kazuyuki Horie*, Takashi Kino[1], Shinjiro Machida[2], H. Furukawa
*Department of Organic and Polymer Materials Chemistry, Faculty of Technology,
Tokyo University of Agriculture and Technology,
2-24-16 Naka-cho, Koganei-shi, Tokyo 184-8588, Japan
TEL/FAX +81-42-388-7233   E-MAIL: horiek@cc.tuat.ac.jp*

Two kind of high-molecular-weight homopolymers consisting of chemically-different monomeric units are usually incompatible and their blends, when cooled from the melt or cast from solution, undergo macroscopic phase separation with segregation of the components at equilibrium. In cases of block copolymers, the mutual incompatibility of their blocks leads to microphase separation with a characteristic morphology existing throughout the samples.

On the other hand, a random copolymer is the one where the different monomers are covalently bonded in the main chain randomly, which gives the idea that the random copolymer behaves like a microscopically homogeneous polymer. It is believed so far that a bulk film of a random copolymer usually exhibits no microphase separation.

Nanoscopic aggregation in random copolymers of methyl methacrylate (MMA) with n-butyl methacrylate (n-BMA) or benzyl methacrylate (BzMA) in bulk films has been studied for the first time at low temperatures by using photochemical hole burning (PHB) spectroscopy for tetraphenylporphine (TPP) dispersed in the copolymers. Temperature cycle experiments were carried out for the copolymers with different ratios of comonomer groups. The increases in hole widths due to structural relaxation of butyl groups or benzyl groups in the copolymers of n-BMA or BzMA with MMA were much larger than those expected for hypothetical systems where MMA and comonomer groups with the corresponding molar ratios are randomly dispersed. The results have been attributed to the nanoscopic aggregation of n-BMA or BzMA units with the preferential inclusion of TPP within them in the films. PHB spectroscopy provides a new tool for studying nanoscopic aggregation in transparent random-copolymer bulk films.
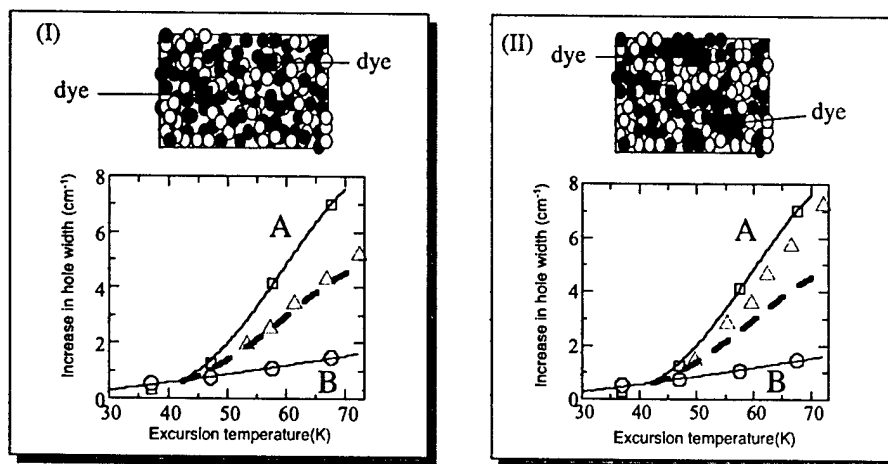

Figure. Schematic pictures of PHB measurements for (I) random copolymer films with randomly located comonomer units at nanoscopic level and for (II) random copolymer films with the existence nanoscopic aggregation and preferential distribution of dye molecules into one of the nanodomains. □: homopolymer A, ○: homopolymer B, △: random copoymer, poly(A/B) (experimental), ---: hypothetical curve for the case (I).

PARAMETER DISTRIBUTIONS OF SINGLE-MOLECULE SPECTRA AND LOW-TEMPERATURE DYNAMICS OF DISORDERED SOLIDS

Yu.G. Vainer[1,*], A.V. Naumov[1], M. Bauer[2], L. Kador[2], E. Barkai[3]

(1) *Institute of Spectroscopy, Russian Academy of Sciences, Troitsk, Moscow reg., 142190, Russia.*

(2) *Institute of Physics and BIMF, University of Bayreuth, D-95440 Bayreuth, Germany.*

(3) *University of Notre Dame, IN 46556, Notre Dame, USA.*

The spectra of single molecules (SMs) embedded in a glassy matrix vary from one molecule to the other, reflecting the random nature of the environments of the SMs. Typical lines of SMs are multi-peaked and fluctuating in time, indicating the dynamical nature of the glass. Hence the characterization of SM lines is a difficult problem. We discuss two approaches. The first one is based on the distribution of line widths. In the second approach, we calculate the cumulants k_1, k_2 etc for each line and then, by measuring many molecules, obtain $P(k_1)$, $P(k_2)$ .... Advantages and disadvantages of the two approaches are discussed, depending on the physical situation and the questions we wish to address.

We measured and simulated distributions of the line widths for the spectra of single *tetra-tert-butylterrylene* (TBT) molecules embedded in amorphous *polyisobutylene* (PIB), at different low temperatures. The simulations were based on the standard tunneling model of low-temperature glasses with appropriate modifications and on the Geva-Skinner stochastic theory of single molecule spectra in glasses [1]. Fig. 1 presents the measured and simulated distributions of line widths.
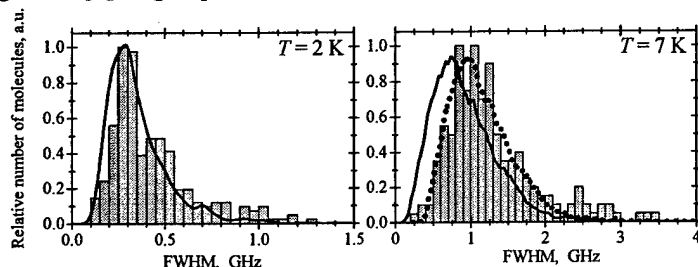
Figure 1. Line width distributions of SM as measured (histograms) and calculated (lines) for TBT in PIB at T=2K and 7K (244 and 187 SM, correspondingly). Solid lines represent the calculations without taking into account the LFM contribution, dotted lines with taking it into account.

The comparative analysis of these data allowed us to evaluate the contribution of quasi-localized low frequency modes to the total spectral shape of SM spectra for different temperatures.

According to the theory of Barkai, Silbey, and Zumofen [2], based on the standard tunneling model of glasses, the probability densities $P(k_1)$, $P(k_2)$, $P(k_3)$ .... are Lévy stable. This result is related to the long-range dipolar interaction between the SM and two-level systems. Analyzing our experimental results for TBT in PIB at 2 K, we show that the distributions of the first two cumulants are compatible with Lévy statistics. Thus the generalized Central Limit Theorem is applicable to this problem. Fig. 2 shows the measured probability densities of the first and second cumulants (dots), together with the results of fits using Lévy statistics (lines).
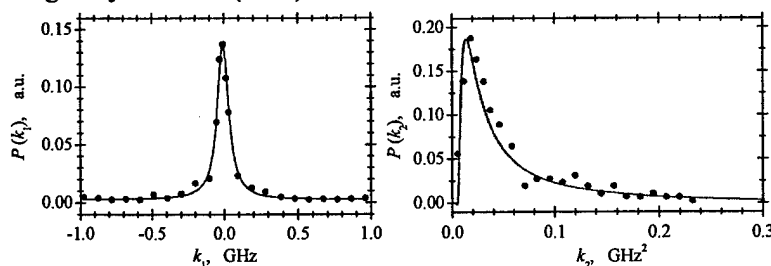

Figure 2. Distributions of the first (a) and second (b) cumulant k_1 and k_2 of SM spectra for TBT in PIB. The curves are one-parameter fits to a Lorentzian and Smirnov's laws, respectively.

[1] E. Geva, J.L. Skinner, *J. Phys. Chem.B*, v. 101, p. 8920 (1997).

[2] E. Barkai, R. Silbey, G. Zumofen, *Phys. Rev. Lett.*, v.84, p. 5339 (2000).

Microscopic exciton properties of fibril-shaped molecular J-aggregates prepared in ultra-thin polymer films

Toshiro Tani, Masaaki Saeki, Yoshihiro Yamaguchi, Toshihide Hayashi and Masaru Oda

Department of Applied Physics, Tokyo University of Agriculture and Technology
[the 21st Century COE program of "Future Nano-Materials"]

2-24-16 Naka-cho, Koganei, Tokyo 184-8588, Japan
Phone: +81-42-388-7153, Fax: +81-42-385-6255, ttani@cc.tuat.ac.jp

Self assembled linear molecular J-aggregates has been attracting attention over a large number of years due to their specific optical properties, due to crucial roles they play in many biological processes such as photosynthesis, and due to great potential they have in technological applications as linear and non-linear nano-optical materials. In linear J-aggregates, the transition moment of the monomer units are more or less arranged to parallel to each other. If an angle with respect to the aggregate axis is less than 54.7 deg, it gives rise to a so-called Frenkel exciton band in which optically allowed states are at the bottom of the energy spectrum. Thus a single red-shifted and usually rather narrow J-band is observed when there is one molecule per unit cell. The structure of J-aggregates may considerably be more complicated than that of a simple linear molecular chain, particularly in case of cyanine dyes. When there are two or more translationally nonequivalent molecules in the unit cell, a split absorption band of two or more Davydov components is expected. For such aggregations with a unit cell composed of more than one molecule, different structural constructions have been proposed to account for the observed optical spectra: zigzag angled chains, herringbone-like structures and even helical structures. As far as based on the extended dipole model developed by Kasha, however, even in these latter cases the directions of the transition dipoles of the optically allowed lowest J-band seem to be aligned parallel to that of their aggregations.

Using micro-spectroscopic techniques of reflection together with AFM we have been studying intensively excitonic properties of higher-order structured fibril-shaped pseudoisocyanine (PIC) J-aggregates in thin ionic polymer PVS films. The most notable features in these investigations are as follows: (1) Large variety of reflection spectra on sub-micrometer size locations of the aggregated structures from simple exciton-like to polariton-like ones characterized with increased reflectivity and broadening. (2) Together with these spectral changes, directions of the local transition dipoles start to deflect from that of the long axis of the fibril structures to almost perpendicular. This behavior is correlated with the onset of polariton-like characters in the local spectra. The above optical features are in some aspect considered to be a common feature for fibril-shaped J-aggregates prepared in different thin-film polymers such as PVS, PVA and polystyrene and are independent of the actual aggregate formation mechanisms. We will also describe and discuss in particular with our recent results of fluorescent imaging and local fluorescent spectra of the J-aggregate fibrils prepared in PVS.

[Ref] *Chem. Phys. Lett.* 331 (2000) 387, *J. Phys. Chem. B* 105 (2001) 12226, *J. Chem. Phys.* 115 (2001) 4973, *Chem. Phys.* 285 (2002) 149, *J. Lumin.* (2003) in press.

Vibrational dynamics of H(D)Cl in cryogenic matrices : from van der Waals interaction to weak hydrogen bond

C. Crépin[a*], M. Broquier[a], A. Cuisset[a], H. Dubost[a], J.-P. Galaup[b], J.-M Ortéga[c], P. Roubin[d]

[a]LPPM, CNRS, Bât 210, Université Paris-Sud, 91405 Orsay, France
[b]Laboratoire Aimé Cotton, CNRS, Bât 505, Université Paris-Sud, 91405 Orsay, France
[c]L.U.R.E., Bât 209, Université Paris-Sud, 91405 Orsay, France
[d]P2IM, Université de Provence, Centre Saint-Jérôme, 13 397 Marseille cedex 20, France

Dynamics in the electronic ground state are essential in the understanding of chemical and biological processes. Hence, we probe vibrational dynamics and focus our attention on the effect of environment on the vibrational coherence times. The study of H(D)Cl embedded in nitrogen or rare gas matrices allows the observation of the behavior of both van der Waals interactions between isolated molecules and the matrix, and weak hydrogen bonds involved in dimers or complexes trapped in the same sample.

Time-resolved one-color DFWM experiments are performed with the Free Electron Laser of Orsay (CLIO). We observe IR accumulated photon echoes and the specific time structure of our experiment gives access to different vibrational processes occurring in very different timescales [1] : dephasing process in the picosecond time scale and spectral diffusion in the nanosecond time scale.

Our results exhibit a dependence of the dephasing time on the strength of the hydrogen bond. This is clearly shown in the investigation of DCl dimers involving two stretching modes perturbed in different ways by the hydrogen bond. A dependence of this time on the lattice host is also observed. In solid nitrogen, spectral diffusion due to energy transfer between isolated DCl molecules is a very rapid process. This efficiency is explained by an enhancement of the vibrational transition dipole moment of the molecule in this peculiar host [2]. In particular, vibrational energy transfers between isotopic species result in the observation of "quantum beats" in DFWM signals which are induced by spectral diffusion between independent two-level systems [3].

[1] C. Crépin, M. Broquier, H. Dubost, J. P. Galaup, J. L. Le Gouët, J. M. Ortéga, Phys. Rev. Lett., 85 (2000) 964.
[2] M. Broquier, C. Crépin, A. Cuisset, H. Dubost, J. P. Galaup, P. Roubin, J. Chem. Phys. (to be published).
[3] C. Crépin, Phys. Rev. A, 67, 013401 (2003).
*tel : (33) 1 69 15 75 39 ; fax : (33) 1 69 15 67 77 ; e-mail : claudine.crepin-gilbert@ppm.u-psud.fr

SITE-SELECTION SPECTROSCOPY OF LOW-TEMPERATURE INCOMMENSURATE PHASES

J. Kikas[1,2], A. Suisalu[2], A. Laisaar[2] and An. Kuznetsov[2]

[1] Department of Physics, University of Tartu, Tähe 4, Tartu 51010, Estonia
phone: +372 7375541, fax: +372 7375540, e-mail: jaakk@physic.ut.ee
[2] Institute of Physics, University of Tartu, Riia 142, Tartu 51014, Estonia

Incommensurate systems represent an interesting intermediate between crystals and more disordered condensed phases [1]. Solid biphenyl is one of very few systems where the incommensurate phase survives down to very low temperatures [2, 3], resulting in peculiar temperature dependence of dopant spectra [4]. This makes it especially appealing for studies by high-resolution methods of optical probing like fluorescence line narrowing and spectral hole burning [3, 5].

The following results will be reported and discussed within the frame of existing theories of incommensurate phases.

A. 2D-excitation/emission spectra were measured for biphenyl doped with free base and Zn-chlorin at 5...50 K. Site energy distributions were obtained and their transformation with temperature is discussed and related to the phase diagram. Beside the features related to zero phonon lines and their phonon sidebands, broad spectral bands were observable in the 2D-spectra attributed to emission after structural relaxation in matrix.

B. Pressure evolution of 2D-spectra of free base chlorin in biphenyl was observed at 5 K for pressures up to 2.2 kbar. The obtained inhomogeneous distribution function (IDF) showed drastic variations with the increase of pressure: the triplet structure observable at normal pressure in the incommensurate phase ICIII converges to a single Lorentzian line in the high-pressure commensurate phase. Calculated spectral moments point to a critical nature of this convergence (critical exponent 0.5) [6].

C. Spectral holes were selectively recorded and compared in (would-be) resonant and nonresonant bands of chlorin dopant, spectral hole burning in a 2D spectrum is demonstrated.

D. Thermal evolution of phosphorescence spectra of pyrene and phenanthrene probes were measured and analyzed. The temperature dependence of the spectral maxima positions for pyrene exhibits discontinuity at 17 K and a critical convergence at 40 K (critical exponent of 0.41). For both pyrene and phenanthrene the incommensurate-incommensurate phase transition at 17 K results in quite a noticable change in the observable Debye-Waller factor as well.

[1] R. Blinc, Phys. Rep., 79 (1981) 33.
[2] J. Etrillard, J. E. Lasjaunias, B. Toudic, and H. Cailleau, Europhys. Lett. 38 (1997) 347.
[3] A. Suisalu, V. Zazubovich, J. Kikas, J. Friebel, and J. Friedrich, Europhys. Lett. 44 (1998) 613.
[4] R. M. Hochstrasser and G. J. Small, J. Chem. Phys. 48 (1968) 3612.
[5] V. Zazubovich, A. Suisalu, and J. Kikas, Phys. Rev. B 64, 104203 (2001).
[6] V. Zazubovich, A. Suisalu, K. Leiger, A. Laisaar, An. Kuznetsov, and J. Kikas, Chem. Phys. 288 (2003) 57.

# Impulsive stimulated scattering on metal and semiconductor interfaces under high pressure

Eric L. Chronister*, Bruce J. Baer, and Masashi Yamaguchi
Department of Chemistry, University of California, Riverside CA 92521
909-787-3288 (phone), 909-787-3420 (fax), eric.chronister@ucr.edu (email)

Impulsive stimulated scattering (ISS) is used to measure the orientation dependence of surface acoustic wave (SAW) velocities on crystalline metal and semiconductor surfaces. ISS data is presented for nickel (100), germanium (100), and aluminum (111) at ambient pressure, and for aluminum under variable high pressure in a diamond anvil cell. The ISS technique is found to be an accurate and robust non-contact method of probing the surface acoustic properties of metal and semiconductor crystalline interfaces.

Brillouin scattering spectroscopy (BS) is a traditional method for studying surface acoustic modes, however, BS can suffer from low scattering efficiency. In contrast, ISS coherently drives surface acoustic modes yielding a relatively large scattering efficiency [1]. In the present study, ISS is used to probe the directional dependence of surface acoustic velocities on crystalline metal and semiconductor interfaces under high pressure in a diamond anvil cell. ISS data is obtained continuously from the Rayleigh surface wave (RSW) branch through the pseudo RSW branch, which is typically not possible with classical Brillouin scattering.

Orientationally resolved acoustic velocity data on crystal surfaces can be used to determine the elastic constants of the material, and the materials studied have significantly different anisotropy factors ($\eta = 2c_{44}/(c_{11}-c_{12})$), leading to different acoustic properties. The ISS results for Ni were found to be more robust than Brillouin scattering with respect to surface quality. The ISS results also correlated well with theoretical calculations, yielding accurate bulk elastic constants. ISS measurements on aluminum under high pressure in a diamond anvil cell have also been obtained, showing the pressure dependence of the Rayleigh and Sholte surface acoustic modes associated with the solid-fluid interface.

The ISS power spectrum for Al at high pressure in shows two frequencies. At high pressure, the sample surface is in contact with a pressure-mediating fluid (nitrogen in this case), and the liquid-solid interface supports the propagation of a Sholte surface mode in addition to the generalized Rayliegh wave, both of which are resolved in the ISS power spectrum below.
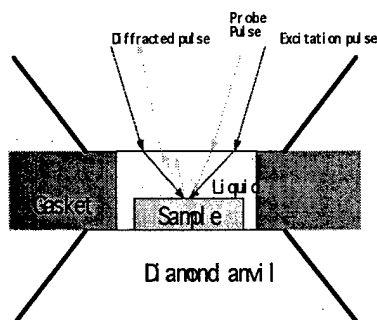
ISS of surfaces in a high pressure diamond anvil cell.
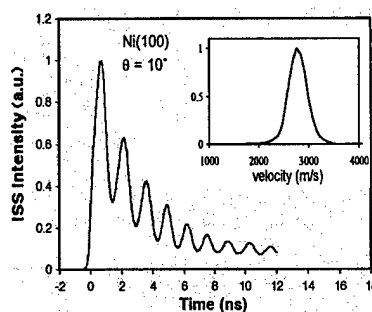
Acoustic velocity for one propagation direction on Ni (100). Inset: power spec.
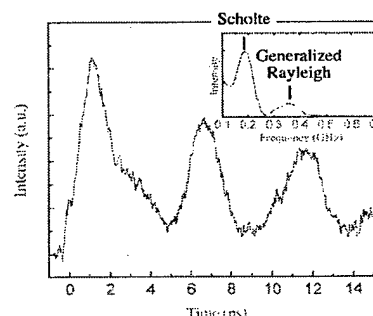
ISS of Al at 1.0 GPa. Inset: ISS power spectrum.

[1] J.A.Rogers, A.A.Maznev, M.J.Banet, K.A.Nelson, *Annu.Rev.Mater.Sci.* **30**, 117-157, 2000.

Single-Molecule Nanosecond Anisotropy Dynamics of Tethered Protein Motions

Dehong Hu[a] and H. Peter Lu[b]

Pacific Northwest National Laboratory, Fundamental Science Division,
P.O. Box 999, Richland, Washington 99352, USA

Confined and hindered protein motions generally exist in living cells, with tethered proteins or protein domains particularly associated with the early events of molecular interactions in cell signaling at extra- and intracellular membrane surfaces. Ensemble-averaged, time-resolved fluorescence anisotropy has been extensively applied to study the protein rotational and conformational motion dynamics under physiologically relevant conditions. However, the spatial and temporal inhomogeneities of the stochastic protein rotational and conformational motions are very difficult to characterize with such ensemble-averaged measurements. Here we demonstrate the use of single-molecule nanosecond anisotropy to study the tethered protein motion of T4 lysozyme molecules on a biologically compatible surface under water.[1] The rotational motions of the tethered proteins are confined in a half-sphere whose volume is primarily defined by the linker and the surface. We observe dynamic inhomogeneities of the rotational diffusion dynamics, i.e., diffusion rate fluctuation, because of interactions between the proteins and the surface. However, we also find that the long-time averages of the dynamically inhomogeneous diffusion rates of single molecules are essentially homogeneous among the single molecules examined. These results suggest that the motions of proteins tethered to surfaces are dynamically inhomogeneous, even if the surfaces or the local environments are homogeneous. Furthermore, the tethered-proteins are found to be in solution without rotational rate fluctuations for most of the time during the measurements, suggesting that he tethered protein molecules stay predominately in solution, rather than being fixed on the modified surface. The infrequent surface interactions are not energetic enough to fix the protein rotational motions. Our results also suggest that the use of tethered proteins on modified glass surfaces under water is a reasonable way to study protein dynamics in solution, as many single-molecule experiments have demonstrated. Our approach allows the recording of time trajectories of the single-molecule rotation rate fluctuation and reveals the single-molecule rotational motion over a wide time scale from sub-nanoseconds to seconds.

Reference:

1. Dehong Hu and H. Peter Lu, "Single-Molecule Nanosecond Anisotropy Dynamics of Tethered Protein Motions", *J. Phys. Chem. B*, 107 (2), 618-626, 2003

a)   Presenting author. Email: dehong.hu@pnl.gov, Phone: (509)376-5709, FAX: (509)376-6066
b)   Email: peter.lu@pnl.gov, Phone (509)376-3897, FAX: (509)376-6066

UV HOLE BURNING OF PROTEINS VIA PHOTOBLEACHING OF INTRINSIC AMINOACIDS

Markus Stübner, Christoph Hecht and Josef Friedrich

Physik-Department E14 und Lehrstuhl für Physik Weihenstephan, TU-München, 85350 Freising, Germany

We investigated the 58-aminoacid protein *bovine pancreatic trypsin inhibitor (BPTI)*at a concentration level of about 9.10^{-3} M in a glycerol/water solvent. BPTI is a globular protein with a molecular weight of 6511 Da. The main secondary structural features are 2 α-helices, 2 β-strands and 3 disulfide bonds. As to the aromatic aminoacids, there are 4 phenylalanins as well as 4 tyrosines. The red edge range of the BPTI-UV-absorption ($33000\text{-}36000$ cm^{-1}) is due to the absorption of the 4 tyrosines. Narrow bandwidth hole burning is possible in a frequency window around 35000 cm^{-1} covering roughly 1000 cm^{-1}. The associated photoreaction is most probably a light induced proton rearrangement reaction involving the hydroxy-group at the aromatic ring. The longwavelength part of the red edge absorption outside the above mentioned frequency window, however, is not sensitive to laser photochemistry. Possible reasons could be due to energy transfer between the respective tyrosines, to structural restrictions which prohibit persistent proton displacement or to strong electron phonon coupling.

Although the UV-holes were rather shallow, the signal to noise ratio was good enough to investigate the influence of pressure and electric fields on the holes. In order to come up with distinct conclusions we compared the behavior of the holes in the protein with the respective one in a frozen solution of tyrosine in the same solvent.

As to the response to pressure, tyrosine in the glycerol/water glass shows a behavior which is very similar to the respective one of the protein. The conclusion is that the elastic properties (i.e. the compressibility) of the nearby environments of the probe must be the same in both cases. The protein surface is likely to be hydrated, even in a glycerol/water solvent. There is one tyrosine out of the 4 in BPTI, namely tyrosine 10, which sticks out considerably into the hydration shell. If it is tyrosine 10 which is photobleached in the hole burning reaction, then the local environment is largely water. On the other hand, it is not unlikely that hydrophobic probe molecules like tyrosine induce a micro phase separation in a glycerol/water mixture which results in a locally ordered solvent cage of water molecules with rather strong hydrogen bonds. Hence, depending of the range of the probe solvent interaction, it is possible that, in both solutions, the tyrosine molecules may largely probe similar environments.

As to the response to the external Stark-field, there are distinct differences between Tyr 10 in the protein and Tyr in glycerol/water solution: Although the Stark-spectra show a splitting in both cases which results from a significant dipole moment of the probe, the splitting is considerably larger in the solution than in the protein. Consequently, the respective dipole moment differences are larger in the solution than in the protein. We conclude that the rather ordered structure of the protein generates a local matrix field which counteracts the charge separation in the free Tyr so that the dipole moments are reduced. Quantum chemistry calculations for the phenol moiety (*A. L. Sobolewski, W. Domcke, J. Phys. Chem. A 105 (2001), 9275*) show that the elctrostatic differences between the ground state and the excited state is most likely due to the formation of complexes with water molecules involving the phenolic H-group.

Phone: ++49 8161-713293   *Fax:* ++49 8161-4517 *Email:* J.Friedrich@lrz.tu-muenchen.de

Correlation Between Energy Disorder and Excitonic Couplings in the LH 2 Complex from *Rhodopseudomonas Acidophila*. (A High Pressure Spectral Hole Burning Study.)

V. Zazubovich, K. Riley, R. Jankowiak, G. J. Small
Ames Laboratory, USDOE and Department of Chemistry, Iowa State University,
Ames, IA 50011.
Phone: (515)-294-69-42; Fax: (515)-294-16-99; E-mail: valterz@iastate.edu

Summary:

We studied the effects of high pressure (up to 1015 MPa) on excitonic coupling energies and energy disorder in the light-harvesting complex 2 (LH-2) from *Rhodopseudomonas Acidophila* (strain 10050) at 5K. The pressure dependences of the widths and positions of the B850 and B870 bands were determined. The latter band corresponds to the lowest exciton level of the B850 ring and is forbidden in absorption in the absence of disorder. While the parameters of the B850 band could be obtained directly from the absorption spectra, hole burning action spectra were used to determine the parameters of the B870 band. The results show that the parameters of the B850 and B870 bands are linearly correlated, consistent with recent theoretical predictions [1].
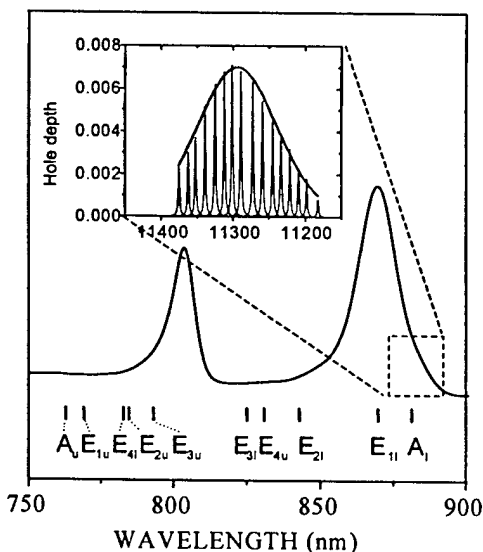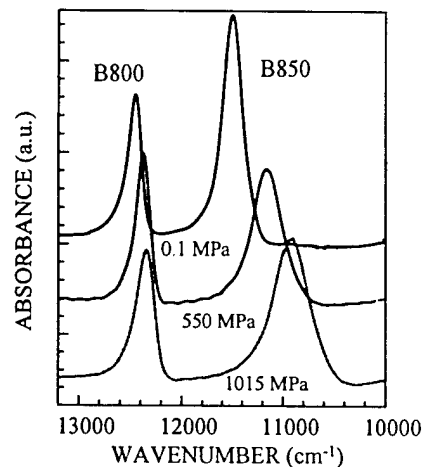
Excitonic calculations for the B850 ring of bacterio-chlorophyll *a* molecules were performed in the nearest dimer-dimer coupling approximation. It was shown in [2] that any arbitrary diagonal or off-diagonal energy disorder in LH-2 can be presented as a superposition of disorders with different symmetries, and that the response of the B870 band (intensity, absorption bandwidth, displacement from the B850 band maximum) to arbitrary energy disorder can be successfully approximated by its response to E_{1+} type diagonal disorder. Coupling parameters and the extent of disorder were deduced by comparing experimental results with these calculations. It was demonstrated that the pressure dependences of the nearest-neighbor coupling energies and the width of the distribution function for energy disorder are positively correlated, both increasing with pressure. An effective pressure-dependent excitonic Hamiltonian for the B850 ring was obtained.

References:
1: Jang et al. *J. Phys. Chem.* B 2001, 105, 6655.
2: Wu et al. *J. Phys. Chem.* B 1997, 101, 7654.

A Quantum-Mechanical Model for Determination of Internal Electric Fields at Protein Active Sites from the Stark Effect on Persistent Spectral Holes

Peter Geissinger*, Jörg C. Woehl[*], and Barry J. Prince[§]

*Department of Chemistry
University of Wisconsin-Milwaukee
3210 N. Cramer Street
Milwaukee, WI 53211
U.S.A.
Phone: +1 414 229-5230; Fax: +1 414 229-5530; E-mail: geissing@uwm.edu

[*]Laboratoire de Spectrométrie Physique
Université Joseph Fourier Grenoble et CNRS
BP 87 - 38402 Saint Martin d'Hères cedex
France
E-mail: jorg.woehl@ujf-grenoble.fr

[§]Research School of Chemistry
Australian National University
Canberra, ACT 0200
Australia
E-mail: baz@rsc.anu.edu.au

In condensed matter the electric fields that originate from the charge distributions of the individual molecules combine to form an internal molecular electric field. Such molecular electric fields can play crucial roles for the functions of biological systems. We are investigating methods for the experimental determination of the magnitude of these internal molecular fields at molecular or even at atomic resolution. By monitoring the external-field induced changes of spectral holes burnt into the inhomogeneously broadened absorption bands of specific "detector" molecules, information about the internal electric field that is present at the detector molecule sites can be extracted. For the determination of the internal fields in molecular resolution, the numerical diagonalization of the Hamiltonian of the detector molecule is required. We will discuss the effects of basis set size and local field factor on the magnitude of the internal fields.

Rotational Diffusion of the Transmembrane Anion Exchange Protein *AE1* at the Single Molecule Level

M. Andreas Lieb and Lukas Novotny

The Institute of Optics, University of Rochester, Wilmot Building, Rochester, NY 14627

Phone: (585) 275 5104, Fax: (585) 244 4936, email: lieb@optics.rochester.edu

Prithwish Pal and Philip A. Knauf

Department of Biochemistry and Biophysics, University of Rochester School of Medicine and Dentistry, Rochester, NY 14642

We present measurements of the rotational diffusion of the human erythrocyte anion exchange protein *AE1* (also called *band 3*) in the red blood cell membrane at the single molecule level. *AE1* carries out a very tightly coupled one-for-one exchange of anions, namely Cl^- for bicarbonate HCO_3^-, and plays a fundamental role in CO_2 transport. It is known to be partly bound to the membrane skeleton and partly freely diffusing in the membrane, leading to fractions with different rotational correlation times [1, 2]. Fluorescence labeling of *AE1* is performed using an oxonol dye, which is known to bind rigidly to the protein [3]. This ensures that the fluorophore rotational diffusion reports directly the protein rotational diffusion.
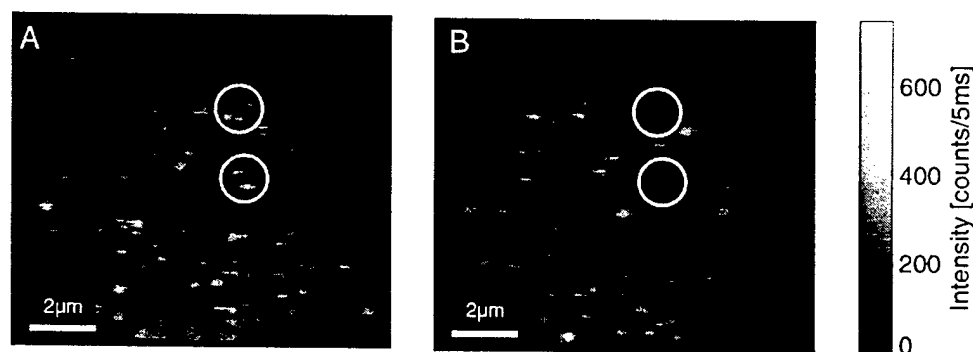
Fig. 1: Labeled *AE1* proteins in red blood cell ghosts: A) initial image, B) image after bleaching of several dyes, e.g. those marked by the white circles.

Measurements of the correlation times were performed using a polarization correlation method as described in [4]. In Fig. 1 images of labeled red blood cell ghosts (sliced cells with removed cytoplasm) are presented, showing single molecule sensitivity and good background suppression. Whereas the correlation times of the fastest diffusing fractions can not be accessed experimentally, those of the slower fractions can be measured.

References:

[1] R. J. Cherry, A. Burkli, M. Busslinger, G. Schneider, and G. R. Parish, "Rotational diffusion of band 3 proteins in human erythrocyte-membrane," *Nature* **263**, 389-393 (1976).

[2] E. D. Matayoshi and T. M. Jovin, "Rotational diffusion of band-3 in erythrocyte-membranes. 1. Comparison of ghosts and intact-cells," *Biochemistry* **30**, 3527-3538 (1991).

[3] N. M. Raha, L. J. Spinelli, and P. A. Knauf, "WW781, a potent reversible inhibitor of red cell Cl⁻ flux, binds to band 3 by a two-step mechanism," *Am. J. Physiol. (Cell Physiol.)* **265**, C521-C532, (1993).

[4] T. Ha, J. Glass, T. Enderle, D. Chemla, and S. Weiss, "Hindered rotational diffusion and rotational jumps of single molecules," *Phys. Rev. Lett.* **80**, 2093–2096, (1998).

Hole burning study of cyanobacterial Photosystem II complexes containing small putative chlorophyll-binding proteins

J. Hála[a], R. Dědic[a], J. Pšenčík[a], M. Kořínek[a], K. Promnares[c], M. Tichý[b,c], J. Komenda[b,c], Ch. Funk[d]

[a] Department of Chemical Physics and Optics, Charles University,
Ke Karlovu 3, CZ–121 16 Prague 2; Czech Republic
[b] Department of Autotrophic Microorganisms, Institute of Microbiology,
Academy of Sciences of the Czech Republic,
Opatovický Mlýn, CZ–379 81 Třeboň, Czech Republic.
[c] Institute of Physical Biology, University of South Bohemia, Zámek 136, CZ-373 33 Nové
Hrady, Czech Republic
[d] Department of Biochemistry and Umeå Plant Science Center, Umeå University, SE-901 87
Umeå, Sweden

Hole burning spectroscopy is widely applied to various chlorophyll-proteins of oxygen evolving photosynthetic systems [1,2]. In this contribution we present low temperature absorption and both broad band and site selective excited fluorescence spectra together with persistent hole burning of photosystem II complexes from the cyanobacterium *Synechocystis PCC* 6803 differing in the content of small cap-like proteins. These proteins are homologous to light-harvesting complex of higher plants and may bind pigments [3,4]. Observed zero phonon hole-widths enabled us to determine excited state lifetimes. The ratio of phonon side-band and zero-phonon hole areas together with spectral shape of inhomogeneously broadened function provided additional information concerning chlorophyll-protein coupling. Comparison of these values to those obtained previously with cyanobacterial chlorophyll-protein complexes CP47 and CP34 [5,6] enabled us to evaluate functions previously proposed for these high light induced proteins.

REFERENCES
[1] H.C. Chang, R. Jankowiak, C.F. Yocum, R. Picorel, M. Alfonso, M. Siebert and G.J. Small, J. Phys. Chem. 98, 7717–7724 (1994).
[2] F.T.H. den Hartog, J.P. Dekker, R. van Grondelle and S. Voelker, J. Phys. Chem. B 102, 11007–11016 (1998).
[3] G. Shen and W.F.J. Vermaas, J. Biol. Chem. 269, 13904-13910 (1994).
[4] Q. Hess, N. Dolganov, O. Bjoerkmann and A. Grossman, J. Biol. Chem. 276, 306–314 (2001).
[5] T. Polívka, P. Kroh, J. Pšenčík, D. Engst, J. Komenda and J. Hála, J. Luminescence 72-74, 600-602 (1997)
[6] M. Lovčinský, R. Dědic, J. Komenda and J. Hála, J. Luminescence 86, 415–419 (2000)

Author that is responsible for further correspondence: J. Hala, Department of Chemical Physics & Optics, Charles University, Ke Karlovu 3, CZ 121 16 Prague 2; Czech Republic, fax: (4202) 2191 1249, phone: (4202) 2191 1421, E-mail: hala@karlov.mff.cuni.cz

OPTICAL DEPHASING IN
LIGHT-HARVESTING COMPLEXES OF PURPLE BACTERIA

J. Gallus[1], S. Bonsma[1], F. Könz[1], S. Jezowski[1],
M. Wendling[2], R. van Grondelle[2] and S. Völker[1,2]

[1] *Huygens and Gorlaeus Laboratories, University of Leiden, The Netherlands.*
[2] *Department of Biophysics, Free University, Amsterdam, The Netherlands..*

The degree of excitonic coupling in light-harvesting (LH) complexes of photosynthetic bacteria is still a controversial issue and much work has and is being done to clear it up [1-6]. Purple bacteria have two ring-shaped LH-complexes, a peripheral LH2-complex containing 9 bacteriochlorophyll (BChl) molecules and a core-complex LH1 with 18 closely packed BChls, and a reaction center (RC) that is surrounded by LH1 [7]. Energy from the sun is collected by the LH2-complexes and transferred very efficiently to LH1 and subsequently to the RC, where charge separation takes place. The absorption spectrum of the LH2-complex shows two bands, one at ~ 800 nm and another at ~850 nm (see figure). They correspond to BChl-molecules in the B800 and B850 rings.
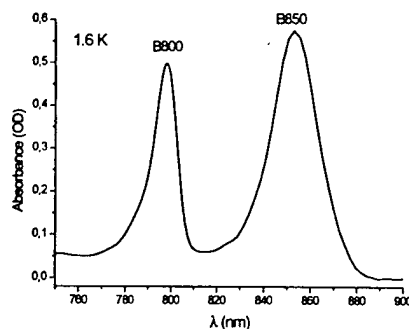
The large interaction energies between nearest neighbor molecules in the B850 band lead to a delocalization of the excitation energy, which is limited by static and dynamic disorder. Since there is no agreement in the literature about the extent of this delocalization, we have studied the excitation dynamics of the B850 band of *Rb. Sphaeroides G1C* by spectral hole-burning. Very narrow holes have been found from which the homogeneous linewidth Γ_{hom} was derived. From the temperature dependence of Γ_{hom}, we draw conclusions about the optical dephasing process, which we compare to results reported in the literature on hole-burning [3] and accumulated photon echoes [8]. The spectral distributions of holes will be discussed in relation to simulations that yield an estimate of the static disorder and the coupling strength between BChl-molecules.

[1] V. Sundström et al., *J.Phys.Chem.B* **103** (1999) 2327-2346.
[2] V. Novoderezhkin et al., *J.Phys.Chem. B* **103** (1999) 10540-10548.
[3] H.M. Wu et al., *J.Phys.Chem. B* **101** (1997) 651-656; *J.Phys.Chem. B* **101** (1997) 7654-7663.
[4] A.M. van Oijen et al., *Science* **285** (1999) 400-402; *Biophys. J.* **80** (2001) 1591-1603.
[5] M.V. Mostovoy and J. Knoester, *J.Phys.Chem.B* **104** (2000) 12355-12364.
[6] S. Jang et al., *J.Phys.Chem.* **105** (2001) 6655-6665.
[7] G. McDermott et al., *Nature* **374** (1995) 517-521
[8] S.S. Lampoura et al., *J.Phys. Chem. B* **104** (2000) 12072-12078.

Quantitative predictions of fluorescence quantum yields for tryptophan in proteins

Patrik R. Callis* and Tiqing Liu
Department of Chemistry and Biochemistry
Montana State University
Bozeman, MT 59717

One of the most remarkable observations related to the widely-used intrinsic fluorescence of tryptophan (Trp) in proteins is the large variation of fluorescence quantum yields (F_f) and lifetimes in different protein environments. The yields vary from near 0.35 down to 0.01 or less. This is particularly interesting because the light-absorbing part of Trp, effectively 3-methylindole (3MI), shows little variability in F_f when dissolved in different solvents varying in polarity from pure hydrocarbon to water, being always near 0.3.

New Paradigm for Tryptophan Fluorescence Brightness in Proteins: Location is everything: No longer think of certain amino acids as electron acceptors. Instead, any charged amino acid can tune the energy gap between the usual fluorescing state and the charge transfer state on local amide. When the charge transfer (CT)state is stabilized, quenching occurs.
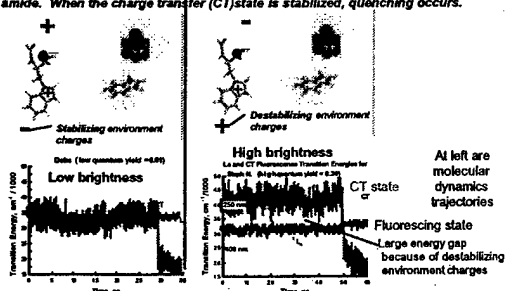
A reasonable basis for the puzzling variation is revealed through quantum mechanics-molecular mechanics simulations in which the energy of the lowest Trp ring-to-amide backbone charge transfer (CT) state is monitored during dynamics trajectories for 20 Trps in 17 proteins. The energy, fluctuations, and relaxation of the high lying CT state are found, unexpectedly, to be extremely sensitive to protein environment (local electric field) and rotamer conformation, leading to large variations in ^1L_a fluorescence yield and lifetime.
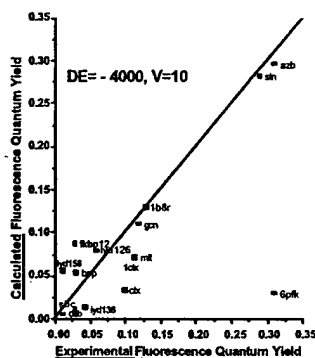
Using a semiempirically adjusted energy gap and electronic coupling, the energy gap variance from molecular dynamics simulations, and a Franck-Condon weighted density of states from ab initio computations in Marcus theory captures the general behavior of the quantum yields for this randomly selected set of single Trp proteins. The basic idea is that those proteins for which the local electric field and fluctuations allow the fluorescing state and CT state to become degenerate often, there will be high probability for trapping the excitation in the non-fluorescent CT state due to fast relaxation of the protein/solvent lattice

* Corresponding Patrik Callis Ph: 406-994-5414, Fax 406-994-5407, email: pcallis@montana.edu

Intraband relaxation of Frenkel excitons in molecular aggregates of low dimensionality

J.P. Lemaistre

Laboratoire des Milieux Désordonnés et Hétérogènes, CNRS UMR 7603, Université P. et M. Curie Tour 22, 4 place Jussieu 75252 Paris Cedex 05, France

Abstract

Dynamic processes of Frenkel excitons in mesoscopic aggregates of molecules forming nanostructures are currently investigated. Many experimental and theoretical works are devoted to the exciton dynamics in molecular systems of low dimensionality like H [1,2] or J [3-5] aggregates, dye aggregates exhibiting a Davydov splitting [6,7], or cyclic aggregates [8]. In general, these aggregates of finite size, are characterized by relatively strong intermolecular interactions due to the long range dipole-dipole couplings. Thus, the cooperative effects are dominant (even at room temperature) and are generally discussed in terms of collective excitation states.

In this contribution, a theoretical model, based on the numerical calculations of the Frenkel exciton eigenstates and their participation ratios, is presented in order to analyze the photophysical properties of interest (oscillator strengths, delocalization lengths, optical lineshapes, radiative lifetimes). The exciton dynamics originating from the coupling of excitons to the vibrations creates temperature dependent local fluctuations in the molecular site energies which are characterized by their amplitude and their correlation time. A microscopic model of exciton-phonon coupling is introduced assuming a Bose-Einstein distribution for the phonon occupation density. The phonon-assisted scattering from the initially excited states redistributes the oscillator strengths within the states of the quasi exciton band. Using a stochastic exciton-phonon model, the intraband scattering among excitons is described as an incoherent energy transfer. The scattering rates are calculated and used in a master equation to obtain the time evolution of the exciton populations after initial excitation of the exciton band. Thus, the optical lineshapes (absorption and fluorescence) and radiative lifetimes are discussed as a function of the temperature and of the exciton-phonon coupling parameters.

Our theoretical results are checked against experimental data available on various types of one-dimensional molecular aggregates.

[1] J.P. Lemaistre, Chem. Phys. 246 (1999) 283.
[2] D. Markovitsi, L.K. Gallos, J.P. Lemaistre and P. Argyrakis, Chem. Phys. 269 (2001), 147
[3] V.K. Kamalov, I.A. Struganova and K. Yoshihara, J. Phys. Chem. 100 (1996) 8640.
[4] M. Bednarz and J.P. Lemaistre, Int. J. of Mod. Phys. B15 (2001) 3761.
[5] M. Bednarz, V.A. Malyshev, J.P. Lemaistre and J. Knoester, J. of Lum. 94/95 (2001) 271.
[6] L.K. Gallos, A.V. Pimenov, I.G. Scheblykin, M. van der Auweraer, G. Hungerford, O.P. Varnavsky, A. G. Vitukhnovsky and P. Argyrakis, J. Phys. Chem. B104(2000)3918.
[7] D.M. Basko, A.N. Lobanov, A.V. Pimenov and A. G. Vitukhnovsky, Chem. Phys. Letters 369 (2003) 192.
[8] M.V. Mostovoy and J. Knoester, J. Phys. Chem B104 (2000) 12355.

Optically induced spin polarisation of the nitrogen-vacancy centre in diamond.

J. Harrison, M. J. Sellars, and N. B. Manson

Laser Physics Centre, Australian National University.

(Dated: March 1, 2003)

Optical readout of the ground state electron spin of a single nitrogen-vacancy (N-V) centre in diamond has potential applications in quantum computing and spintronics. The optical detection of single N-V centres is now well established, using such techniques as confocal microscopy and fluorescence excitation spectroscopy[1,2]. The centre has a paramagnetic ground state (total spin angular momentum S = 1) with an optical transition (at 1.945eV) to the lowest lying triplet excited state. There is strong evidence that a preferential population of the m_s=0 ground state spin level results from even weak optical pumping of this transition[3,4]. However, quantum computing applications require a cyclic transition, i. e. that the m_s=0 (ground state) $\rightarrow$ m_s=0 (excited state) transition can be excited, and the fluorescence (from the subsequent decay) observed, for many cycles (on a time scale long enough to make a spin measurement) before a transition to the ground state m_s=1 (or m_s=-1) spin level occurs. To date, the cyclic nature of the N-V optical transition has not been elucidated by experiment. We have used the results of electron paramagnetic resonance spectroscopy, in the "dark" and with laser illumination of the sample, to determine the degree to which this transition is cyclic. The results of these measurements, at room temperature and low temperature, will be presented and possible implications for the use of the N-V centre in quantum computing applications discussed.

Contact details:
Email: jph111@rsphysse.anu.edu.au
Phone: (+612) 6125 4129
Fax.: (+612) 6125 0029

[1] A. Gruber, A. Dräbenstedt, C. Tietz, L. Fleury, J. Wrachtrup, and C. von Borczyskowski, Science **276** 2012 (1997).

[2] F. Jelezko, C. Tietz, A. Gruber, I. Popa, A. Nizovtsev, S. Kilin, and J. Wrachtrup, Single Mol. **2** 255 (2001).

[3] J. H. N. Loubser and J. A. van Wyk, Diamond Research 11 (1977).

[4] D. A. Redman, S. Brown, R. H. Sands, and S. C. Rand, Phys. Rev. Lett. **67** 3420 (1991).

Persistent Spectral hole burning studies in Lithium fluoride color centers

William Conway and B. Rami Reddy*
Alabama A&M University, Department of Physics, P. O. Box 1268, Normal, AL 35762
Tel: 256-858-8101; Fax: 256-851-5622; *E-mail: brreddy@aamu.edu

Summary

High-resolution spectroscopy and optical hole burning (HB) studies are performed on lithium fluoride color centers. Color centers were produced by exposing the material to gamma radiation. Room temperature measurements revealed broad absorption extending up to 660nm having a strong peak at 445nm with a full width at maximum of 3883 cm^{-1}. Its optical density is 3.42 and the corresponding absorption coefficient is 7.9cm^{-1}. However the low temperature transmission measurements revealed several zero-phonon lines. In this presentation we will discuss the high resolution spectroscopy measurements of 601nm zero-phonon line (ZPL). It was observed in transmission as well as emission. Hole burning studies were not performed at this wavelength previously[1,2]. Under 580 nm excitation it showed broad emission peaking at 645nm.

A high resolution excitation spectrum of 645nm emission revealed a strong ZPL at 600.7nm and weak ZPL at 601.3nm. The inhomogenous broadening of the strong ZPL varied from 5.3 cm^{-1} (10K) to 34cm^{-1} (80K). Above 100K the ZPL is not detected at all. At high irradiation densities >3.9kW/cm^2 we were able to burn holes. At lower powers hole burning was not observed at all. This clearly indicates that the HB requires more than one photon. Hole kinetics are performed as a function of temperature and time. Hole depths of ~30% were achieved very easily. We were able to burn multiple holes in this material up to 40K. All the holes remained for the whole day at low temperature without any change in shape or depth. This implies that this material is very useful for long term information storage. Even if the temperature of the material is increased to 100K, it did not lose the hole. The hole reappeared after it is cooled back.

There is also energy transfer occurring in the material. That is when the main peak at 600.7nm is exposed to laser light another peak is produced at 600nm. We were able to burn persistent holes in all the peaks at 600, 600.7 and 601.3nm. This clearly indicates that all these peaks are zero-phonon lines belonging to different sites.

References:

1. W. E. Moerner, P. Pokrowsky, F. M. Schellenberg and G. C. Bjorklund, Phys. Rev. B33, 5702 (1986).
2. V. V. Federov, S. B. Mirov, M. A. Ashenafi and L. Xie, Appl. Phys. Lett. 79, 2318 (2001).

Optical hole burning in europium doped borate glasses

Rajamohan R. Kalluru, Elizabeth Schoolfield and B. Rami Reddy*
Alabama A&M University, Department of Physics, P. O. Box 1268, Normal, AL 35762
Tel: 256-858-8101; Fax: 256-851-5622; *E-mail: brreddy@aamu.edu

Summary

Our effort is to improve hole burning efficiency of sodium borate glasses. We made sodium borate glasses doped with europium in ambient air, nitrogen and reducing atmosphere. In some glasses the dopant concentration is ~ 2mol%. The samples are made by mixing appropriate chemicals thoroughly and then melted in a high temperature furnace at 1400°C for an hour. Afterwards the melt was cooled in ambient air. It was polished manually using different grades of sand papers and polishing compounds. For comparision we made two undoped glasses under similar conditions.

A room temperature absorption revealed Eu^{3+} peaks at 393 ($^7F_0 \rightarrow ^5D_3$) and 465nm ($^7F_0 \rightarrow ^5D_2$). Under Argon ion laser excitation it did reveal Eu^{3+} emission at 612nm ($^5D_0 \rightarrow ^7F_2$). The $^7F_0 \rightarrow ^5D_0$ absorption peak did not appear in conventional absorption measurements even at cryogenic temperatures. However an excitation spectrum of 612nm ($^5D_0 \rightarrow ^7F_2$ emission) revealed the $^7F_0 \rightarrow ^5D_0$ absorption centered at 579nm having a fullwidth at half maximum of $62.6cm^{-1}$. For hole burning experiments a low resolution dye laser of linewidth $2cm^{-1}$ was resonantly tuned to the center of the excitation maximum. Typical irradiance is $12kW/cm^2$. The sample was exposed to the laser for about 15 to 30 minutes. The excitation spectra recorded before after exposure was compared to identify the hole. For excitation spectral recording the same laser power was reduced by a factor of 80 and the laser wavelength was scanned simultaneously monitoring the strong emission at 612nm.

In our measurements we did not observe hole burning in glasses made in the ambient air or nitrogen atmosphere. But we observed holes in glasses made in a reducing atmosphere. The hole lasted for a couple of hours and disappeared above 100K. However when a 5% yttrium oxide was added to the base glass (hereafter called co-doped glass) the hole burning was observed even above the room temperature. In the latter glass we are able to burn deeper holes ~24% in depth, very easily. Hole burning efficiency was estimated in both the glasses using the formulations given elsewhere[1].

The hole burning efficiency increased from 4.3×10^{-5} to 2.6×10^{-3} in the co-doped glass. To understand the effect of reducing gas as well as Y^{3+} on the hole burning, we compared the absorption spectra of undoped and doped glasses. It appeared that the co-doped glass developed more defects. Moreover a larger amount of Eu^{3+} reduced to Eu^{2+} in the co-doped glass. Hole burning is due to charge exchange with the traps.

[1] W.E.Moerner, M. Gehrtz and A.L. Hustor, J. Phys. Chem. 88, 6459 (1984).

A new way to model spectral hole burning.

T. Reinot, N. C. Dang, and G. J. Small
Iowa State University and Ames Laboratories, Ames, Iowa, USA

It has been known since its discovery that a spectral hole burning has complicated spectral and temporal characteristics, such as: highly non-exponential growth; hole broadening, which depends on time and intensity of the burn; spontaneous and light-induced hole filling (SHF, LIHF); interference between hole, photoproduct, and phonon sidebands; and spectral diffusion (SD). On the other hand, large inhomogeneous/homogeneous linewidth ratios (often in the order of 10^5) force one to use million point data arrays in simulations. The complexity of the burn and the volume of necessary calculations has been the biggest obstruction in hole growth modeling. Due to progress in personal computing and due to a better understanding of HB processes it is now possible for the first time to provide a single model, which describes the evolution of the hole burned spectrum including all above mentioned hole growth and filling aspects.

Initially, this model was created to describe the experimental observation - a ZPH can be filled 100% using LIHF, either by white light or using a laser. To provide the required photomemory a 2-dimensional site distribution function (SDF) was created. While the abscissa describes the site's 'regular' absorption frequency, the ordinate labels the site's origin frequency it possesses before any interaction with the light. Due to the discrete nature of computer modeling, a site distribution matrix is created, the diagonal of which describes the educt and all off-diagonal elements describe the product. As hole burned spectrum is observed (or hole is burned) the absorption occurs due to both educt and product sites, which are at resonance with the observation (burn) frequency. A temperature dependent single site absorption spectrum can be calculated in usual manner e.g. as treated in [1]. The size of the matrix is reduced by introducing non-linear frequency axes. Hole burning at frequency ω_{B1} occurs using dispersive hole growth model, which is described in [2]. The strong point of this model is that successive holes are burned into already hole burned spectrum. Although product formation is treated phenomenologically (due to lack of information of the underlying processes), LIHF occurs automatically due to the absorption of product states created by previous burns. Similarly to the hole growth, SHF displaces sites dispersively in the matrix bringing off-diagonal, i.e. product sites, back to the diagonal, thus reversing product into educt. Hole growth and filling occur iteratively in small time intervals enabling interplay between filling and growing of the same hole. Spectral diffusion is treated analogously to a '2D-Gaussian blur filter', which is used in image processing.

This model has been successfully applied to describe hole evolution in free base phthalocyanine in hyperquenched 1,2-dichlorobenzene glass [3]. Free base phthalocyanine is known to hole burn due to photo-tautomerization, therefore, hole burning takes place intramolecularly and exponential growth kinetics is expected. Experimental results, however, show highly dispersive kinetics, which was assigned to coupling of the glassy matrix with the tautomerizing protons.

1. J. M. Hayes, P. A. Lyle, G. J. Small, J.Phys.Chem.,98 (1994), 7337.
2. T. Reinot, G. J. Small, J. Chem. Phys., 114 (2001) 9105.
3. T. Reinot, N. C. Dang, G. J. Small, submitted to J.Chem.Phys.

Hole Burning of Inorganic-Organic Hybrid Materials Prepared by Sol-Gel Method

H. Hanzawa[a], Y. Kanematsu[b], E.Tashiro[c], D. Ueda[c], G. Adachi[c], and K. Machida[d],

[a]Division of Materials Physics, Graduate School of Engineering Science, Osaka University,

1-3 Machikaneyama-cho, Toyonaka, Osaka 560-8531, Japan.

[b]Venture Business Laboratory, Osaka University, 2-1 Yamadaoka, Suita, Osaka 565-0871, Japan.

[c]Department of Materials Chemistry, Graduate School of Engineering, Osaka University,

2-1 Yamadaoka, Suita, Osaka 565-0871, Japan.

[d]Collaborative Research Center for Advanced Science and Technology, Osaka University,

2-1 Yamadaoka, Suita, Osaka 565-0871, Japan.

The persistent spectral hole burning (PSHB) properties for the Eu(III) 15-cown-5 ether complex, Eu(15C5)Cl$_3$, incorporated in composite glass matrices in binary systems of SiO$_2$-M$_x$O$_y$(Al$_2$O$_3$, ZrO$_2$ and Ta$_2$O$_5$) by sol gel method were characterized by monitoring the excitation spectrum based on the $^7F_0$-$^5D_0$ transition of Eu^{3+} ion befor and after dye laser light irradiation (Rhodamin 6G). The hole peaks were rapidly formed on the composite materials (SiO$_2$-M$_x$O$_y$):Eu(15C5)$^{3+}$ compared with the conventional inorganic glasses doped with Eu^{3+} ions partially reduced by heating in H$_2$. The 40-50% of peak intensity of excitation spectra of (SiO$_2$-ZrO$_2$):Eu(15C5)$^{3+}$ was decreased by irradiation of dye laser (100 mW/mm^2) to form a deep hole at the higher rate even than SiO$_2$:Eu(15C5)$^{3+}$.

The thermal stability of hole peaks for the composite materials (SiO$_2$-M$_x$O$_y$):Eu(15C5)$^{3+}$ were considerably improved compared with that of SiO$_2$:Eu^{3+} or SiO$_2$:Eu(15C5)$^{3+}$: The temperature cycling measurements showed that the hole peaks as formed at the laser irradiation at 77 K were still maintained even at room temperature (see Fig.1). Futhermore, the half-width of hole peaks were decreased by mixing SiO$_2$ with M$_x$O$_y$. These are due to the lowered lattice vibration (phonon) effect by the addition of M$_x$O$_y$ to the binary composite glass matrices.
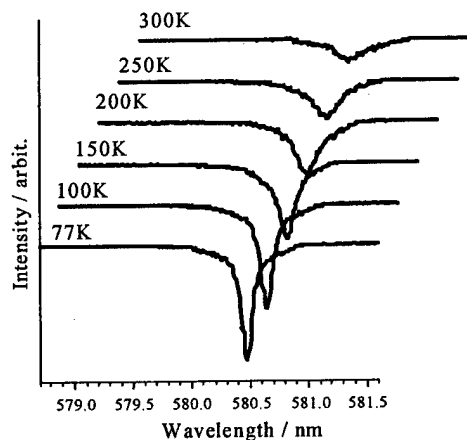

Fig. 1. Hole spectra measured by temperature cycling method for (SiO$_2$-ZrO$_2$):Eu(15C5)$^{3+}$. The hole peak was formed under irradiation of rhodamin 6G dye laser (100mW/mm^2) at 77 K.

Corresponding Author : H. Hanzawa

Address : Division of Materials Physics, Graduate School of Engineering Science, Osaka University,

1-3 Machikaneyama-cho, Toyonaka, Osaka 560-8531, Japan

Phone & Fax : +81 (0)6-6850-6452

E-mail : hanzawa@mp.es.osaka-u.ac.jp

HOLE BURNING AND SINGLE-MOLECULE SPECTROSCOPY OF TERRYLENE IN INCOMMENSURATE BIPHENYL

V. Palm[1], M. Pärs[1,2], and J. Kikas[1,2]

[1]Institute of Physics, University of Tartu, Riia 142, 51014 Tartu, Estonia
phone: +372 7428882, fax: +372 7383033, e-mail: viktor@fi.tartu.ee
[2]Department of Physics, University of Tartu, Tähe 4, 51010 Tartu, Estonia

Biphenyl forms at normal pressure and temperatures below 40 K an incommensurate structure with properties varying in space on a scale of nanometers [1]. To detect these variations, one can dope biphenyl with impurity molecules, which perform as sensitive probes of their local environment [2]. We use terrylene molecules as such molecular probes. Thin films of terrylene-doped biphenyl have been studied using methods of high-resolution laser spectroscopy at temperatures between 1.7 K and 2.1 K.

Due to its favourable properties, as high fluorescence quantum yield and absence of photochemical hole burning mechanism, terrylene is extensively used as a dopant with several crystalline and amorphous hosts in experiments on single-molecule spectroscopy (SMS) [3]. A very low probability of photoinduced spectral transitions (spectral hole burning) of an impurity molecule is one of the most important conditions making SMS study of this molecule possible.

Unlike terrylene in crystalline and amorphous matrices studied so far, intensive processes of non-photochemical spectral hole burning with significantly nonexponential kinetics have been observed. At 1.7 K, a holewidth of 2.7 GHz have been determined by extrapolating to zero burning fluence. Together with the results on non-photochemical hole burning for chlorin dopant in biphenyl [4], this points to existence of a universal (independent on dopant) burning mechanism. Surprisingly, in spite of the hole burning, also the single-molecule spectra with some extremely stable single molecule lines have been obtained for low-concentration samples. Single molecule lines with well reproducible shape and linewidths between 160 and 400 MHz have been observed at 1.7 K. Thus the observed zero-phonon lines of single terrylene molecules are several times broader than in other matrices studied so far at similar temperatures, indicating a different broadening mechanism.

Our experimental results demonstrate a large variety of spectral behavior of terrylene impurity molecules, indicated by a very wide range of probabilities of photoinduced transitions: we observe very fast initial phases of the hole-burning kinetics, but also very stable molecules for which single molecule spectra can be recorded. Large holewidths also indicate differences between stable and less stable impurities. We attribute these effects to spatial variations of local environment of terrylene molecules in an incommensurate matrix of biphenyl. The broadening of single molecule lines is probably induced by elementary excitations specific for an incommensurate matrix.

[1] H. Cailleau, J.C. Messager, F. Moussa, F. Bugaut, C.M.E. Zeyen and C. Vettier, Ferroelectrics **67**, 3 (1986).
[2] A. Suisalu, V. Zazubovich, J.Kikas, J. Friebel, and J.Friedrich, Europhys. Lett., **44**, 613 (1998).
[3] W.E. Moerner and M. Orrit, Science **283**, 1670 (1999).
[4] V. Zazubovich, A. Suisalu, and J. Kikas, Phys. Rev. B **64**, 104203 (2001).

Room-Temperature Persistent Spectral Hole Burning of Eu^{3+} in Alkali Borate Glasses

Koji Fujita, Masayuki Nishi, and Kazuyuki Hirao

Department of Materials Chemistry, Graduate School of Engineering, Kyoto University,

Sakyo-ku, Kyoto 606-8501, Japan

E-mail: koji@collon1.kuic.kyoto-u.ac.jp

TEL +81-75-753-5541 FAX +81-75-753-3345

The phenomenon of spectral hole burning has attracted considerable attention because of its potential application to high-density optical storage utilizing frequency domain. Also, the spectral hole burning is a powerful tool for performing high-resolution optical spectroscopy in solids. As for Eu^{3+} in inorganic solids, it is known that an optical pumping brings about spectral hole burning at very low temperatures. The spectral hole burning caused by the optical pumping mechanism was observed in Eu^{3+}-doped silicate glass below 10K[1].

Recent efforts of the studies on spectral hole burning of Eu^{3+} have been devoted to the discovery of high-temperature PSHB in amorphous and crystalline materials. Nogami and Abe [2] reported high-temperature PSHB of Eu^{3+} in sol-gel-derived SiO_2 and Al_2O_3-SiO_2 glasses. Recently, we found that PSHB is observed even at room temperature for Eu^{3+} in sodium aluminosilicate and silicate glasses [3]. As for the sodium silicate glasses, glasses prepared in air do not show spectral hole burning at room temperature, whereas the room-temperature PSHB is observed in glasses melted in a nitrogen atmosphere.

Similar PSHB phenomenon was reported in other glass systems as well [4]. In all the reported cases, europium ions were present as both Eu^{3+} and Eu^{2+} in the glass matrix. We also examined the effect of the degree of reduction on PSHB of Eu^{3+} in sodium borate glasses, and found that the efficiency of hole burning changes with the concentration of the coexisting Eu^{2+} [5]. Nonetheless, the mechanism of hole burning of Eu^{3+} in glasses prepared by melting in reducing conditions is less clear. It is anticipated that different glass hosts lead to changes in hole-burning properties. Here, we present the dependence of hole-burning efficiency on the kind of alkali ions in R_2O-B_2O_3 glasses (R=Li, Na, and K).

References

[1] R. M. Macfarlane, and R. M. Shelby, *Opt. Commun.*, **45**, 46 (1983).

[2] M. Nogami, and Y. Abe, *Appl. Phys. Lett.*, **71** 3465 (1997), M. Nogami, and Y. Abe, *J. Opt. Soc. Am. B*, **15**, 680 (1998).

[3] K. Fujita, K. Tanaka, K. Hirao, and N. Soga, *Opt. Lett.*, **23**, 543 (1998), K. Fujita, K. Tanaka, K. Hirao, and N. Soga, *J. Opt. Soc. Am. B*, **15**, 2700 (1998).

[4] M. Nogami, T. Hayakawa, and T. Ishikawa, *Appl. Phys. Lett.*, **75** 3072 (1999), D. Ricard, W. Beck, A. Y. Karasik, M. A. Borik, and J. Arvanitidis, *J. Lumin.*, **86**, 317 (2000), N. Murase, Y. Kawasaki, and A. Tomita, *J. Lumin.*, **98**, 301 (2002).

[5] K. Fujita, M. Nishi, K. Tanaka, and K. Hirao, *J. Phys.: Condens. Matter*, **13**, 6411 (2001), K. Fujita, M. Nishi, and K. Hirao, *Opt. Lett.*, **26**, 1681 (2001).

Function of Eu ions and defect centers in photochemical hole-burning in glasses

Norio Murase,[1,*] Rei Nakamoto,[1,2] Jun Matsuoka,[1,2] and A. Tomita[2]

[1] Photonics Research Institute, National Institute of Advanced Industrial Science & Technology (AIST),
Ikeda-City, Osaka 563-8577, Japan,• Tel. +81-72-751-8483, Fax. +81-72-751-9637
*E-mail: n-murase@aist.go.jp

[2] Osaka Electro-Communication University, Neyagawa-city, Osaka 572-8530, Japan

Rare-earth ion doped glasses show photochemical hole-burning even at room temperature. Eu can stay both as divalent and trivalent ions in most of glasses. Therefore, hole-burning in Eu doped glasses have been investigated intensively. There are two mechanisms reported so far for the room temperature hole-burning. One is a photoinduced reduction of Eu^{3+}.[1] The other is a photoreduction of Eu^{3+} by electrons from defects centers.[2] Both experiments are done in glasses prepared in a reducing atmosphere with constant concentration of Eu and defect centers.

We reported a concentration dependence of Eu ions on hole-burning extent.[3] The result suggested a mechanism of an energy or electron transfer between Eu^{3+} and Eu^{2+}. However, a role of defect centers formed by the reduction was not clear. Therefore, we have investigated the concentration dependence of defect centers created by X-ray on hole-burning extent.

Figure 1 shows the result. When the sample is irradiated by X-ray for a long period, the hole-burning becomes obvious. Further, holes burnt in a sample with high Eu concentration are more stable against temperature. This result denies the mechanism previously reported.[2] A possible mechanism of the hole formation at high temperature is electron transfer from Eu^{2+} to Eu^{3+} assisted by adjacent defect centers.
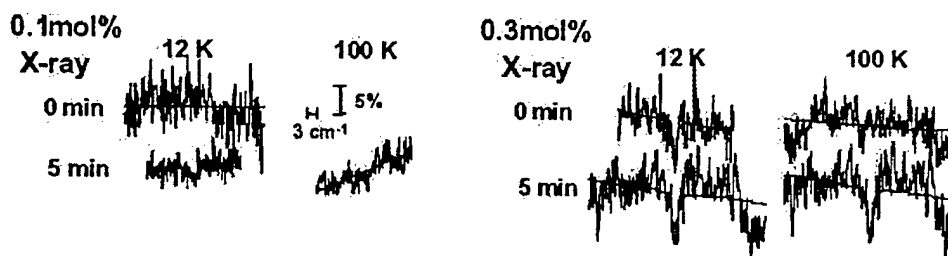
Figure 1• Hole-burning extent and its Eu ion and X-ray irradiation time dependence.

[1] K. Fujita, K. Tanaka, K. Hirao, N. Soga, *J. Opt. Soc. Am. B*, 15, 2700(1998).

[2] W. J. Chung, and J. Heo, *Appl. Phys. Lett.*, 79, 326(2001).

[3] N. Murase, Y. Kawasaki, A. Tomita, *J. Lumin.*, 98, 301(2002).

Persistent spectral hole burning in Mn-doped Al_2O_3 ceramics

I. Sildos, V. Kiisk and V.Palm
Institute of Physics, University of Tartu, Riia 142, 51014 Tartu, Estonia

H. Balzer and U. Bogner, Institute of Physics II, University of Regensburg
Universitätstrasse 31, D-93053 Regensburg, Germany

Persistent spectral hole burning is an attractive method for the sensor techniques of external fields (eg. stress, electrical fields) in functional materials like α-Al_2O_3 ceramic plates used as a substrate in high-power electronic devices. Spectral hole burning in Mn-doped α-Al_2O_3 ceramic plates was for the first time performed in a sol-gel produced ceramic [1].

The samples investigated here were produced by mixing together α-Al_2O_3 powder, Mn_3O_4 powder, and MgO powder. After that the material was sintered in a furnace at 1540°C. This sample behaves optically similarly to a ruby and the analogues of R lines can be found in the luminescence spectrum of Mn^{4+} ion at low temperatures (R_1 and R_2 lines at 676.5 nm and 672.5 nm, respectively).

An excimer-pumped pulsed dye or a continuous single-frequency dye laser was used for the resonant excitation of Mn^{4+} ion to $2\overline{A}$ level (R_2 line). After this resonant illumination of the sample, a spectral hole was detected in the excitation spectrum of the R_2 line monitored via the luminescence of R_1 line. We were also able to detect a spectral hole in a "total luminescence spectrum" (see eg [2]), using a tunable laser as an excitation source in combination with a CCD camera-equipped spectrometer for the detection of the luminescence spectrum.

The hole burning process was more effective when using a pulsed dye laser and, therefore, we suggest a two-step self-gated mechanism.

An electron-irradiation treatment of the samples was carried out to investigate its influence on the burning efficiency.

1. S. Feofilov et al., J. Lumin. **76&77** (1998) 217.
2. K. Palewska, E. Meister, and U. Wild, J. Lumin. **50** (1991) 47.

DIAMOND WITH IMPURITY IONS AS A HOLE BURNING MATERIAL

A.A. Gorokhovsky[a, *], V.A. Martinovich[a,b], A.V. Turukhin [c]

[a] The College of Staten Island and The Graduate Center of CUNY, 2800 Victory Blvd., Staten
Island, NY 10314, USA

[b] Belarussian State University, Minsk, Belarus

[c] JDS Uniphase Corporation, Eatontown, NJ 07724, USA

Diamond is an extremely hard and highly thermally conducting crystal which is optically transparent in the visible and near IR regions of the spectrum. Spectroscopic studies of defect centers in diamond are important for basic understanding of the defect structure and the interaction of defects with the lattice and light. Furthermore, due to the unique properties of diamond, they are potentially useful materials for advanced applications of hole-burning in optical storage and processing.

We report here on spectroscopic, laser induced luminescence and hole burning studies of two types of impurity defects in diamond: the Si center and Xe center. The samples with the Si center were free-standing polycrystalline films grown by microwave-assisted plasma chemical-vapor deposition. In the luminescence spectra, the Si center shows a zero-phonon line (ZPL) at 737 nm (1.682 eV) with inhomogeneous broadening up to 45 cm^{-1}. It was found that the Si center has a quasi-molecular Si_2 structure. Persistent spectral hole burning, as well as photoinduced hole filling by resonance light, were observed at low temperatures.

The samples with the Xe center were natural diamonds (type Ia) irradiated with 500 keV Xe ions at room temperature within the dose range 1×10^{13} - 5×10^{14} cm^{-2}. The Xe center exhibits an isolated ZPL at 811.6 nm (1.527 eV) and a relatively weak vibrational sideband. The width of the ZPL at 1.5 K was determined to be in the range 5 – 15 cm^{-1}, depending on the implantation dose. On the basis of post-implantation thermal annealing studies, it was concluded that the vacancy is involved in the Xe center formation. A growth of a second ZPL at 793.3 nm was observed at elevated temperatures. An excited state energy level splitting of about 130 cm^{-1} was found by studying the temperature behavior of these ZPLs. It was determined that the excited state, as well as the ground state of the optical transition, each have a double level structure, and that ZPL at 811.6 nm is probably not a resonance 0-0 line.

* Corresponding author. Tel.: +1-718-982-2815; fax +1-718-982-2830.
E-mail address: gorokhovsky@postbox.csi.cuny.edu (A. A. Gorokhovsky)

HOLEBURNING IN RARE EARTH DOPED NANOPARTICLES OF MgS & CaS[†]

Aras Konjhodzic[††], Deepika Chhabriya, Omer Salihoglu, Sameh Dardona & Zameer Hasan

Physics Department, Temple University, Philadelphia, PA 19122

Summary:

Nanometer size particles exhibit enhanced structural, electronic, and optical properties. Confinement induced changes in optical and thermal properties may be exploited for optical hole-burning devices especially the ones using only a few atoms. In this paper we report the optical hole-burning in nano-particles of Eu-doped in MgS and CaS. These materials in bulk form are known to have very favorable characteristics for spectral hole-burning based memories. For example, high density, fast storage times, persistence, photo-erasability and operation at relatively high temperature approaching 25K have all been demonstrated in these materials. Nano-particles of MgS:Eu and CaS:Eu have been produced by quench condensing the laser ablated vapors from a solid target. The pressure of the ambient gas in the chamber has been used to control the size of particles. Our experiments produced particles as small as a couple of nanometers in size. Nanoparticles of CaS:Eu and MgS:Eu were dispersed in a polymer (PMMA – Poly-Methyl-Methacrylate) to address particles individually. Results will be presented on hole-burning characteristics of nano-particles especially with reference to Rare Earth based quantum memories.

A possibility of separating the inhomogeneous broadening via coherent Raman spectra

I.Tehver

Institute of Physics, University of Tartu, Riia 142, Tartu 51014, Estonia;
phone:+372-7-383017; fax: +372-7-383033; e-mail: tehver@fi.tartu.ee

The goal of this communication is to draw attention to one more possibility of distinguishing the inhomogeneous broadening from the homogeneous width of vibronic spectra, in addition to the known methods like spectral hole burning, single molecule spectroscopy, fluorescence line narrowing and photon echo. Here the excitation spectra of the resonant coherent Raman scattering, the coherent anti-Stokes Raman scattering (CARS) and the coherent Stokes Raman scattering (CSRS) are used.

The idea is following. The excitation profiles of CARS and CSRS of an ensemble of identical molecules have the same shape, only the excitation spectrum of CSRS being shifted in wavenumber (the frequency of Raman mode) to the high-frequency side. For the molecules in condensed-phase systems, the inhomogeneities/fluctuations of the medium lead to different linewidths and redistribution of line intensities in the excitation profiles of CARS and CSRS and, also, to the shifts of excitation lines [1,2]. A comparison of the inhomogeneously-broadened excitation lines of CARS and CSRS enables one to estimate the homogeneous and inhomogeneous linewidths.

To analyze/calculate coherent Raman excitation profiles, it is convenient to use the transform technique, a method known from the spontaneous resonance Raman scattering, which relates the Raman amplitudes to the molecular absorption spectrum [3-5]. A procedure is proposed which allows one to distinguish homogeneous and inhomogeneous broadening, based on the measured linewidths of the absorption and the excitation lines of CARS and CSRS.

The method enables one to determine very short (of the order of 10^{-13} - 10^{-14} s) relaxation times via a stationary experiment. It can be applied to crystals as well as to glasses and solvents. The advantages of this method are that it can be used at arbitrary (incl. room) temperatures and that the presence of narrow zero-phonon lines is not necessary.

References

1. I.Tehver, J. Raman Spectrosc. **28**, 819, 1997.
2. I.Tehver, J. Luminescence **83-84**, 43, 1999.
3. V.Hizhnyakov and I.Tehver, phys. stat. sol. **21**, 755, 1967.
4. V.Hizhnyakov and I.Tehver, J. Raman Spectrosc. **24**, 653, 1993.
5. J.P.Page, in: Light Scattering in Solids VI, eds. M. Cardona, G.Güntherodt, Springer, Berlin, 1991, p.17.

Near-infrared to visible upconversion studies in Tm^{2+} doped halide crystals

Judith Grimm*, Hans U. Güdel
Department of Chemistry and Biochemistry
University of Bern
Freiestrasse 3
CH – 3000 Bern 9
Switzerland

We report on the synthesis and optical properties of Tm^{2+} doped halide crystals. The energy level scheme of Tm^{2+} ($4f^{13}$) is spectroscopically similar to that of Yb^{3+}, having only two f-levels: The $^2F_{7/2}$ ground state and the $^2F_{5/2}$ excited state. Divalent Thulium has received less attention in the past than other divalent lanthanides (i.e. Eu^{2+}, Sm^{2+}, Yb^{2+}). Tm^{2+} is a dual emitter [1,2], exhibiting $^2F_{5/2} \rightarrow {}^2F_{7/2}$ emission in the near infrared as well as 4f–5d emission in the visible spectral region. This makes Tm^{2+} suitable for near-infrared to visible photon upconversion. Upconversion (UC) is a non-linear optical process that generates short wavelength luminescence upon excitation at long wavelengths, and it is based on the existence of multiple metastable excited states. Tm^{2+} UC was demonstrated for the first time in the system $SrCl_2:Tm^{2+}$ where UC emission is observed up to room temperature [3]. We are now extending the Tm^{2+} UC studies to fluoride compounds. The UC luminescence of Tm^{2+} is broad because of its 4f–5d nature and the energetic position depends on the crystal field strength.

[1]   W. J. Schipper, A. Meijerink, G. Blasse, *J. Lumin.*, **62**, 1994, 55
[2]   C. Wickleder, *J. Alloys Compounds*, **300-301**, 2000, 193
[3]   O.S. Wenger, C. Wickleder, K.W. Krämer, H.U. Güdel, *J. Lumin.*, **94-95**, 2001, 101

*   Tel: + 41 31 631 42 54, fax: + 41 31 631 43 99,
    Email address: judith.grimm@iac.unibe.ch

Single-mode external cavity diode laser rapidly tuneable over 50 GHz

Lars Rippe

Dept. of Physics, Lund Institute of Technology (LTH), Box 118, S-221 00 Lund, Sweden
phone: +46 (0)46 2224877, fax: +46 (0)46 2224250, e-mail: Lars.Rippe@fysik.lth.se

External cavity diode lasers (ECDLs) with Littrow configuration have over the years proven to be very versatile and simple tools to be used in different areas of research and have therefore spread widely. These lasers are often tuned by letting a piezoelectric actuator move the grating, thereby changing the length of the cavity. The mechanical nature of the tuning and the hysteresis, which is inherent to piezoelectric elements, limits the accuracy and maximum tuning speed for this tuning method. In order to reach higher repeatability and tuning speeds one can incorporate an electro-optical crystal (EOC) into the cavity [1]. The index of refraction of the EOC can be changed by applying an electric field across it, thereby accurately changing the effective optical length of the cavity. There are however two disadvantages with this construction. Firstly, the tuning range of the laser is limited to the mode spacing of the cavity, which is ~3 GHz for a 5 cm long cavity [1]. Secondly the feedback efficiency changes when the laser is tuned, which leads to changes in the output power of the laser. This means that the frequency change is accompanied by an amplitude change, which limits its usefulness in some applications.

Laser tuning is governed by the relationship $\Delta\lambda = \Delta L*(\lambda_0 / L_0)$ where $\Delta\lambda$ is the wavelength change caused by a cavity elongation ΔL for a cavity with original length L_0 and initial wavelength λ_0. Most single mode lasers are tuned by moving one of the mirrors, thereby changing the length of the laser cavity. To keep them in one mode when tuning them beyond one free spectral range, a second wavelength selective element, e.g. an etalon, can be used. The wavelength change, $\Delta\lambda$, for the etalon should at all times match the wavelength change for the whole cavity. However, since the etalon is shorter the required elongation will also be smaller.

In general, the requirement for mode-hop free tuning is that the elongation of each cavity should be proportional to the optical length of that cavity. The simplest Littrow cavity consists of a mirror and a grating, from which the first order is reflected back towards the mirror. In such a cavity there are in a sense as many cavity lengths as there are illuminated grooves on the grating, but the same requirement still applies. The elongation should be proportional to the cavity length all across the beam. This can be achieved by inserting a crystal with a uniform length but which is thinner on the longer side of the cavity. The electric field, for a certain applied voltage, will be higher where the crystal is thin causing a larger change of index of refraction and consequently a larger elongation of the cavity's optical length at that side.

We have designed and built a laser using the ideas presented above for use in coherent transient spectroscopy on thulium doped inorganic crystals at 793 nm [2]. The laser has an output power of 60 mW and tuning speeds of 1.5GHz/μs and a single-mode tuning range of 50 GHz have been demonstrated. The repeatability is better than 2 MHz. Since ECDLs are established technology and can be constructed at many different wavelengths, this laser might be suitable for other applications where fast and precise tuning is desired.

[1]   B. Boggs, C. Greiner, T. Wang, H. Lin and T.W. Mossberg, "Simple high-coherence rapidly tunable external-cavity diode laser", Opt. Lett. **23**, 1906, (1998)

[2]   L. Rippe, "Mode-hop-free electro-optically tuned diode laser", Opt. Lett. **27**, 237, (2002)

Spectral hole burning with a mode-locked laser

Joe A. Fischer, Thomas Böttger, Mingzhen Tian, R. L. Cone, and Wm. Randall Babbitt
Department of Physics, Montana State University, Bozeman, MT 59717, USA
phone: (406)994-7988, *Fax*: (406)994-4452, *email*: fischer@physics.montana.edu

Mode-locked (ML) lasers emit a periodic train of pulses whose Fourier transform reveals a comb of equally spaced frequencies with several tens of THz bandwidth. Using this frequency comb as a frequency ruler to link optical frequencies to the RF domain has been the motivation to stabilize these lasers in recent years using a variety of techniques including Fabry-Perot cavities[1]. In stabilizing a ML laser to a Fabry-Perot cavity, the frequency comb of the laser has to be simultaneously locked to a large number of adjacent longitudinal Fabry-Perot cavity modes. Using this technique requires that the modes and absolute frequency between the laser and the cavity must exactly match in order to form a combined error signal needed for stabilization. In addition, the dispersion of the Fabry-Perot cavity allows only a finite number of modes to overlap.

As an alternative approach, we use a spectral hole burning material as a frequency reference that overcomes these difficulties by automatically matching the relative mode spacing and coincidence of absolute frequency over the bandwidth of the material with no adjustment required and overcomes the limitations associated with Fabry-Perot cavity length changes induced by vibrational and acoustical noise as well as thermal expansion. This is an extension of using spectral hole burning frequency references for continuous wave laser stabilization[2] from using only one mode to using a frequency comb of modes spanning the entire inhomogeneously broadened transition.

We demonstrate this concept in Tm^{3+}:YAG at 793 nm using a Kerr-Lens ML Ti: Sapphire laser. Figure 1 shows the frequency comb spectrum burned by the ML laser into the inhomogeneous absorption line of Tm^{3+}:YAG at 4.2 K. The mode spacing of 93 MHz allows to burn ~180 holes over the 17 GHz FWHM wide absorption line. Since the modes of the ML laser pulse train are phase-locked together, stabilizing two fractions at opposite ends of the comb will be sufficient to stabilize all parameters of the entire comb. As for continuous wave laser frequency stabilization, we generate the error signal using frequency modulation spectroscopy of the narrow spectral holes, which in the ML laser case is a superposition of all modes occupying the inhomogeneous line. The property of the spectral hole burning material as a spectrum analyzer was used to evaluate the frequency stability of the ML laser.
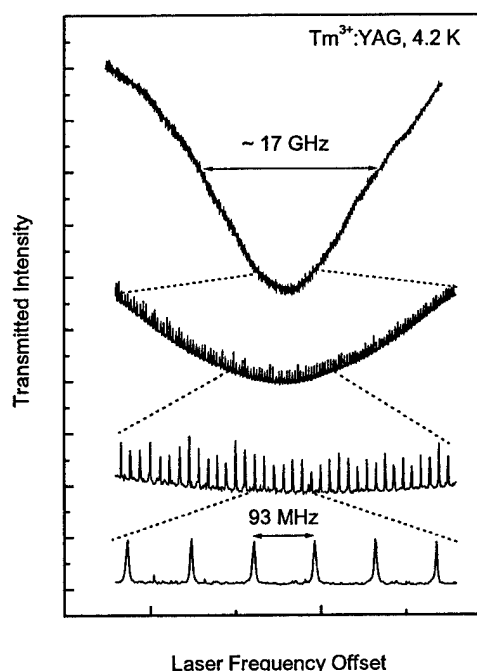
Figure 1: Frequency comb spectrum of the ML laser burned into the inhomogeneous absorption of Tm^{3+}: YAG at 793 nm. The expanded view shows the uniform mode spacing.

1. R. J. Jones and Jean-Claude Diels, Phys. Rev. Lett. **86**, 3288 (2001).
2. T. Böttger, G. J. Pryde, N. M. Strickland, P. B. Sellin, and R. L. Cone, Optics in 2001, Optics & Photonics News **12**, no.12, 23, Dec. 2001.

External Cavity Diode Laser Pumped Intra-Cavity Second Harmonic Generation at 580nm and 589nm

Peter B. Sellin, Kevin S. Repasky, and Ali Belarouci
Spectrum Lab and Physics Department, Montana State University, Bozeman, MT 59717
Phone: (406) 994-6082, Fax: (406) 994-4452, repasky@physics.montana.edu

Quantum dot diode lasers can access the near infrared spectral region by adjusting the size of the three dimensional quantum wells. Quantum dot diode lasers can be frequency double through the process of second harmonic generation to produce light in the visible spectral region at wavelengths not easily accessible. In this paper, initial results of a laser system based on a quantum dot diode laser pumped intra-cavity second harmonic generation is presented. The output of the laser system has low power single mode operation at 580nm for applications in spectral hole-burning and optical data storage and optical processing in $Eu:Y_2SiO_5$. The laser is also capable of operating at 589nm enabling optical trapping and quantum computing experiments with sodium.

A schematic of the external cavity diode laser is shown in fig.(1). The output from quantum dot laser with a center wavelength near 1160nm in a c-mount package is collimated using a Thor Labs aspheric lens. The light is next incident on a 10mm x 27mm clear aperture optical grating with 1200 lines/mm. The zeroth order reflection from the optical grating is incident on a turning mirror and the reflection from the turning mirror is used as the output of the ECDL. The first order reflection from the optical grating is directed back to the laser diode and this optical feedback allows wavelength control of the ECDL. The diode laser is temperature controlled by a peltier cooler and a commercial temperature controller. The external cavity diode laser has continuous wave single mode operation with a side mode suppression ration of greater than 40dB. However, as the output power of the external cavity diode laser was increased, the laser ran in multiple modes. This multimode operation at higher operating powers is attributed to inhomogeneous gain at higher laser diode drive currents.

Figure 1 Schematic diagram of the external cavity diode laser in a Littrow configuration. A quantum dot diode with a center wavelength near 1160nm contained in a C-mount package is used as the gain medium.

A schematic of the intra-cavity frequency doubling is shown in fig.(2). The light from the ECDL is coupled into a bowtie cavity with a LBO non-linear optical crystal placed between the two focusing mirrors. The intra-cavity frequency double has the advantage of optical power build up inside of the optical cavity thus making the second harmonic conversion more efficient. The mirror reflectivity at the pump wavelength for the four mirrors was 98%. The two focusing mirrors had a radius of curvature of 50mm resulting in a 41µm spot size at the center of the LBO crystal. The LBO crystal was 5mm x 5mm x 12mm with antireflection coatings at each 5mm x 5mm face at both the fundamental and second harmonic wavelengths. The crystal was temperature controlled via a peltier cooler a commercial temperature controller. The optical path length around the bowtie cavity can be adjusted via a piezo-electric transducer.
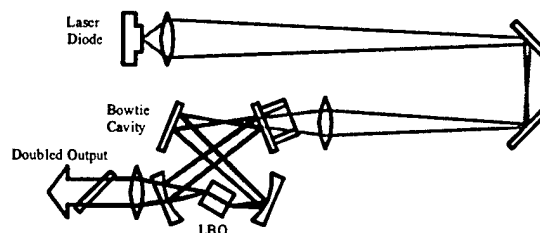

Figure 2 Schematic of the bowtie cavity used for frequency doubling.

The cavity enhance frequency conversion occurs when the output of the external cavity diode laser maintains resonance with the bowtie cavity. To achieve this, an active frequency stabilization of the external cavity diode laser to the optical cavity via the Pound-Drever-Hall stabilization technique was employed. Laser output at 580nm was achieved through this application of second harmonic generation.

Modeling and Simulation of Optical Coherent Transient processes with Complex Configurations

Tiejun Chang, Mingzhen Tian, Zeb W. Barber, and Wm. Randall Babbitt

The Spectrum Lab, Montana State University, Bozeman, MT 59717

Phone: (406)9947308, Fax: (406)9946767, Email: chang@spectrum.montana.edu

Optical coherent transient (OCT) techniques are not only well-established spectroscopic tools, but also the bsis of a variety of optical information storage and processing devices. To model the OCT processes, such as photon echoes, free induction decay and optical nutation, the coupled Maxwell-Bloch equations have been used successfully for the collinear configuration in thick media. In this theory the coherent effects of light on the inhomogeneously broadened absorbers are described by Bloch equations, where the electric field acts as a driving source to the atomic dipoles. The propagation effects are governed by Maxwell's equations, where the macroscopic polarization caused by the atomic dipole moments acts as a source to the electric field. Recently, more complex configurations have been proposed to make practical OCT optical processing devices, such as pulse shaping and arbitrary waveform generation. This kind of devices requires angled beam configurations to discriminate the processed signals from unwanted transmitted inputs. In addition, the electric fields are usually frequency chirped and/or phase and/or amplitude modulated. Frequency jitter and phase noise have to be counted in most practical settings as well.

In this paper, we present a model for multiple angled beams with phase and frequency modulations (including noises) based on the in-phase and in-quadrature Maxwell-Bloch model, where the spatial phase is introduced and the spatial Fourier transform is applied to trace the field along some predefined directions under the small angle assumption.

In the beam direction i, the wave vectors of the field $k^{(i)}$ have components in the transverse directions $k_{xy}^{(i)}$, and propagation direction $k_z^{(i)}$. The angles between beams are assumed very small, so that we have $k_{xy}^{(i)} \ll k_z^{(i)}$ and $k_z^{(i)} \approx k_z$. The electric field of the multiple beams can be written as

$$E(\vec{R},z,t) = \frac{\hbar}{\mu}\left[\Omega_C(\vec{R},z,t)\cos(\omega_0 t - k_z z) + \Omega_S(\vec{R},z,t)\sin(\omega_0 t - k_z z)\right]$$

where

$$\Omega_C(\vec{R},z,t) = \sum_i\left\{\Omega^{(i)}(z,t)\cos\left[\varphi^{(i)}(t) + \vec{k}_{xy}^{(i)}\cdot\vec{R}\right]\right\} \text{ and } \Omega_S(\vec{R},z,t) = \sum_i\left\{-\Omega^{(i)}(z,t)\sin\left[\varphi^{(i)}(t) + \vec{k}_{xy}^{(i)}\cdot\vec{R}\right]\right\}$$

ω_0 is an arbitrary stationary frequency, $\Omega^{(i)}(z,t)$ is the amplitude (in terms of Rabi frequency) propagating along direction i and $\varphi^{(i)}(t)$ is the general phase term that includes phase and frequency modulations of the field in that direction. This field can also be expressed with in-phase and in-quadrature terms. $\Omega_C(\vec{R},z,t)$ and $\Omega_S(\vec{R},z,t)$ are the in-phase and in-quadrature field components driving the atomic dipoles. From the coupled Maxwell-Bloch equations these two field components can be calculated after interaction with a layer of optically thin medium. Applying the spatial Fourier transform, we can obtain the field amplitudes along different directions. A optically thick medium can be sliced into thin layers. Maxwell-Bloch equations are applied to each layer successively from the input side to the output side of the medium. The output field from a layer is applied as the inputs to the next layer. With this method, the tedious computation caused by adding an additional spatial dimension to the Maxwell-Bloch equations is avoided and the simulations with common settings can be done within reasonable time. In most applications, only a few directions need to be tracked and the computation can be reduced significantly.

The simulation results will be presented for pulse shaping and arbitrary waveform generation for various settings including programming with one rate linear frequency chirps and probe with a brief pulse, and programming and probe with multi-rate chirps. The frequency and/or phase noises will be considered. The simulation results will be compared with the experiments.

Reference:
[1] Z. W. Barber, M. Tian, R. R. Reibel, and Wm. R. Babbitt, Opt. Exp. **10**, 1145 (2002)

Coding considerations for analog signal processing applications

R. Krishna Mohan, K. D. Merkel and A. Olson

Spectrum Lab, Montana State University, Bozeman, Montana 59717

Phone: 406-994-7675, Fax: 406-994-6767, Email: krishna@spectrum.montana.edu

Spectral spatial analog signal processors, currently being developed at Spectrum Lab, can be tailored to perform a variety of signal processing applications. These applications vary among true-time delay (TTD) generation, radar range-Doppler correlative processing, and arbitrary analog waveform generation, among others. The end-application will determine the choice of the codes or waveforms used in the optical processor.

This paper covers investigations to identify optimal coding choices suitable to TTD generation and range-Doppler correlative processing using various spread spectrum modulation schemes. The basic operation is the storage of coherent correlations of a pattern and its time delayed replica in a spectral spatial holographic material. Repeated processing with such pattern pairs is performed and the resultant coherent correlations are summed as a spectral grating in the material that can be coherently probed or readout for analysis. The period of the spectral grating has the delay information essential for TTD generation and/or range measurement. Using dynamic codes in integration enhances the primary frequency component while the other spectral features (e.g., temporal sidelobes) change each shot and tend to average in integration. A desirable processor performance is for the eventual output signal strength to scale with the square of the number of chips per pattern, N, (a property of autocorrelation) and square of the number of distinct patterns J, (a result of coherent summation). Device performance in both cases is dependent on the code length, bandwidth, power and spectral composition of the patterns.

For a TTD generator the choice of the code governs the fidelity of the programmed spectral grating. Bandwidth, spectral resolution, temporal jitter, frequency jitter, dynamic range, distortion and non-linearities are the code dependent performance specifications. The code selection for radar signal processor is critical for transmission, processing and unambiguous range and Doppler resolution. In both cases, the performance is evaluated in terms of the auto-correlation structure leading to the peak to maximum sidelobe ratio (PSR). Additional considerations such as high-resolution ranging capability, message screening from eavesdroppers and interference rejection (cross correlation properties) govern code selection for radars.
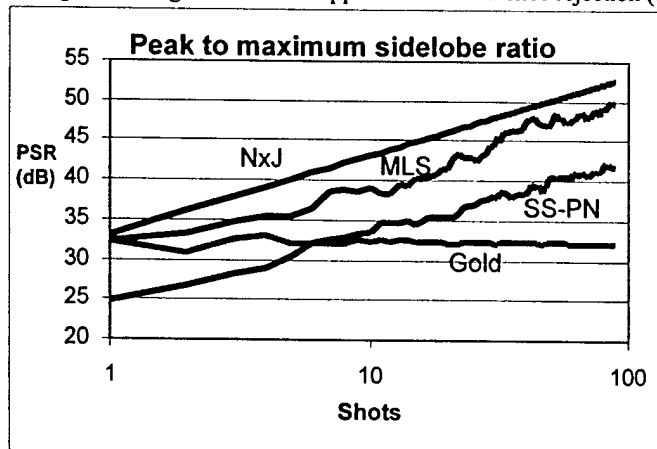
Fig 1 : Peak to Maximum sidelobe Power ratio (PSR) for various coding schemes versus processing shots

A preliminary comparative analysis of various codes in terms of their coherent correlation and integration properties has been performed. The code sets chosen for the investigation are maximal length sequences (MLS), Gold codes and spread spectrum-pseudo random noise (SS-PN) codes being explored at Spectrum Lab. The generated patterns have 2047 chips each and 88 distinct patterns were used for all cases for comparison to the 88 base MLS codes of this length. A comparative chart of the integrated PSR for these codes is shown in Figure 1. The chart shows that the MLS codes exhibit high initial PSR very close to N and continue to grow closely as (NxJ). Thus using these codes could be advantageous for creating a good TTD grating in the material. However since these codes are well known, they are potentially susceptible to jamming and have poor cross-correlation properties which negates their advantages for radar applications. The Gold codes also show high initial PSR, similar to MLS codes, that flattens out after a small number of shots. The use of a subset of MLS and/or Gold codes as initial shots in a radar would result in high initial PSR with rapid growth. The SS-PN codes fall into an intermediate category between MLS and Gold codes. The PSR is low initially, and increases monotonically for large J. The SS-PN code set is very large, thereby enhancing security for radar systems. It can be shown that a suitable down-selection criterion of the SS-PN codes can improve the dynamic range and cross- correlation properties. Optimal code sets for a particular application may therefore be generated from a combination of code types and subsets including these and others under investigation. For example, the initial use of Gold codes followed by randomly selected SS-PN-codes could provide an optimal solution for secure radar scenarios. The results of the current investigations on other possible coding schemes such as complementary sequences, cyclic codes etc., will also be discussed. We gratefully acknowledge the support of both DARPA and NASA Ames Research Center for this research.

Photon Echo Total Recall of a Stored Field

F. de Sèze, V. Lavielle, F. Bretenaker, I. Lorgeré, J.-L. Le Gouët

Laboratoire Aimé Cotton, bâtiment 505, 91405 Orsay Cedex, France
Tel 33 1 69 35 20 00, Fax 33 1 69 35 21 00, jean-louis.legouet@lac.u-psud.fr

Abstract: in the prospect of quantum information storage, we propose a rephasing scheme based on fast adiabatic passage to retrieve the entire field stored in an inhomogeneously broadened condensed material.

One realized recently that a macroscopic group of atoms can be used as a quantum memory, where a quantum state of light can be stored [1]. Since spontaneous emission rapidly destroys entanglement, it has been suggested that quantum information be stored in a ground state Raman coherence. To avoid spontaneous emission one can resort either to a cw scheme, where the driving fields are tuned off-resonance with the optical transitions involved in Raman coherence preparation [2], or to a pulsed scheme, where the intermediate step involving optical coherences is much shorter than the excited state lifetime.

The dark polariton concept[1] offers a way to adiabatically convert a light state into an atomic state and vice versa, without any loss of quantum information. It seems to be much more difficult to save quantum light information in the usual photon echo scheme. However a new arrangement has been proposed [3] where the stored quantum state of a field is totally retrieved. Unfortunately this scheme, relying on the sign properties of the Doppler inhomogeneous phase-shift, apparently only applies to vapors.

Figure: *An inhomogeneously broadened three-level atom collection successively interact with light fields tuned to resonance with transitions a-b, b-c and b-c again (see insert). The phase evolution of three different frequency classes is represented, from initial excitation at time t_1 to final rephasing. The atoms successively evolve as coherences ρ_{ab}, ρ_{ac}, and ρ_{ab} again. The frequency chirped third excitation achieves fast adiabatic passage coherence conversion at appropriate time.*
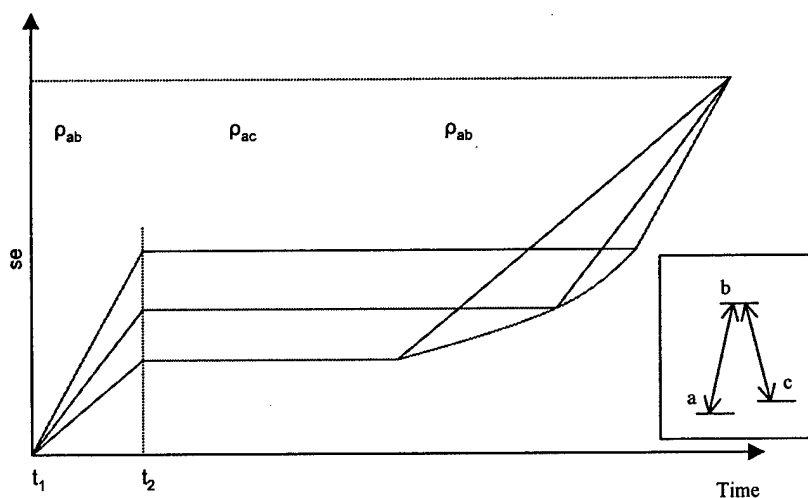
In this presentation we propose a rephasing scheme that applies to solid materials as well. By chirping the probe beam frequency in a specific non-linear way, one makes the different frequency classes undergo a fast adiabatic passage transition to the upper state, converting the stored Raman coherences into radiating optical coherences that ultimately all rephase together as illustrated in the figure.

1. M. D. Lukin, S. F. Yelin, and M. Fleischhauer, Phys. Rev. Lett. **84** 4232 (2000)
2. L. Vernac, M. Pinard, and E. Giacobino, Eur. Phys. J. D **17**, 125-136 (2001)
3. S. A. Moiseev and S. Kröll, Phys. Rev. Lett., **87** 173601 (2001)

Chirped Optical Nutation

C. M. Jefferson[1], J. A. Hoffnagle[1], T. L. Harris[2], G. W. Burr[1], M. Tian[2], and W. R. Babbitt[2]

[1]IBM Almaden Research Center, 650 Harry Road, San Jose, California 95120-6099
[2]The Spectrum Lab, Montana State University, PO Box 173510, Bozeman, Montana 59717-3510
michael@almaden.ibm.com; tel:408-927-2141; fax:408-927-2100

Abstract: The excitation of $Eu^{3+}:Y_2SiO_5$ by linear frequency chirped optical pulses generates a novel nutation-like response which is observed in the transmitted beam intensity. Unlike the periodic response of CW nutation, this response is frequency chirped. Our experimental results are described well by both Maxwell-Bloch simulations and Landau-Zener calculations.

Excitation of the $^7F_0$ to $^5D_0$ transition[1] in 1% doped $Eu^{3+}:Y_2SiO_5$ with a CW square pulse produces a familiar optical nutation signal, observed as a modulation in the transmitted beam power[2]. If linear frequency chirped optical excitation is used, however, the response of the sample is strikingly different. Chirped excitation yields a damped oscillatory response in which the oscillations of the transmitted laser beam power are themselves frequency chirped. This novel effect can only be observed when the coherence time of the laser source is considerably longer than the oscillation damping time.

Figure 1 shows a sequence of observed nutation signals in which the incident laser frequency chirp rate ranged from zero (CW excitation) to rapidly chirped, while the intensity of the beam stayed constant. The transition of the response from that of CW nutation to that which can be characterized as fully chirped occurs for chirp rates between 0.05 and 0.1 MHz/µsec. At this point, the chirp rate exceeds the square of the Rabi frequency as defined for a CW excitation. At chirp rates higher than 1 MHz/µsec, there is too little pumping of the excited state to generate a nutation-like response, and the transmitted beam power simply reflects the sample's absorption.
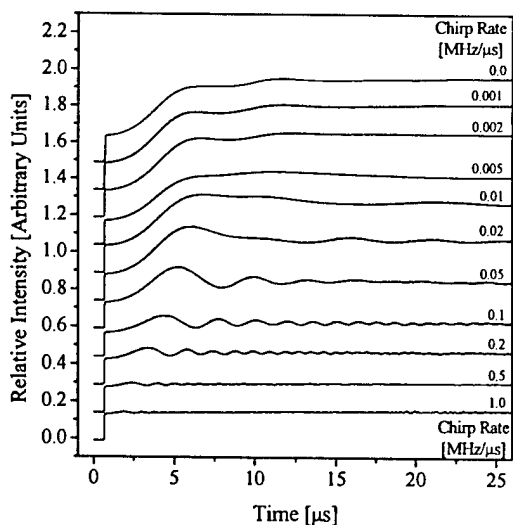
Figure 1: CW and chirped nutation signals. The incident intensity was held constant and the chirp rate varied.
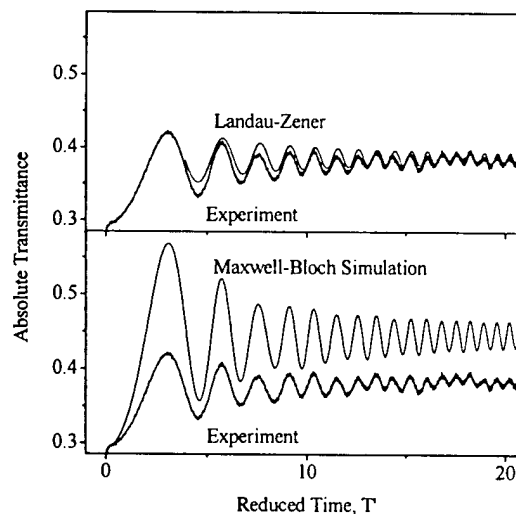
Figure 2: Chirped nutation data and calculated results.

In Figure 2(top) we show a plot of chirp nutation and the analytic result of calculations performed using the Landau-Zener approach[3]. In Figure 2(bottom) we show a similar plot with a chirp nutation signal and the calculated response using a computer simulation with the Maxwell-Bloch model. In both cases, the agreement is striking, particularly in the prediction of the chirped behavior of the nutation. The amplitude discrepancy between the model results and the experimental data is believed to be due to the Gaussian spatial beam profile averaging the effects.

References

1. R. W. Equall, Y. Sun, R. L. Cone, and R. M. Macfarlane, *Phys. Rev. Lett.*, **72**(14), 2179-2181 (1994).
2. Y. Sun, P. B. Sellin, C. Michael Jefferson, and R. L. Cone, "Oscillator strength measurements on $Eu^{3+}:Y_2SiO_5$," unpublished.
3. N. V. Vitanov and B. M. Garraway, *Phys. Rev. A.*, **53**, 4288- 4304 (1996).
4. C. Sjaarda Cornish, W. R. Babbitt, and L. Tsang, *Opt. Lett.* **25**, 1276-8 (2000).

Highly efficient true-time delay echoes

Hongyan Li, Zeb W. Barber, Joe A. Fischer, Mingzhen Tian and Wm. Randall Babbitt
(The Department of Physics, Montana State University, Bozeman, MT 59717, USA)
Phone: (406) 994-7988, *Fax*: (406) 994-4452, *email*: leehongyan@netscape.net

The stimulated photon echo process has been investigated for use in such processing systems as true-time delay (TTD) beam steering of phased array radars[1], time domain memory, range-doppler correlation, broadband RF spectrometers, continuous optical correlators, and pulse shaping and arbitrary waveform generation. The photon echo process has generally been thought of as an inefficient process because of the linear regime requirements of low pulse areas and small optical length αL. This has been a drawback for all these applications, because practical optical coherent transient (OCT) devices will require good efficiency.

Previous investigations have shown that the photon echo process of time domain memory can be made super efficient with efficiencies greater than one [2]. However, no investigation of efficiencies for the OCT process of true time delay has been performed. Using a Maxwell-Bloch simulator, we simulate this process and compare with experimental results. The simulation includes the effect of the gaussian spatial profile of the beams. We show efficiencies versus parameters such as programming pulse area, αL, and programming method. True time delay programming methods used were brief pulses, temporally separated linear frequency chirped pulses(LFC), and temporally overlapped linear frequency chirped pulses(TOLFC) [3]. A comparison is made between required intensities and bandwidths vs. echo efficiencies for each programming method. In addition, experimental results showing efficiencies in the tens of percent range will be presented. In figures 1 and 2, we show just the results for LFC programmings. Note that peak efficiency for the simulation occurs at programming pulse areas greater than 0.5π, similar to the memory studies[2].
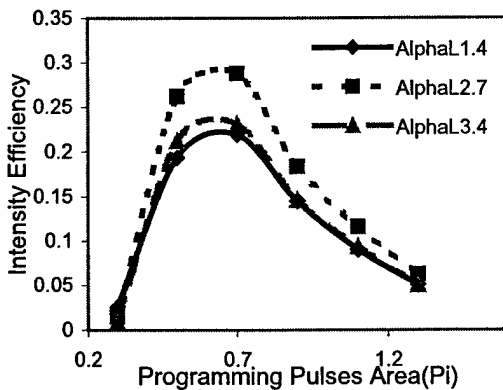
Fig.1. Simulation results for Efficiency V.S Programming pulses area. Using LFC programming method for different αL. The probe pulse area for this simulation is 0.05 Pi.
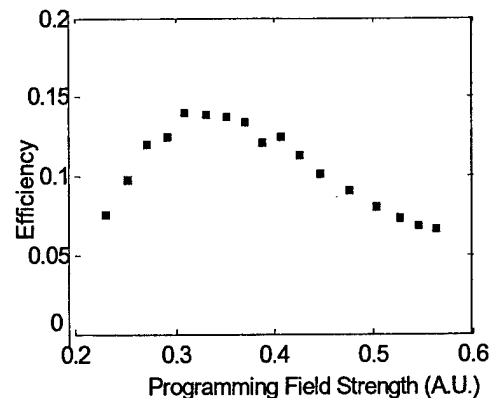
Fig.2. Experiment results for αL=1.4, using LFC programming method. Probe pulse area for this experiment was roughly 0.05 Pi.

[1] "Optical coherent-transient true-time-delay regenerator", K.D.Merkel, W.R.Babbitt Opt.Lett, 21, 1102,1996
[2] "Demonstration of highly efficient photon echoes", C.S.Cornish, W.R.Babbitt, L.Tsang. Opt.Lett, 25,1276-8,2000.
[3] "High bandwidth spectral gratings programmed with linear frequency chirps". R.Reibel, Z.W.Barber, M.Tian, W.R.Babbitt, J.Lumin.98, 355-65,2002.

Theory and Applications of Linear Sideband Chirp Programming

R. Reibel[*], M. Tian, Z. Barber, J. Fischer, and W. R. Babbitt

Department of Physics, Montana State University, Bozeman, MT 59717

The process of true time delay (TTD), where a reference signal is delayed by some time, τ_d, has become a highly desired tool for phased array processes such as beam steering, coherent detection and has application to arbitrary waveform generation. Currently, phased array processes are driven with phase shifting devices (PSD), which produce beam squint when used at wide bandwidths (> 1 GHz). The inherent problem with PSD's is that they do not impart each frequency component of the signal with the same time delay. TTD, however, delays each frequency component by the same delay time eliminating beam squint. In this presentation, we present the theoretical background as well as experimental demonstrations for a novel TTD programming technique. The demonstrations utilized state of the art, off-the-shelf commercial equipment in a compact optical setup to program spatial-spectral gratings into an inhomogeneously broadened absorber.

Broadband TTD applications have been shown before using either high-powered pulsed lasers or specialized chirped external cavity diode lasers. Because of the expense of high-powered pulse lasers and the complexity of stabilizing chirped lasers, other programming methods were investigated. It is desirable to have a highly stable, extremely precise, large bandwidth chirping source. Through the use of integrated optics phase modulators, these requirements can be met in a compact, affordable, large bandwidth, commercially available package. In order to create a linear sideband chirp, these modulators are driven with a chirping square wave from an extremely fast pulse pattern generator. Such a function, in essence, creates cw sidebands at the start frequency, f_{start}, and slowly ramps the sidebands linearly in time to the stop frequency, f_{end}. In order to produce a TTD grating, we interfere two identically chirped pulses offset slightly in frequency by δ. Figure 1 shows a colormap depicting the population difference for the inhomogeneously broadened absorber as a function of frequency detuning and time. Here, as the sidebands chirp, the two pulses spectrally interfere to create a TTD grating. The time delay set up using this method is $\tau_d = \delta\tau_c / B$. Here τ_c is the chirp temporal duration and B is the bandwidth of the chirp given by $B = f_{start} - f_{end}$.

A discussion of the theoretical aspects of programming with linear sideband chirps will be presented. Specifically, results from a Maxwell-Bloch simulator that includes arbitrary phase show the beneficial features of programming with this method compared to other approaches. Experimental demonstrations using the linear sideband approach will also be presented. Here we have demonstrated time delays from 100 ns to 1 μs. Figure 2 shows the heterodyned echo signals resulting from probing different TTD gratings with 666 Mbit/s BPSK probe pulses. TTD of 1 Gbit/s sequences will also be presented as well as how this programming technique can be applied to steer phased array radar systems.

With the availability of wide bandwidth off-the-shelf integrated optics phase modulators and stabilized lasers, this technique will be able to program and accumulate multi-gigahertz TTD gratings in the near future, having a significant impact upon both phased array processes as well as arbitrary waveform generation.
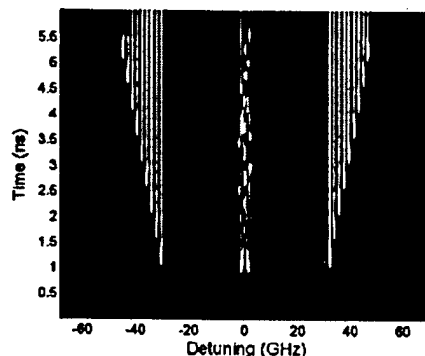

Figure 1. Modeled spectral gratings using a temporally overlapped linear sideband chirped programming method.
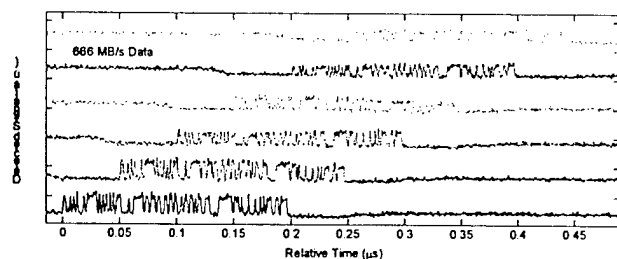

Figure 2. Various echoes with time delays ranging from 50 to 300 ns. Here the bits are 666 Mbits/s BPSK data that has been heterodyned.

*Present Address: Directed Energy Solutions, 949 Elkton Dr., Colorado Springs, CO, 80907

WITHDRAWN

DYNAMICS OF GLASSES AT TEMPERATURES WHEN THE TWO-LEVEL SYSTEM MODEL FAILS (4.5-30 K): STUDY BY SINGLE MOLECULE SPECTROSCOPY

A.V. Naumov[1], Yu.G. Vainer[1], M. Bauer[2], L. Kador[2]

(1) *Institute of Spectroscopy, Russian Academy of Sciences, Troitsk, Moscow reg., 142190 Russia*
(2) *Institute of Physics and BIMF, University of Bayreuth, D-95440 Bayreuth, Germany*

The anomalous dynamics of glasses at temperatures below 1-2 K are usually described with the standard two-level system (TLS) model. Also at higher temperatures, amorphous materials exhibit a number of anomalous properties (in comparison with perfectly ordered crystals) which are still poorly understood. The TLS model cannot explain most of these phenomena. Some answers are given by the soft potential model (SPM), which was developed to describe the dynamics of glasses at temperatures above 2-3 K. According to the SPM model, thermally activated transitions in TLSs and the quasi-localized low-frequency modes (LFMs) of the matrix exist in addition to acoustic phonons and tunneling TLSs and contribute to the total dynamics of disordered solids. But the SPM model is also purely phenomenological and cannot answer many principal questions. For example, important questions concerning the dynamics of glasses, such as interactions between TLSs, the existence of three or more level systems, or the role of structural relaxations are still open.

We present the results of a SMS study on purely amorphous *polyisobutylene* doped with *tetra-tert-butylterrylene* (TBT) in the temperature region $T = 4.5 - 30$ K, where the main assumptions of the tunneling TLS model are expected not to be valid. The measurements were aimed at obtaining new knowledge about the spectral dynamics of doped amorphous solids on a microscopic level. We observed the temporal evolution of a number of fluorescence excitation spectra of single TBT molecules detected by scanning repeatedly over the same frequency region (see examples in the Figure). The analysis of the widths of the recorded spectral trails and their frequency jumps allowed us to obtain new information about the spectral dynamics in the system under study. We indeed observed many single molecules (SMs), whose spectral trajectories were not consistent with the model of tunneling TLSs. At the same time the temporal behavior of a large part of SM spectral trails looks similar to the spectral histories observed at $T \leq 2$ K (with the exception of larger spectral widths). Some of the observed effects look very intriguing and we cannot explain them. To obtain more general information about the dynamics of the matrix we detected a large number of SM spectra and analyzed the distributions of their parameters. These distributions are invariable and characteristic for the matrix properties. By comparing the measured and simulated distributions of the parameters we concluded some points about the system under study.

The following results were obtained: ❶ At $T = 2$ K the spectral histories of most SM were found to be consistent with the TLS model. ❷ At higher T more and more trajectories began to show anomalous behavior, demonstrating that the TLS model is not adequate at these temperatures. ❸ The contribution of LFMs of the matrix to the total spectral shape of SM spectra was measured.
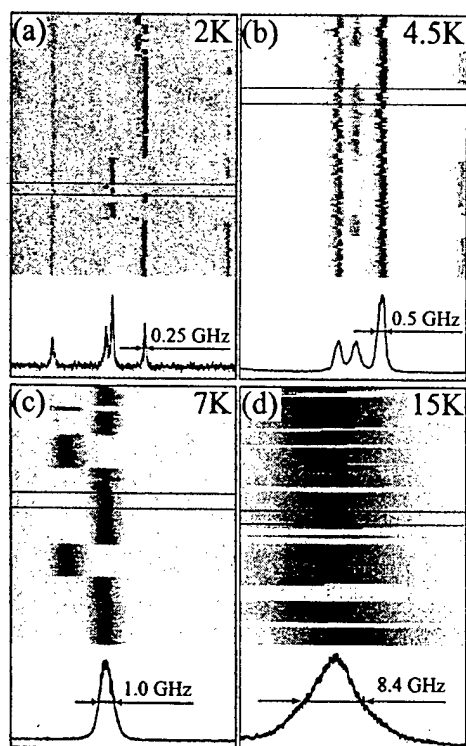
Nonperturbative theory of multiphonon transitions: critical dependence on the interaction strength

V. Hizhnyakov, H. Kaasik, and M. Selg

Institute of Physics, University of Tartu, Riia 142, 51014 Tartu, Estonia;
E-Mail: hizh@fi.tartu.ee

The multiphonon transitions in molecular systems and in solids are usually considered in the framework of the time-dependent perturbation theory. According to this theory the transition rate is described by the Fermi Golden Rule and it increases with the interaction causing the transition. The theory is applicable only in the case when the latter interaction is weak.

Recently, a new theory was proposed [1], which gives a nonperturbative description of the two-phonon relaxation. In this theory, the rate of emission of phonons is evaluated analogously to the emission of photons by a black hole: it is determined by the transformation of phonon (photon) operators in time. In this communication, we generalize method [1] in order to extend its applicability to: a) the multiphonon relaxation of high-frequency local modes, b) the multiphonon nonradiative electronic transitions caused by the quadratic nondiagonal vibronic interaction.

It has been found that the multiphonon relaxation of a strongly excited local mode exhibits a critical behavior with respect to the strength of the anharmonic interaction and the energy of the mode: the rate of relaxation is strongly enhanced at the critical value(s) of the given parameter(s). Analogously, in the case of the nonradiative transitions caused by the quadratic nondiagonal vibronic interaction, the rate of the transition displays a critical behavior with respect to the interaction strength and the temperature. E.g. it has been found that if the nondiagonal quadratic interaction has a value close to the critical one, V_{cr}, then even at low temperatures the rate of transitions may be very high (comparable to the mean phonon frequency). Besides, in this case there may exist a temperature interval where the usual increase of the transition rate with temperature is replaced by the decrease. It has also been found that a strong quadratic nondiagonal interaction leads to a strong renormalization (increase) of the activation energy. These results may be important for understanding of the mechanisms of catalysis of chemical reactions [2].

The critical behavior of two-phonon transitions has recently been observed on studying the hot luminescence of self-trapped excitons in solid Xe at low temperatures [3]. Xe crystal is the most suitable object to verify the theoretical predictions, as two-phonon relaxation channel is dominant in a wide range of the vibrational levels ($n = 20 - 44$) of the quasi-molecular emission centers Xe_2^*. As expected, a sharp maximum of the relaxation rate has been observed, which corresponds to the "critical" level $n_{cr} = 22$.

1. V. Hizhnyakov, Phys. Rev. B **53**, 13981 (1996); Europhys. Lett., **45**, 508 (1999);
2. V. Hizhnyakov, H. Kaasik, J. Chem. Phys. **114**, 3127 (2001).
3. V. Hizhnyakov, et al. Physica B, **263-264**, 683 (1999).

TEMPERATURE BROADENING OF SPECTRAL HOLES IN GLASS UNDER HIGH HYDROSTATIC PRESSURE: ISOTHERMAL AND CYCLING EFFECTS

J. Kikas[1,2], V. Hizhnyakov[1,2], J. Takahashi[1,2*], A. Suisalu[2], A. Laisaar[2] and An. Kuznetsov[2]

[1] Department of Physics, University of Tartu, Tähe 4, Tartu 51010, Estonia
phone: +372 7375541, fax: +372 7375540, e-mail: jaakk@physic.ut.ee
[2] Institute of Physics, University of Tartu, Riia 142, Tartu 51014, Estonia

We demonstrate that the pressure effects observed in a polymeric glass in two basically different types of spectral hole burning experiments, isothermal and temperature cycling, can both be coherently handled within the same theoretical approach based on the soft potential model (SPM) [1]. For this we assume a linear coupling of soft systems to pressure P: $U_P(x) = U_0 (\eta x^2 + \xi x^3 + x^4 + \kappa P x)$ [2], and, contrary to a conventional assumption, an *asymmetric* (in ξ) distribution of the SPM parameters:

$$F(\eta, \xi) \propto |\eta| (1 - \beta \eta \xi).$$

Irreversible broadening of spectral holes in chlorin-doped polystyrene glass was studied in the thermal cycling experiments under high pressure (by raising the temperature from 5 K to various magnitudes up to 18 K and returning to 5 K at various fixed pressures between 0 and 5 kbar). At all pressures the increment in the hole width after completion of a thermal cycle exhibits a slightly superlinear ($\sim T^{3/2}$) dependence on the cycling temperature. The magnitude of this increment is essentially reduced under high pressure (at 5 kbar it is about twice less than at ambient pressure). The residual broadening of holes is interpreted as a result of irreversible spectral diffusion arising from interaction of the electronic transition in a dopant molecule with two-level systems (TLSs, $\eta < 0$) which perform thermally activated overbarrier jumps between two possible states. In order to explain the observed pressure reduction of the residual broadening one has to assume that the most numerous TLSs are those having double-well potentials with the "right" well (associated with a larger local volume) located at a higher energy than the "left" well corresponding to smaller local volume ($\beta > 0$). In this case pressure reduces the number of almost symmetric TLSs, which provide the largest contribution to hole broadening.

Our earlier results [3] on isothermal hole burning at various fixed pressures, where the main contribution to the holewidth comes from single-well soft local modes ($\eta > 9\xi^2/32$), also qualitatively fit into this picture, i.e., again $\beta > 0$ consistently with the result from cycling experiments.

* Present address: Japan Science and Technology Corporation (CREST), 758-65 Bibi, Chitose, Hokkaido 066-8655, Japan

[1] V. G. Karpov et al., Sov. Phys. JETP **57** (1983) 439.
[2] U. Buchenau et al., Phys. Rev. B **46** (1992) 2798.
[3] V. Hizhnyakov et al., Phys. Rev. B **62** (2000) 11296.

Method of extending hyperfine coherence times in $Pr^{3+}:Y_2SiO_5$

E. Fraval, M. J. Sellars, and J. J. Longdell
Laser Physics Center, Australian National University.
(Dated: March 3, 2003)

There is currently great interest in using nuclear spin states in a solid state host to store and manipulate quantum information. Long nuclear spin state coherence times will be required for these applications. Long nuclear spin coherence times are challenging to achieve in a solid state system due to interactions with other spins within the environment. One approach is to use spin free hosts, however not many centers of interest are chemically compatible with such hosts. We have demonstrated a method for increasing the coherence times for transitions associated with spin systems of $I > 1$. $Pr^{3+}:Y_2SiO_5$ was chosen to demonstrate this technique as it's use has been proposed for quantum computing[1] and it has already been used in a slow light demonstration[2].

The method for increasing the coherence time of praseodymium hyperfine ground state transitions is to apply an external magnetic field such that the Zeeman splitting of the hyperfine transition is at a critical point in three dimensions, making the first order Zeeman shift vanishingly small for the transition. Therefore small magnetic field perturbations originating from host lattice spin flips do not cause any appreciable change in transition frequency, negating the dominant dephasing mechanism in $Pr^{3+}:Y_2SiO_5$. Using this method a phase memory time of 82ms, two orders of magnitude greater than the previously reported value[3] was achieved as shown in Figure 1. A new dephasing mechanism that is caused by electric field interactions now limits the coherence time.

The system was investigated with two and three pulse Raman heterodyne spin echos using the $^3H_4 - ^1D_2$ optical transition at 605.977nm. Using these techniques the coherence time as a function of magnetic field in the region of the critical point was investigated. Directions to further increase the coherence time of the system are also discussed.

contact details:
email: elliot.fraval@anu.edu.au
phone: (+612) 6125 4129
(+612) 6125 0379 (LAB)
fax: (+612) 6125 0029

---

[1] K. Ichimura, Opt. Commun. **196**, 119 (2001).
[2] A. V. Turukin, V. S. Sudarshanam, M. S. Shahrier, J. A. Musser, B. S. Ham, and P. R. Hemmer, Phys. Rev. Lett. **88**, 023602 (2002).
[3] B. S. Ham, M. S. Sharier, and P. R. Hemmer, Phys. Rev. B **58**, R11825 (1998).
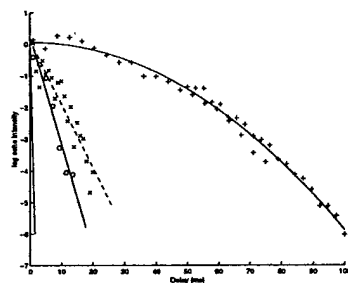
FIG. 1: Two pulse echo sequences taken at the critical point magnetic field $B_{CP} = \{732, 172, -219\}\,G$ for transition $m_I = +1/2 \leftrightarrow +3/2$ at site 1a (+). The $m_I = +1/2 \leftrightarrow +3/2$ site 1b transition ($\times$); the $m_I = -3/2 \leftrightarrow +3/2$ transition (o) and the zero field $T_2 = 500\mu s$ decay line shown for comparison.

Characterization of Individual Two-Level Systems (TLSs) by Stark Effect Tuning of Single-Molecule Spectra

Markus Bauer, Lothar Kador[†]

University of Bayreuth, Institute of Physics and "Bayreuther Institut für Makromolekülforschung (BIMF)", D–95440 Bayreuth, GERMANY

The spectra of single dopant molecules in disordered matrices are usually affected by two-level systems (TLSs) at cryogenic temperatures. The interaction with TLSs can lead to broadening and/or splitting of the lines, often giving rise to complicated spectral shapes [1,2]. If only one TLS is coupled strongly to a dye molecule, its line is split into two components.

We performed Stark effect experiments on the spectra of single terrylene molecules in the Shpol'skiĭ matrix *n*-hexadecane. Apart from the familiar linear Stark shift, some molecules underwent distinct spectral changes with the electric field strength. Figure 1 summarizes the data for one example. The two components of the molecular line do not shift uniformly with the electric field, but the splitting and the intensity ratio exhibit distinct and reproducible variations. The data can be well described by assigning permanent dipole moments to the localized states of the TLS [smooth lines in Fig. 1 (b) and (c)]. This allows us to fully characterize the parameters of the specific TLS, *i. e.*, to determine its zero-field asymmetry, tunnel parameter, and dipole moment difference. For some of the TLSs, dipole moment differences as large as 8 D were found. Possible ranges of the TLS parameters for the observation of this effect will be discussed.
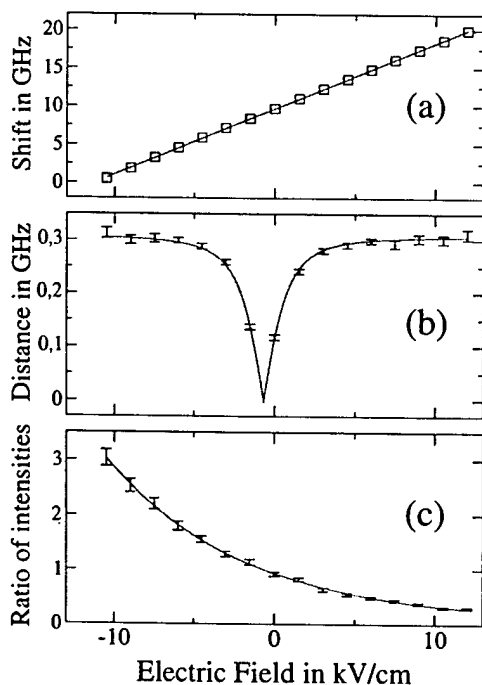
Fig. 1: Spectral changes of a single terrylene molecule in *n*-hexadecane with the external electric field strength. The line consists of two components due to coupling to a single TLS. Part (a) shows the overall spectral shift (linear Stark effect), part (b) the splitting, and part (c) the intensity ratio of the components as a function of field strength. The smooth lines were obtained by model calculations.

[1] E. Geva and J. L. Skinner, J. Phys. Chem. B **101**, 8920 (1997).
[2] A.-M. Boiron *et al.*, Chem. Phys. **247**, 119 (1999).

[†]Phone (+49-921) 55-3182, Fax (+49-921) 55-3250, e-mail: lothar.kador@uni-bayreuth.de

Differences of the radiative linewidth in single-impurity molecule spectroscopy

Inna Rebane

Institute of Physics, University of Tartu, Riia 142, 51014 Tartu, Estonia

Phone +372 7 428164, Fax +372 7 383033, E-mail inna@fi.tartu.ee

A theory of the dependence of the spontaneous emission rate and, consequently, the dependence of the radiative linewidth of the single-impurity molecule on the orientation of the transition dipole moment in a birefringent host crystal [1] is developed for the case of the quadrupole radiation. The dependences of the density of the final states of the emitted photon (expressed through the phase and the ray velocities of the photon) and the local and the average electric fields' strengths on the orientation of the wave vector of the photon in the host crystal and on the principal refractive indices are taken into account.

In a uniaxial host crystal, if the ordinary principal refractive index n_o is larger than the extraordinary one, n_e, the spontaneous emission rate of the quadrupole radiation has a maximal value when the transition dipole moment is directed along the optical. When the dipole moment is perpendicular to the optical axis it has the minimal value. For $n_e > n_o$ the situation is the opposite: the spontaneous emission rate of the quadrupole radiation reaches its maximum when the dipole moment is perpendicular to the optical axis. Note that for the case of the dipole radiation the situation is the opposite.

For $n_o = 1.5$ the spontaneous emission rates of the dipole radiation for different dipole moment orientations differ by more than 10%, if $n_e < 1.366$ or $n_e > 1.630$. For the same n_o the spontaneous emission rates of the quadrupole radiation differ by more than 12%, if $n_e < 1.366$ and more than 11%, if $n_e > 1.630$. Thus, at the same difference $| n_o - n_e |$ the spontaneous emission rates of the quadrupole radiation differ a little more than in the case of the dipole radiation.

References

[1] I. Rebane, Optics Commun. **217** (2003) 265.

Molecular Aggregation at Single Molecule Scale

Jui-Hung Hsu, Urs P. Wild, Sheng-Hsien Lin, Ta-Chau Chang

Institute of Atomic and Molecular Sciences, Academia Sinica
Taipei, Taiwan 106, Republic of China

We have investigated the aggregation of DiI molecules embedded in polyvinyl alcohol (PVA) film. The sample of PVA water solution with DiI concentration of ~ 0.1 nM was spin coated on a cover slip. Since water in the polymer matrix can preserve for several tens of minutes, it facilitates the hydrophobic DiI molecules to form aggregates. The much bright spots, red-shifted spectra and non-single exponential decays characterized the J-aggregates of DiI molecules. For example, a lifetime distribution in the range between 3.0 and 4.2 ns was measured for individual DiI molecules in PMMA matrix. However, very different decay dynamics were observed for the DiI molecules in PVA. Figure 1 shows several fluorescence decays obtained from various bright spots. Different decay dynamics are attributed to different sizes of aggregates. The distribution of various aggregates and the correlation between aggregate size and its photophysics will be discussed.
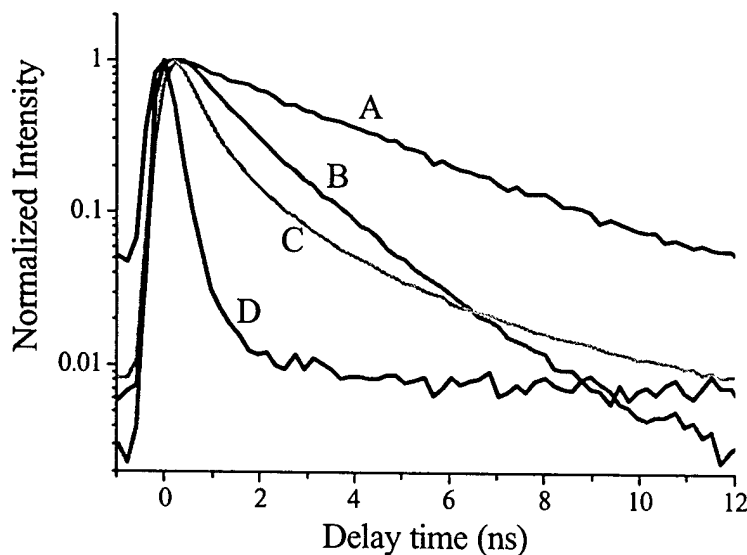
Coherence of photons originating from a single quantum system

F.Jelezko[1], A.Volkmer[1], I.Popa[1], K.K.Rebane[2] and J.Wrachtrup[1]

[1] 3. Physikalisches Institut, Universität Stuttgart, Pfaffenwaldring 57, 70569 Stuttgart, Germany
tel: 0049-711-685-5276; e-mail: f.jelezko@physik.uni-stuttgart.de
[2] Institute of Physics, Tartu University, 142 Riia Str., 51014, Tartu, Estonia;
tel.: 372-7-428159; fax: 372-7-383033; e-mail rebanek@fi.tartu.ee

Single quantum systems as sources of single photons open novel possibilities to learn about the fundamental feature – dualism of light. A new experimental technique based on single impurity molecule spectroscopy is demonstrated [1], which allows to characterize the coherence length of a single photon source using single photon interferometry of single center in solids. The first-order correlation function has been recorded and analyzed in terms of a single exponential decay time. A coherence time of ~ 5 ps has been obtained, which is in good agreement with the corresponding spectral line width and demonstrates the feasibility of Fourier-transform spectroscopy of singe quantum systems. Further prospective single molecule spectroscopy – single molecule interference experiments – are discussed.

References:

[1] F.Jelezko, A.Volkmer et al., submitted to Phys. Rev.

Three-dimensional orientation of single molecules measured by far-field and near-field fluorescence microscopy

Martin Vacha

Department of Organic and Polymer Materials Chemistry, Tokyo University of Agriculture and Technology, Nakacho 2-24-16, Koganei, Tokyo 184-8588, Japan
tel.: +81-42-388-7050; fax: +81-42-381-7979; e-mail: vacha@cc.tuat.ac.jp

Masahiro Kotani

Department of Chemistry, Gakushuin University, Mejiro 1-5-1, Toshima-ku, Tokyo 171-8588 Japan; e-mail: masahiro.kotani@gakushuin.ac.jp

Spatial three-dimensional orientation is an important parameter in single molecule studies. Here, we present a simple method that allows determination of the orientation of absorption transition dipole moments of single molecules by combined far- and near-field fluorescence polarization microscopy. Conventional far-field microscopy provides projection of the dipole orientation into the sample plane. Near field at total internal reflection surface has a strong z-component. For a given in-plane angle ϕ, the amplitude and phase shift of the fluorescence signal excited by the polarization-modulated near field are determined unambiguously by the value of the out-of-plane angle θ. Both the far-field and near-field excited fluorescence traces are fitted with expressions for the electric field in the respective excitation modes. The figure below shows the fluorescence traces together with the fitting parameters ϕ, θ for a molecule that underwent an orientation change during the course of the measurement. As a result, the phase shift between the far- and near-field traces is different in the left and right parts of the figure. To monitor such orientation changes in real time both excitation modes are periodically alternated. An example of the results is an observation of conformation dynamics of individual rhodamine molecules covalently attached to a quartz substrate.
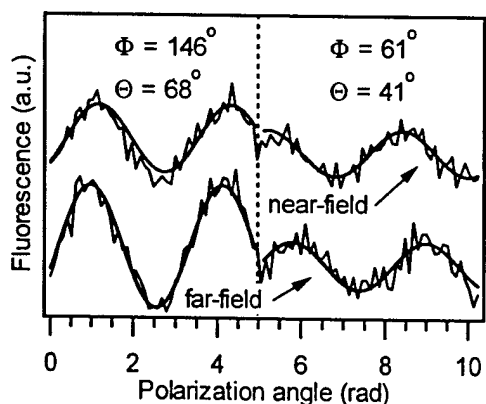
M. Vacha and M. Kotani, *J. Chem. Phys.* 118 (2003), in press

Single molecule optical detection of carboxytetramethylrhodamine connected by alkyl chains on glass and quartz substrates

Toshiro Tani, Yoshihiro Yamaguchi, Kenji Ohuchi and Masaru Oda

Department of Applied Physics, Tokyo University of Agriculture and Technology
[the 21st Century COE program of "Future Nano-Materials"]

2-24-16 Naka-cho, Koganei, Tokyo 184-8588, Japan
Phone: +81-42-388-7153, Fax: +81-42-385-6255, ttani@cc.tuat.ac.jp

Recent developments in room temperature imaging and spectroscopy of single fluorescent molecules are promising particularly for biological studies because they allow the observation of conformational changes of macromolecules in action. However, single fluorophores in such systems often display various kinds of fluorescence intensity and spectral fluctuations, even in the absence of biologically relevant events. This may indicate that once we go into the field of microscopic intermolecular interactions there exist much issues in particular the dynamics of conformation, energy transfer, dipolar orientations etc., to be elucidated in single molecule detection levels. We have already constructed original scanning laser microscope using graded-index rod-shaped micro lens with "0" working distance and have investigated single molecule vs. matrix interactions at 1.6K. At low temperature observations, there are sometimes claimed that physics itself seems to be nice but it is still not suitable for comprehension of biological functions. Thus we have also fabricated rather simple version of room-temperature single molecule imaging as well as spectroscopy apparatus by specific modification from ordinary optical microscope (Nikon, TE2000-U) and started investigation on the dynamical aspect of fundamental processes mentioned above more directly. In this paper, we will describe our initial stage of single molecule detections at room temperatures. The prototype systems we have adopted here are the fluorescent dye molecules connected covalently by the alkyl chains on to the surface of glass and quartz substrates: Dye molecules, 5-(and-6)- carboxytetramethyl-rhodamine, succinimidyl ester (5(6)-TAMRA, SE), are kind of derivatives of rhodamine-6G and used as leveling reagents. As for silanization reagent, `-aminopropyltriethoxysilane (3-APTEOS) is used. First in about 40-mL ethanol silanizations on to the cleaned surfaces of glass or quartz substrates are performed by adding 5 ˙L of 3-APTEOS and reacted for about 30 min at room temperature. Then in anhydrous ethanol, labeling reactions of primary amine with the succinimidyl esters are proceeded by adding 0.1 mL of 1.9 ~10^{-6} M/L TAMRA-SE /a-DMF solution. For comparison simple rhodamine-6G spin-coated samples are also prepared. Imaging observations are performed in air by N.A.= 0.90 objective (Nikon, EPI-P: ~100) in air under evanescent light excitation configuration. Using Kodak KAF-1400 CCD chip as a detector we have obtained successful imaging of the single molecules. Detailed descriptions of our results as well as instrumentations will be presented.

Single molecule detection of a phosphorescent organometallic iridium(III) complex

Martin Vacha, Yohei Koide

Department of Organic Materials Chemistry, Tokyo University of Agriculture and Technology, Naka-machi 2-24-16, Koganei, 184-8588 Tokyo, Japan
Tel.: +81-42-388-7050; Fax: +81-42-388-7050; e-mail: vacha@cc.tuat.ac.jp

Masahiro Kotani

Department of Chemistry, Gakushuin University, Mejiro 1-5-1, Toshima-ku, 171-8588 Tokyo, Japan

Hisaya Sato

Graduate School of Bio-Applications and Systems Engineering (BASE), Tokyo University of Agriculture and Technology, Naka-machi 2-24-16, Koganei, 184-8588 Tokyo, Japan

Efficient intersystem crossing to a long-lived triplet state is a major obstacle in the optical detection of organic dyes at the level of individual molecules. Further requirements for single-molecule detection include strong absorption, high emission quantum yield, and high photostability. Here, we report room temperature detection of single molecules of a phosphorescent organometallic complex tris(2-phenylpyridine)-iridium [Ir(ppy)$_3$]. In recent years, this material has attracted considerable attention as an electroluminescent (EL) emitter due to its high quantum efficiency. The high EL yield is a result of efficient phosphorescence from a triplet metal-to-ligand charge transfer state. At room temperature, the phosphorescence quantum yield is more than 0.5, and the triplet state lifetime is on the order of 1 μs. These parameters make Ir(ppy)$_3$ a possible candidate for photoluminescence detection at single molecule level, which is a necessary first step towards single molecule EL studies. In this contribution, photostability was examined for Ir(ppy)$_3$ dispersed in poly(methyl methacrylate) films at moderate concentrations. Photobleaching of the samples shows a two-exponential decay with characteristic times on the order of seconds and tens of seconds. For single molecule experiments, low concentration spin-cast samples were imaged by a wide-field microscope with a cooled CCD camera. Individual Ir(ppy)$_3$ molecules were characterized by their phosphorescence time traces (one- or multi-step photobleaching, blinking) and by polarization modulated excitation.

Emission of Dye Molecules on Silicon Nanocrystal Surfaces

Jörg Martin, Frank Cichos and Christian von Borczyskowski
Institute of Physics 122501, Chemnitz University of Technology
09107 Chemnitz, GERMANY
Phone: +49/(0)371 531 3066
Fax: +49/(0)371 531 3060
email: j.martin@physik.tu-chemnitz.de

Individual silicon nanocrystals exhibit the same blinking features in emission time traces as other semiconductor nanocrystals. To explore if the dark state of the particle is also coupled to a charged state of the nanocrystal, we have deposited potential sensitive dye molecules on top of smaller silicon nanocrystal clusters. The dye is able to detect positive and negative electrostatic potentials by a blue or red shift of the emission spectrum, which is well separated from the nanocrystal emission.

To measure the emission spectrum of the dye molecules we utilize confocal microscopy with an excitation wavelength suited to excite the dye molecules as well as the silicon nanocrystals. The emission spectrum of the dye is measured at each point along a line (with a silicon nanocrystal cluster at the line) in the confocal image. Thus the changes in the spectral position at the location of the particle can directly be compared to other points in the line with dye molecule but without silicon. The experiments show, that the dye molecules exhibit a clearly visible red shift of the emission at the position of the particle from which we conclude an increased negative potential close to the dye. An electron trapping at the interface or in the close environment of the silicon is thus a potential explanation for the observations.

Semiconductor nanocrystals covered with organic molecules: crystal growth, characterization and its optical properties

Masaru Oda, Masayuki Matsubayashi, Jyunpei Tsukamoto, Shinji Suzuki,
Izumi Hagiwara, Atsushi Hasegawa and Toshiro Tani

Department of Applied Physics, Tokyo University of Agriculture and Technology
[the 21st Century COE Program of "Future Nano-Materials"]

2-24-16 Naka-cho, Koganei, Tokyo 184-8588, Japan
Phone: +81-42-388-7428, Fax: +81-42-385-6255, odamasa@cc.tuat.ac.jp

In the last decade, semiconductor nanocrystals covered with organic molecules have been extensively investigated due to their unique hybrid properties of quantum confined luminescence and chemical reaction itself. It provides us well-defined and high-quality 3D quantum confined dot systems in the field of basic material sciences and also possible biological and/or electronic and optoelectronic applications in future technologies as well. We also are interested in the aspect of hybrid organic-inorrganic nature of this system and have started our investigation from the initial stage of synthesis and growth of CdSe and CdSe/ZnS nanocrystals hybridized with regand molecules such as trioctylphosphine oxide (TOPO) and hexadecylamine (HDA) by ourselves totally.

In this paper we will describe at first our way of the synthesis and present performance with optical properties as well as TEM observations. Our synthetic pathways are based on the original methods by Bawendi's [1] and Arivisatos' [2] but fairly modified at present. One of the improvements is to use rather highly purified TOPO and the reaction scale is order of magnitude decreased, which bring us increased reproducibility. We have also been inspecting the effect of stronger regand e.g.. teradecylphosphonic acid (TDPA) and others mixed in TOPO, and the effect of CdO for precursors of CdSe instead of dimethyl cadmium. Effect of the former for instance is marvellous: Typically the FWHMs of luminescence spectra are improved to about 26.4 nm for the nanocrystals having average diameter of 4.3 nm, while those of our previous ways show 46.9 nm for the ones with similar diameters. Among notable features which displayed in these systems so-called blinking of luminescence is also interesting. It is a kind of "instability" and on-and-off behavior of luminescent, which is different from ordinary singlet anti-bunching. Surface states may participate in the phenomena, while it is still far from comprehension yet. From applicational point of view, the blinking should be removed. To understand more detailed nature of the phenomena, we have also been investigating luminescence properties emitted from single nanocrystals. On-off behaviour and photo-induced increment of luminescence intensity, i.e. photobrightening effect [3], are observed at room temperatures, detailed results of which are also described.

[1] J. Am. Chem. Soc. 115 (1993) 8706. [2] Angew. Chem. Int. Ed. Engl. 36 (1997) 45.
[3] J. Phys. Chem. B105 (2001) 8281.

REVEALING THE PRIMARY PHOTON ECHO'S SATELLITES IN RUBY

V.V.Samartsev, A.M.Shegeda, A.V.Shkalikov, V.A.Zuikov

Kazan Physical-Technical Institute of Russian Academy of Sciences, Sibirsky Trakt Str. 10, Kazan, 420029, Russia.
Phone: 7-8432-729333 Fax: 7-8432-725075 e-mail: samartsev@kfti.knc.ru

The search experiments are carried out on the special setup of photon echo and the primary echo's satellites are discovered in ruby (energy transition: $^4A_2 - {}^2E(\bar{E})$; wavelength is 693.4 nm; temperature is 2 K) as a result of the computer statistical data processing of large number of echo signals.

The theoretical analysis of the experimental data shows that appearance of satellites is due to magnetic hyperfine interaction of the nuclear spin I of isotope Cr-53 with electron spin. The number of satellites is equal to $2I+1$ that is 4 for $I = 3/2$ (Cr-53). The results of this theoretical analysis agree with the experimental data.

(a)
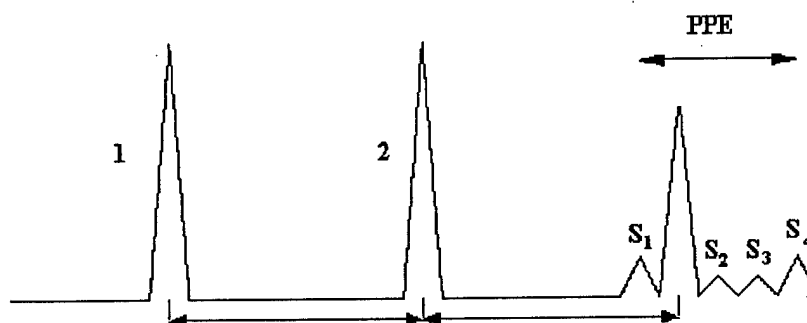
(b)
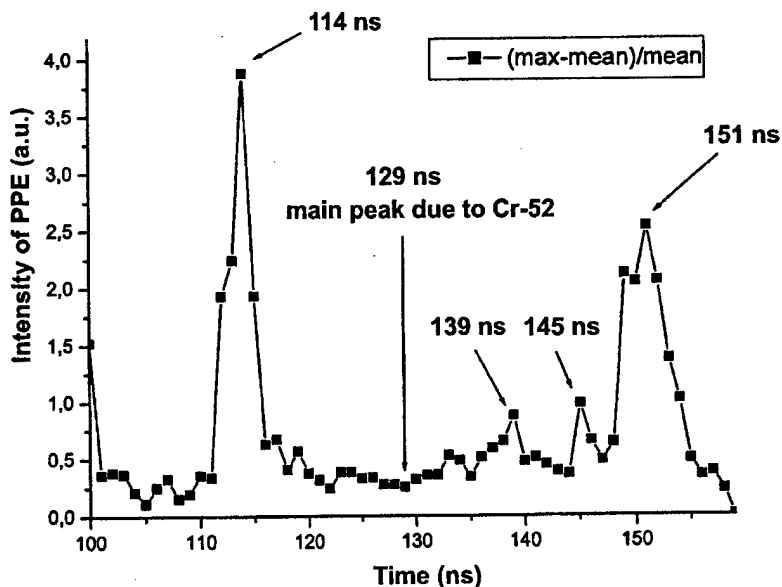
Figure 1. (a) Exciting pulses (1 and 2) and primary photon echo (PPE) with satellites (S_1, S_2, S_3, S_4); (b) results of the search for satellites in ruby (without PPE, due to Cr-52) .

Amplification of nonclassical states of light under triggered superradiance regime

A.A.Kalachev, V.V.Samartsev

Kazan Physical-Technical Institute of RAS,

10, Sibirsky Trakt str., 420029, Kazan, Russia

phone: +7 8432 729333; fax: +7 8432 725075

e-mail: kalachev@kfti.knc.ru

Recently, nonclassical states of light have been intensively investigated in quantum optics. These states attract considerable attention in part because of many practical applications such as quantum communication, quantum imaging and quantum information processing. In this connection the problem of amplification of light in nonclassical state is of important. This amplification can be realized under optical superradiance regime when quantum correlations transfer from optical centers to emitted photons.

In this work the possibility of amplification of pulses of squeezed light in the regime of triggered optical superradiance is analyzed. The kinetic equations are obtained which describe the dynamics of cooperative development of the population inversion and variance of quadrature components of polarization of optical centers interacting with each other through the common radiation field. The triggering pulse field may be in the squeezed vacuum state or in the squeezed coherent state. The former corresponds to the case of triggering superfluorescense. The dependence of the squeezing degree of the superradiance field on the squeezing degrees of the triggering pulse field and polarization of an amplifying medium is determined. It is shown that in the case of a sufficiently strong squeezing of the medium, the intensity of the squeezed quadrature component of the superfluorescense signal is lower than that of an incoherent spontaneous background. Therefore, the superradiance field can be characterized not only by a classical squeezing (when the variances of quadratures are not identical) but also by a quantum squeezing (when the variance of one quadrature is smaller than its vacuum value).

The possible applications of such amplification regime for the systems of quantum information processing are discussed. In part the amplification of weak pulses with conservation of quantum correlations may be exploited to produce nonclassical states of light, sub-shot-noise microscopy and quantum holography.

Author Index

Recep Avci
Montana State University
MSU Physics EPS 264
Bozeman, MT   59717
(406) 994-6164
avci@physics.montana.edu

Randy Babbitt
Montana State University
Spectrum Lab
P.O. Box 173510
Bozeman, MT   59717
(406) 994-6156
babbitt@physics.montana.edu

Zeb Barber
Montana State University
Physics Department
264 EPS Building
Bozeman, MT   59717
(406) 994-7988
pezinator@yahoo.com

Eli Barkai
University of Notre Dame
Dept. of Chemistry & Biochemistry
251 Nieuwland Science Hal
Notre Dame, IN   46556-5670
(574) 631-5235
jbarkai@nd.edu

Mariusz Bednarz
University of Groningen
Nijenborgh 4
Groningen, The Netherlands   9747 AG
M.Bednarz@phys.rug.nl

Laurent Bigot
CNRS-Alcatel
Alcatel R&I - Route de Nozay
Marcoussis Cedex, France   91461
laurent.bigot-carre@laposte.net

Rami Bommareddi
Alabama A&M University
Physics Department, PO Box 1268
Normal, AL   35762
(256) 372-8101
brreddy@aamu.edu

Sybrand Bonsma
University of Leiden
Molecular Physics - Huygens Laboratory
P.O. Box 9504
Leiden, NL   2300 RA
sbonsma@molphys.leidenuniv.nl

Geoffrey Burr
IBM Almaden Research Center
650 Harry Rd.
San Jose, CA   95014
(408) 927-1512
burr@almaden.ibm.com

Patrik Callis
Montana State University
Dept. of Chemistry
Bozeman, MT   59717
(406) 994-5414
pcallis@montana.edu

Ta-Chau Chang
Academia Sinica
P.O. Box 23-166
Taipei, Taiwan   106 ROC
tcchang@po.iams.sinica.edu.tw

Tiejun Chang
Montana State University
Spectrum Lab
P.O. Box 173510
Bozeman, MT   59717
(406) 994-7596
chang@spectrum.montana.edu

Eric Chronister
University of California, Riverside
6561 Aerial Court
Riverside, CA   92506
(909) 787-3288
eric.chronister@ucr.edu

Frank Cichos
Chemnitz Technical University
Institute of Physics
Reichenhainer Str. 70
Chemnitz, Germany   D-09126
371 531 3066
cichos@physik.tu-chemnitz.de

Zachary Cole
Montana State University
Spectrum Lab
P.O. Box 173510
Bozeman, MT   59717
(406) 994-5239
cole@spectrum.montana.edu

Rufus Cone
Montana State University
Physics Department
Bozeman, MT   59717
(406) 994-6175
cone@montana.edu

Alan Craig
Montana State University
Physics Department
Bozeman, MT   59717
(406) 994-6869
craig@physics.montana.edu

Claudine Crepin-Gilbert
CNRS-LPPM
LPPM Bat210, Universite Paris-Sud
Orsay, FRANCE   91405
claudine.crepin-gilbert@ppm.u-psud.fr

Jason Dahl
Montana State University
264 EPS Building
Bozeman, MT   59717
(406) 994-7988
sakana_78@hotmail.com

Volkmar Dierolf
Lehigh University
16 Memorial Drive East
Bethlehem, PA   18015
(610) 758-3915
vod2@lehigh.edu

Mikhail Drobizhev
Montana State University
Physics Dept ESP 264
Bozeman, MT   59717
(406) 994-7809
drobijev@physics.montana.edu

Yuliya Dzenis
Montana State University
Physics Department
Bozeman, MT   59717
(406) 994-7826
dzenis@physics.montana.edu

Randy Equall
Scientific Materials Corp.
310 Icepond Road
Bozeman, MT   59715
(406) 585-3772
rwesm@montana.com

Michael Fayer
Stanford University
Department of Chemistry
Stanford, CA   94305-5080
(650) 723-4446
fayer@stanford.edu

Joe Fischer
Montana State University
264 EPS Building
Bozeman, MT   59717
(406) 994-7988
fischer@physics.montana.edu

Elliot Fraval
LPC, ANU
51 Learmouth Dve, Kambah
Canberra, Australia   2902
elliot.fraval@anu.edu.au

Josef Friedrich
Munich Technical University
Dept. of Physics
Vöttinger Str. 40
Freising, Germany   85350
8161 71 3294
j.friedrich@lrz.tu-muenchen.de

Koji Fujita
Kyoto University
Department of Material Chemistry
Yoshidahonmachi, Sakyo-ku
Kyoto, Japan   606-8501
koji@collon1.kuic.kyoto-u.ac.jp

Jean-Pierre Galaup
Laboratoire Aime Cotton-CNRS
Bat 505 Centre d Orsay
Orsay, FR   F91405
jean-pierre.galaup@lac.u-psud.fr

Peter Geissinger
University of Wisconsin
Dept. of Chemistry
3210 N Cramer Street
Milwaukee, WI   53211
(414) 229-5230
geissing@uwm.edu

Anshel Gorokhovsky
CUNY/CSI
2800 Victory Blvd.
Staten Island, NY   10314
(718) 982-2815
gorokhovsky@postbox.csi.cuny.edu

Judith Grimm
University of Bern
Dept. of Chemistry & Biochemistry
Freiestrasse 3
Bern, Switzerland   3012
judith.grimm@iac.unibe.ch

Jan Hala
Charles University
Ke Karlovu 3
Prague, CZ121,   16
hala@karlov.mff.cuni.cz

Hiromasa Hanzawa
Osaka University
1-3 Machikaneyama-cho
Toyonaka-shi, Japan   560-8531
hanzawa@mp.es.osaka-u.ac.jp

Todd Harris
Montana State University
Spectrum Lab
P.O. Box 173510
Bozeman, MT   59717
(406) 994-6073
harris@spectrum.montana.edu

Joanne Harrison
Australian National University
29 Strong Place
Belconnen, Australia   ACT 2617
jph111@rsphysse.anu.edu.au

John Hayes
Iowa State University
116 Arizona Ave.
Ames, IA   50014
(515) 294-4872
jmhayes@iastate.edu

Vladimir Hizhnyakov
University of Tartu
Riia 142
Tartu, Estonia   51014
(372) 738-3017
hizh@eeter.fi.tartu.ee

Christopher Hollars
Lawrence Livermore National
Laboratory
7000 East Ave., L-232
Livermore, CA   94513
(925) 422-5155
hollars1@llnl.gov

Kazuyuki Horie
Tokyo University of Agriculture and
Technology
2 24 16 Nakacho Koganei shi
Tokyo, Japan   184-8588
(042) 388-7233
horiek@cc.tuat.ac.jp

Dehong Hu
Pacific Northwest National Lab
P.O. Box 999
Richland, WA   99352
(509) 376-5709
dehong.hu@pnl.gov

Ralph Hutcheson
Scientific Materials Corp.
310 Icepond Road
Bozeman, MT   59715
(406) 585-3772
scimat@montana.com

Mark Ivey
Montana State University
Spectrum Lab
P.O. Box 173510
Bozeman, MT   59717
(406) 994-1797
ivey@spectrum.montana.edu

Ryszard Jankowiak
Iowa State University
0706 Gilman
Ames, IA   50014
(515) 294-4394
jankowiak@ameslab.gov

Michael Jefferson
IBM Almaden Research Center
650 Harry Road
San Jose, CA   95125
(408) 927-2141
michael@almaden.ibm.com

Lothar Kador
University of Bayreuth
Institute of Physics
Bayreuth D-95440
Germany
921-55-31 82
lothar.kador@uni-bayreuth.de

Aliaksandr Karotki
Montana State University
Physics Department
Bozeman, MT   59717
(406) 994-7826
karotki@physics.montana.edu

Jaak Kikas
University of Tartu
Tähe 4
Tartu, Estonia   51010
(372) 737-5541
jaakk@physic.ut.ee

Flurin Könz
University of Leiden
Molecular Physics - Huygens Laboratory
P.O. Box 9504
Leiden, The Netherlands   NL-2300 RA
flurin@molphys.leidenuniv.nl

Stefan Kröll
Lund Institute of Technology
Box 118
Lund, Sweden   221 00
Stefan.Kroll@fysik.LTH.se

Katrina Kujawa
Montana State University
264 EPS Building
Bozeman, MT   59717
(406) 994-7988
mortalfools@hotmail.com

Mark Lasher
Spaywar Systems Center
53490 Dow St.
San Diego, CA   92152
(619) 553-2540
mark.lasher@navy.mil

Jean-Louis Le Gouët
CNRS-Laboratoire Aime Cotton
Campus Universitaire, batiment 505
Orsay, France   91405
jean-louis.legouet@lac.u-psud.fr

Jean-Pierre Lemaistre
CNRS-Laboratoire Aime Cotton
Universite Paris 6, 4 place Jussieu
Paris, France   F-75252
jp.lemaistre@wanadoo.fr

Andreas Lieb
University of Rochester
Optics, Wilmot Bldg
Rochester, NY   14627
(585) 275-5104
lieb@optics.rochester.edu

H. Peter Lu
Pacific Northwest National Laboratories
P O Box 9999
Mail Stop K8-88
Richland, WA   99352
(509) 376-3897
peter.lu@pnl.gov

Roger Macfarlane
IBM Almaden Research Center
650 Harry Road
San Jose, CA   95125
(408) 927-2428
macfarla@almaden.ibm.com

Alfred J. Meixner
University of Siegen
Adolf-Reichwein Str.
Siegen, Germany   57068
meixner@chemie.uni-siegen.de

Richard Meltzer
University of Georgia
Dept. of Physics and Astronomy
Athens, GA   30602
(706) 542-5515
rmeltzer@hal.physast.uga.edu

Kris Merkel
Montana State University
Spectrum Lab
P.O. Box 173510
Bozeman, MT   59717
(406) 994-7241
merkel@spectrum.montana.edu

W. E. Moerner
Stanford University
Dept. of Chemistry
M/C 5080
Stanford, CA   94305
(650) 723-1727
wmoerner@stanford.edu

Norio Murase
National Institute of AIST
Midoriagaoka
Ikeda-City
Osaka, Japan   563-8577
n-murase@aist.go.jp

Andrei Naumov
Institute of Spectroscopy RAS
Troitsk, Moscow Region, Russia
142190
(095) 3340236
naumov@isan.troitsk.ru

Masura Oda
Tokyo University of Agriculture and
Technology
Nakacho 2-24-16
Koganei
Tokyo, Japan   184-8588
odamasa@cc.tuat.ac.jp

Andy Olson
Montana State University
Spectrum Lab
P.O. Box 173510
Bozeman, MT   59717
(406) 994-7881
andyo@spectrum.montana.edu

Michel Orrit
Universiteit Leiden
MoNOS, Huygens Laboratorium
Postbus 9504
2300, RA   Leiden
orrit@molphys.leidenuniv.nl

Taras Plakhotnik
ETH Zurich
Laboratory for Physical Chemistry
ETH Hönggerberg
Zurich, Switzerland   CH-8093
taras@phys.chem.ethz.ch

Aleksander Rebane
Montana State University
Physics EPS 264
Bozeman, MT   59717
(406) 994-7831
rebane@physics.montana.edu

Inna Rebane
University of Tartu
Institute of Physics
Riia Str 142
Tartu, Estonia   51014
(372) 742-8164
inna@fi.tartu.ee

Karl Rebane
University of Tartu
Institute of Physics
Riia Str 142
Tartu, Estonia   51014
rebanek@fi.tartu.ee

Randy Reibel
Directed Energy Solutions
6360 Shirecliff Dr.
Colorado Springs, CO   80918
(719) 333-7797
randyr@denergysolutions.com

Tõnu Reinot
Iowa State University
0712 Gilman
Ames, IA   50011
(515) 294-6942
tonu@iastate.edu

Christoffer Renner
Montana State University
264 EPS Building
Bozeman, MT   59717
(406) 994-7988
cliffkopy@aol.com

Kevin Repasky
Montana State University
Spectrum Lab
P.O. Box 173510
Bozeman, MT 59717
(406) 994-6082
repasky@physics.montana.edu

Lars Rippe
Lund Institute of Technology
Box 118
Lund, Sweden S22100
lars.rippe@fysik.lth.se

Krishna Rupavatharam
Montana State University
Spectrum Lab
P.O. Box 173510
Bozeman, MT 59717
(406) 994-7675
krishna@spectrum.montana.edu

Seishiro Saikan
Tohoku University
Aramaki
Sendai, Japan 870-8578
(022) 217-6461
saikan@laser.phys.tohoku.ac.jp

Yoko Saikan
Tohoku University
c/o Seishiro Saikan
Aramaki
Sendai, Japan 870-8578
(022) 217-6461
saikan@laser.phys.tohoku.ac.jp

G. MacKay Salley
Wofford College
429 N. Church Street
Spartanburg, SC 29303
(864) 597-4610
salleygm@wofford.edu

Vitaly Samartsev
Kazan Physical-Technical Institute RAS
Sibirski Trakt Str. 10
Kazan, 420029 Russia
8432-729-333
samartsev@kfti.knc.ru

Friso Schlottau
University of Colorado at Boulder
Electrical & Computer Engineering
Boulder, CO 80309-0425
(303) 492-4716
friso.schlottau@colorado.edu

Marlan Scully
Texas A&M University
Physics Dept.
Institute for Quantum Studies
College Station, TX 77843
(979) 862-2333
scully@physics.tamu.edu

Matthew Sellars
Laser Physics Center, Research School
of Physical Science and Engineering
Australian National University
Canberra, ACT, 0200, Australia
matthew.sellars@anu.edu.au

Vladimir Shalaev
Purdue University
School of Electrical Engineering
1285 EE Building
West Lafayette, IN 47907
(765) 494-9855
shalaev@ecn.purdue.edu

Yongchen Sun
Montana State University
Physics Department
Bozeman, MT 59717
(406) 994-6163
sun@physics.montana.edu

Toshiro Tani
Tokyo University of Agriculture and
Technology
Nakacho 2-24-16 Koganei
Tokyo, JP   184-8588
ttani@cc.tuat.ac.jp

Imbi Tehver
University of Tartu
Institute of Physics
Riia 142
Tartu, Estonia   51014
(372) 738-3017
tehver@eeter.fi.tartu.ee

Erwin Thiel
University of Siegen
Physical and Theoretical Chemistry
Laboratory
Adolf-Reichwein Str.
Siegen, Germany   57068
+0175 74 55 129
thiel@physics.montana.edu

Charles Thiel
Montana State University
Physics Department
Bozeman, MT   59717
(406) 994-4363
e.thiel@zess.uni-siegen.de

Mingzhen Tian
Montana State University
264 EPS Building
Bozeman, MT   59717
(406) 994-6286
tian@physics.montana.edu

Martin Vacha
Tokyo University of Agriculture and
Tech.
2-24-16 Naka-machi, Koganei
Tokyo, Japan   184-8588
vacha@cc.tuat.ac.jp

Yuri Vainer
Institute of Spectroscopy RAS
Troitsk, Moscow Region, Russia
142190
(095) 3340236
vainer@isan.troitsk.ru

Silvia Völker
Huygens Laboratory, Leiden University
Niels Bohrweg 2, P.O. Box 9504
Huygens Laboratory, Leiden University
Leiden, The Netherlands   2300 RA
silvia@molphys.leidenuniv.nl

Kelvin Wagner
University of Colorado at Boulder
Electrical & Comp Engineering
Boulder, CO   80309-0425
(303) 492-4661
kelvin@java.colorado.edu

Jörg Woehl
University of Grenoble
Laboratoire de Spectrometrie Physique
Saint Martin d'Heres, France   38402
jorg.woehl@ujf-grenoble.fr

Ijaz Zafarullah
Montana State University
Dept. of Physics
264 EPS Building
Bozeman, MT   59717
(406) 994-7988
Ijaz@montana.edu

Valter Zazubovich
Iowa State University
Department of Chemisty ISU
Ames, IA   50011
(515) 294-6942
valterz@iastate.edu

Montana State University – Campus Map

Physics Labs are on the first floor of the EPS Bldg.

Spectrum Lab

Visitor Information & Parking Kiosk

University Police

$2 P

'The Campus Visitor Information and Parking Kiosk' will sell you a one day parking permit for $2 if you need to drive to Montana State University and park during the hours of 8 AM to 5 PM. Evening parking is free in the lots indicated by 'P.'

Butte 90 mi
Missoula 200 mi

Belgrade 10 mi
Airport 9 mi

I-90 Exit 306

N

Oak St
W Oak St

GranTree Inn
1325 N 7th Ave
Bozeman, MT 59715

Aspen St

Durston Rd
W Peach St E Peach St

W Beall St

E Lamme St

W Main St Bozeman E Main St
W Babcock St

W Olive St E Olive St

Scientific Materials Corp.
310 Ice Pond Rd
Bozeman, MT 59715

E Story

W College St W College St W College St

Livingston 25 mi
Billings 140 mi

Montana State University
EPS Building
W Grant St & S 6th Ave

Montana State University
Spectrum Lab

W Grant St

W Lincoln St

Holly

W Kagy Blvd W Kagy Ave

1 mile

1 km